

AIR TOXIC EMISSIONS FROM MOBILE SOURCES IN WINTER

By

FARAH N. ABEDIN

A thesis submitted in partial fulfillment of
the requirements for the degree of

MASTER OF SCIENCE IN ENVIRONMENTAL ENGINEERING

WASHINGTON STATE UNIVERSITY
Department of Civil and Environmental Engineering

DECEMBER 2011

To the Faculty of Washington State University:

The members of the Committee appointed to examine the thesis of
FARAH N. ABEDIN find it satisfactory and recommend that it be
accepted.

Bertram T. Jobson, Ph.D., Chair

Brian K. Lamb, Ph. D.

Joseph K. Vaughan, Ph.D.

ACKNOWLEDGEMENT

Many people have helped me in the process of writing this thesis. I would like to take this opportunity to thank some of the individuals.

First and foremost, I would like to thank my academic advisor, Dr. Tom Jobson. He has been an amazing guide and an excellent teacher throughout this whole process. He never shied away from my numerous silly questions and showed extraordinary patience while explaining things to me. He always encouraged me to look at the big picture, beyond all the numbers and equations. I have learned a lot from him about chemistry, logic and life's intricate philosophy. I feel very lucky that I got to work with him for the past two years.

I would also like to thank my thesis committee members, Drs. Brian Lamb and Joseph Vaughan. They have helped me, along with my advisor, to achieve my goals in my research and guided me through some rocky territories. I thank Dr. Brian Lamb for taking an interest in my research and for encouraging me to explore the possibilities beyond this thesis. I cannot thank Dr. Vaughan enough for helping me understand some of the key aspects of AIRPACT. He patiently guided me through the process of extracting the modeled data. I am deeply grateful for his insights and suggestions on writing this manuscript.

Many thanks go to past and present graduate students of LAR. I am very grateful to my fellow graduate students and office mates, Will Wallace and Matt Erickson for helping

me with Igor codes to manipulate my data. Had they not, I would be still crunching numbers the old way and develop a permanent carpal tunnel syndrome.

I would specially like to thank Rasa Grivicke, Kara Yedinak and Celia Faiola for all the conversations we had over the years about school and beyond. I would also like to show appreciation to my fabulous office mates: Andrew Rengel, Vincent Fricaud, Sarah Waldo, Rodrigo Gonzalez-Abraham, George Mwaniki and Farren Herron-Thorpe. Thank you all for your friendship and support.

Lastly, I would like to thank my family and friends, around the globe, for their endless love, support and patience.

AIR TOXIC EMISSIONS FROM MOBILE SOURCES IN WINTER

Abstract

by Farah N. Abedin, M.S.
Washington State University
December 2011

Chair: Bertram T. Jobson

The US Environmental Protection Agency has labeled six air toxics to be the most hazardous to human health, including formaldehyde, acetaldehyde and benzene. In urban areas, these are mainly emitted by vehicles when lower temperature inhibits biogenic emissions. Among these toxics benzene is a well known carcinogen and the aldehydes (formaldehyde and acetaldehyde) can also contribute to ground level ozone formation besides affecting human health. To estimate toxic emissions from mobile sources, toxic assessment programs can use emission ratios along with ambient monitoring data. In this study, emission ratios relative to vehicle exhaust tracers (CO and NO_x) were calculated by using parameters from regression analysis.

Formaldehyde, acetaldehyde and benzene along with other volatile organic compounds (VOCs) and trace gases (CO, NO_x) were measured in winter from December 2008 to January 2009 as a part of the Treasure Valley PM_{2.5} campaign in Meridian, Idaho. By analyzing the morning rush hour period, we found that the emissions ratios with respect to CO were 3.30 ± 0.29 pptv/ppbv, 2.11 ± 0.20 pptv/ppbv and 1.30 ± 0.07 pptv/ppbv for formaldehyde, acetaldehyde and benzene respectively. The emission ratios with respect

to NO_x were 11.9 ± 1.2 pptv/ppbv, 7.99 ± 1.03 pptv/ppbv and 5.06 ± 0.47 pptv/ppbv for formaldehyde, acetaldehyde and benzene respectively. These emission ratios with CO were found to be in reasonable agreement with previous studies done in various cities. The measured emission ratios were also compared with calculated ones from modeled data generated by AIRPACT-3. The measured emission ratios, for aldehydes with respect to NO_x and for benzene with respect to CO, were comparable to the modeled ones. The good agreement for AIRPACT versus observations, for NO_x correlations compared to those with CO, suggests that the CO emission from the model is over predicted by a factor of 5.2.

TABLE OF CONTENTS

ACKNOWLEDGEMENT	iii
ABSTRACT.....	v-vi
LIST OF TABLES	viii
LIST OF FIGURES	x
CHAPTER 1: INTRODUCTION.....	1
1.1. Air toxics	1
1.2.Sources of air toxics	3
1.2.1. Acetaldehyde.....	5
1.2.2. Benzene.....	6
1.2.3. Formaldehyde	7
1.3. Air toxics in urban areas.....	10
1.4. Modeling air toxics.....	14
1.5. Objective.....	16
CHAPTER 2: EXPERIMENTAL.....	17
2.1. Site description	17
2.2. Measurements.....	19
CHAPTER 3: RESULTS AND DISCUSSION.....	23
3.1. Data description.....	23
3.2. Morning rush hour Analysis	34
3.3. Selection criteria for morning rush hour periods.....	37
3.4. Air toxics correlation analysis for rush hour periods	39
3.4.1. Correlation with CO.....	39

3.4.1.1. Formaldehyde	39
3.4.1.2. Acetaldehyde	44
3.4.1.3. Benzene	47
3.4.1.4. Other species.....	50
3.4.1.4.1. m/z = 69	50
3.4.1.4.2. m/z = 137	51
3.4.1.4.3. Aromatics.....	52
3.4.2. Correlation with NO _x	55
3.4.2.1. Formaldehyde	55
3.4.2.2. Acetaldehyde	58
3.4.2.3. Benzene	62
3.4.2.4. Other species.....	65
3.4.2.4.1. m/z = 69	66
3.4.2.4.2. m/z = 137	67
3.4.2.4.3. Aromatics.....	68
3.5. Comparison to AIRPACT-3	70
3.5.1. Formaldehyde	71
3.5.2. Acetaldehyde.....	73
3.5.3. Benzene.....	76
3.5.4. Aromatics	77
3.6. Summary and discussion	80
CHAPTER 4: CONCLUSION	85
BIBLIOGRAPHY	89

LIST OF TABLES

Table 1.1. List of EPA Mobile Source Air Toxics	2
Table 3.1. Summary of statistics of measured volatile organic compounds (VOCs) and carbon monoxide and nitrogen oxides (5 - minute averages)	23
Table 3.2. Parameters for linear regressions of HCHO vs. CO for the selected morning rush hour periods. The average temperature and relative humidity are included	40
Table 3.3. Parameters for linear regressions of HCHO vs. CH ₃ CHO for the selected morning rush hour periods	43
Table 3.4. Parameters for linear regressions of CH ₃ CHO vs. CO for the selected morning rush hour periods.....	46
Table 3.5. Parameters for linear regressions of benzene vs. CO for the selected morning rush hour periods.....	48
Table 3.6. Parameters for linear regressions of aromatics vs. CO for the selected morning rush hour periods.....	54
Table 3.7. Parameters for linear regressions of HCHO vs. NO _x for the selected morning rush hour periods. The average temperature and relative humidity are included	56
Table 3.8. Parameters for linear regressions of CH ₃ CHO vs. NO _x for the selected morning rush hour periods	60

Table 3.9. Parameters for linear regressions of benzene vs. NO _x for the selected morning rush hour periods.....	63
Table 3.10. Parameters for linear regressions of unknown #2 (m/z =137) vs. NO _x for the selected morning rush hour periods	67
Table 3.11. Parameters for linear regressions of aromatics vs. NO _x for the selected morning rush hour periods	69
Table 3.12. Emission ratios of VOCs from Meridian, Idaho and modeled data from AIRPACT-3	82
Table 3.13. Emission ratios of air toxics with respect to CO from Meridian, Idaho and other cities. Units are in pptv/ppbv CO	84

LIST OF FIGURES

Figure 1.1. Sources of urban air toxics	4
Figure 1.2. Block diagram of O ₃ production driven by HCHO, HOX and NOX chemistry.	13
Figure 2.1 Map of the study site in Meridian, Idaho.	18
Figure 2.2. Close-up of the measurement trailer equipped with the instruments	20
Figure 3.1.1. Plots of 5 - minute averaged data of temperature, relative humidity, formaldehyde (HCHO), nitrogen oxides (NO _x) and carbon monoxide (CO) mixing ratios in Meridian, Idaho, from 1 December, 2008 to 31 January, 2009.	25
Figure 3.1.2. Plots of 5 - minute averaged data of acetaldehyde, acetone, acetonitrile and benzene mixing ratios in Meridian, Idaho, from 1 December, 2008 to 31 January, 2009.	26
Figure 3.1.3. Plots of 5 - minute averaged data of C2-benzene, C3-benzene, C3-benzene and methanol mixing ratios in Meridian, Idaho, from 1 December, 2008 to 31 January, 2009.	27
Figure 3.1.4. Plots of 5 - minute averaged data of naphthalene, pentenes, phenol and toluene mixing ratios in Meridian, Idaho, from 1 December, 2008 to 31 January, 2009.	28
Figure 3.1.5. Plots of 5 - minute averaged data of unknown #1 (m69) and unknown #2 (m137) mixing ratios in Meridian, Idaho, from 1 December, 2008 to 31 January, 2009.	29
Figure 3.2. Diel profiles of formaldehyde, acetaldehyde, benzene and CO mixing ratio as half hour averages	30
Figure 3.3. Wind rose plots showing wind speed and fractional occurrence of wind flow direction in 30° increment bins for day and night during the entire campaign and the stagnation period	31

Figure 3.4.1. Plots of 5 - minute averaged mixing ratios of CO and formaldehyde as a function of wind direction in 30° increment bins.	32
Figure 3.4.2. Plots of 5 - minute averaged mixing ratios of Acetaldehyde and Benzene as a function of wind direction in 30° increment bins.....	33
Figure 3.5. Hourly vehicle miles travelled (VMT) of gasoline vehicles over a week	36
Figure 3.6. Hourly vehicle miles travelled (VMT) of diesel vehicles over a week	37
Figure 3.7. Relationships between HCHO and CO mixing ratios in Meridian, Idaho.	39
Figure 3.8. Measured and calculated (using HCHO/CO ratio) HCHO mixing ratios	41
Figure 3.9. Histogram plots of the ratio of observed and predicted (using HCHO/CO ratio) formaldehyde mixing ratios	42
Figure 3.10. Relationships between formaldehyde and acetaldehyde mixing ratios	43
Figure 3.11. Relationships between acetaldehyde and carbon monoxide mixing ratios in Meridian, Idaho.	44
Figure 3.12 Measured and calculated (using CH ₃ CHO/CO ratio) CH ₃ CHO mixing ratios.	45
Figure 3.13. Histogram plots of the ratio of observed and predicted (using CH ₃ CHO/CO ratio) of acetaldehyde mixing ratios.	47
Figure 3.14. Relationships between benzene and carbon monoxide mixing ratios in Meridian, Idaho	48
Figure 3.15. Measured and calculated (using benzene/CO ratio) benzene mixing ratios.	49
Figure 3.16. Histogram plots of the ratio of observed and predicted (using benzene/CO ratio) of benzene mixing ratios.	50

Figure 3.17. Relationships between unknown #1 ($m/z = 69$) and carbon monoxide mixing ratios in Meridian, Idaho.	52
Figure 3.18. Relationships between unknown #2 ($m/z = 137$) and carbon monoxide mixing ratios in Meridian, Idaho	53
Figure 3.19. Relationships between aromatics and carbon monoxide mixing ratios in Meridian, Idaho.....	54
Figure 3.20. Relationships between HCHO and NO _x mixing ratios in Meridian, Idaho.	55
Figure 3.21. Measured and calculated (using HCHO/NO _x ratio) HCHO mixing ratios.	57
Figure 3.22. Histogram plots of the ratio of observed and predicted (using HCHO/NO _x ratio) formaldehyde mixing ratios	58
Figure 3.23. Relationships between CH ₃ CHO and NO _x mixing ratios in Meridian, Idaho.	59
Figure 3.24. Measured and calculated (using CH ₃ CHO/NO _x ratio) CH ₃ CHO mixing ratios	60
Figure 3.25. Histogram plots of the ratio of observed and predicted (using CH ₃ CHO/NO _x ratio) of acetaldehyde mixing ratios	61
Figure 3.26. Relationships between benzene and NO _x mixing ratios in Meridian, Idaho.	62
Figure 3.27. Measured and calculated (using benzene/NO _x ratio) benzene mixing ratios	63
Figure 3.28. Histogram plots of the ratio of observed and predicted (using benzene/NO _x ratio) of benzene mixing ratios	65
Figure 3.29. Relationships between unknown #1 ($m/z = 69$) and NO _x mixing ratios in Meridian, Idaho.	66

Figure 3.30. Relationships between unknown #2 ($m/z = 137$) and NO_x mixing ratios in Meridian, Idaho	68
Figure 3.31. Relationships between aromatics and NO_x mixing ratios in Meridian, Idaho	69
Figure 3.32. AIRPACT-3 domain. Satellite image of AIRPACT-3 domain showing major cities and interstate highways (red lines).	70
Figure 3.33. Comparison of HCHO/CO slopes from AIRPACT-3 model and measurements.	72
Figure 3.34. Comparison of HCHO/NO_x slopes from AIRPACT-3 model and measurements.	73
Figure 3.35. Comparison of $\text{CH}_3\text{CHO}/\text{CO}$ slopes from AIRPACT-3 model and measurements.	74
Figure 3.36. Comparison of $\text{CH}_3\text{CHO}/\text{NO}_x$ slopes from AIRPACT-3 model and measurements.	75
Figure 3.37. Comparison of benzene $/\text{CO}$ slopes from AIRPACT-3 model and measurements.	76
Figure 3.38. Comparison of benzene $/\text{NO}_x$ slopes from AIRPACT-3 model and measurements.	77
Figure 3.39. Comparison of mono aromatics/ CO slopes from AIRPACT-3 model and measurements.....	78
Figure 3.40. Comparison of mono aromatics/ NO_x slopes from AIRPACT-3 model and measurements.....	79

ABBREVIATIONS

ACS	American Cancer Society
AIRPACT	Air Indicator Report for Public Awareness and Community Tracking
BVOC	Biogenic volatile organic compounds
CAA	Clean Air Act
CI	Compression ignition
CMAQ	Community Multi-Scale Air Quality
DHHS	Department of Health and Human Services
EPA	Environmental Protection Agency
HAPs	Hazardous air pollutants
IARC	International Agency for Research on Cancer
IDEQ	Idaho Department of Environmental Quality
IUATS	Integrated Urban Air Toxic Strategy
MACL	Mobile atmospheric chemistry lab
MSATs	Mobile Source Air Toxics
MTBE	Methyl tertiary butyl ether
NAAQS	National ambient air quality standards
NEI	National Emission Inventory
NESHAPS	National emissions standards for hazardous air pollutants
PM	Particulate matters
PMSATs	Priority Mobile Source Air Toxics
PTR-MS	Proton transfer reaction mass spectrometer

SI	Spark ignition
SOA	Secondary organic aerosol
TOG	Total organic gases
VMT	Vehicle miles travelled
VOCs	Volatile organic compounds

NOMENCLATURE

C_5H_8	Isoprene/ 2-methyl-1,3 butadiene
C_6H_6	Benzene
$C_{10}H_{15}$	Monoterpenes
CH_3CHO	Acetaldehyde
CH_4	Methane
CO	Carbon monoxide
HCHO	Formaldehyde
HO	Hydroxyl radical
HO_2	Hydroperoxy radical
NO	Nitric Oxide
NO_2	Nitrogen dioxide
NO_3	Nitrogen trioxide or nitrate radical
NO_x	Nitrogen Oxides
O_3	Ozone

SO₂ Sulfur dioxide

Units

ppbv parts per billion by volume

pptv parts per trillion by volume

CHAPTER 1: INTRODUCTION

1.1. Air toxics

Air toxics, also known as hazardous air pollutants (HAPs), are those air pollutants which are known or suspected to cause serious effects on human health. The pollutants can be volatile organic compounds (VOCs) or chemicals found in particulate matter (PM). Some important air toxics found in urban environments are benzene, toluene, alkyl benzenes, formaldehyde (HCHO) and acetaldehyde (CH₃CHO). The health effects of HAPs on humans can be acute or chronic depending on the pollutants and nature of exposure (ATSDR, 1999, 2007; EPA, 1988). Usually, the health risks from these pollutants are higher in the areas closest to where they are emitted. Some of these pollutants have a long residence time in the atmosphere or can accumulate in the food chain, thus impacting people far removed from HAP sources.

The HAPs are different from the six criteria pollutants which are regulated by the U.S. Environmental Protection Agency (EPA). The criteria air pollutants include carbon monoxide (CO), and ozone (O₃), nitrogen dioxide (NO₂), sulfur dioxide (SO₂) and PM_{2.5} and are the most abundant air pollutants in an urban atmosphere. Criteria pollutants are regulated by EPA by the national ambient air quality standards (NAAQS). EPA has been also trying to reduce the emissions of these air toxics because of their impact on health and environment. The federal Clean Air Act (CAA) Amendment recognizes 187 chemicals or chemical classes as hazardous air pollutant or air toxics. To limit the release of HAPs from specific sources, EPA has established National Emissions Standards for

Hazardous Air Pollutants (NESHAPs), according to Section 112 of the CAA (EPA, 2000b).

The EPA has also devised a strategy, known as the National Air Toxics Program: The Integrated Urban Air Toxic Strategy (IUATS), for air toxics in urban areas by looking at stationary, mobile, and indoor source emissions. In this strategy, EPA established a list of 33 urban HAPs which pose the greatest threats to public health in urban areas, considering emissions from major, area and mobile sources. At the same time, the agency compared the lists of compounds identified in the motor vehicle emission databases and studied them with the toxic compounds listed in the Integrated Risk Information System, IRIS. Thus, U.S. EPA identified 21 Mobile Source Air Toxics (MSATs) (EPA, 2000b), each of which has the potential to cause serious adverse health effects as reflected in IRIS and in the ongoing agency scientific assessments. Table 1 shows the list of the 21 MSATs

Table 1.1. List of EPA's Mobile Source Air Toxics (Reprinted from (EPA, 2000b))

Acetaldehyde	Diesel Particulate Matter & Diesel Exhaust Organic Gases	MTBE
Acrolein	Ethylbenzene	Naphthalene
Arsenic Compounds	Formaldehyde	Nickel Compounds
Benzene	n-Hexane	Polycyclic Organic Matter
1,3-Butadiene	Lead Compounds	Styrene
Chromium Compounds	Manganese Compounds	Toluene
Dioxin/Furans	Mercury Compounds	Xylene

which include various volatile organic compounds, VOCs, and metals, as well as diesel particulate matter, and diesel exhaust organic gases, collectively called DPM + DEOG.

Among these pollutants, six air toxics are considered to be priority mobile sources air toxics (PMSATs) due to their higher risk to human health, according to the U.S. EPA's IUATS and the MSATs regulations. These are: acrolein, acetaldehyde, benzene, 1,3-butadiene, formaldehyde, and DPM (EPA, 2000a). The focus of this thesis is on acetaldehyde, benzene and formaldehyde.

1.2. Sources of air toxics

Most of the air toxics in the atmosphere come from anthropogenic sources as a result of incomplete combustion of fossil fuels including roadway emissions (e.g., cars, trucks, buses etc.), non-roadway emissions (e.g., locomotive, aviation etc.), area sources (e.g. home heating, biomass burning etc.) and point sources (e.g., factories, refineries, power plants, etc.). VOCs, like benzene, can be also emitted in the atmosphere through fuel evaporation and solvent use (Borbon et al., 2004). Air toxics, like formaldehyde and acetaldehyde, can be produced in the atmosphere photochemically from other VOCs or biogenic volatile organic compounds (BVOCs) (Altshuller, 1993). Secondary photochemical formation depends on various factors of the atmosphere, including precursor concentrations and the abundance of oxidants. During summer, high emissions of biogenic hydrocarbons (BVOCs) from plants can be a major source of secondary formaldehyde, and lead high levels of formaldehyde during summer compared to winter (Possanzini et al., 2002; Tago et al., 2005). Figure 1.1 shows the intricate relationship

between these various sources and how they contribute to toxic concentrations in the ambient environment.

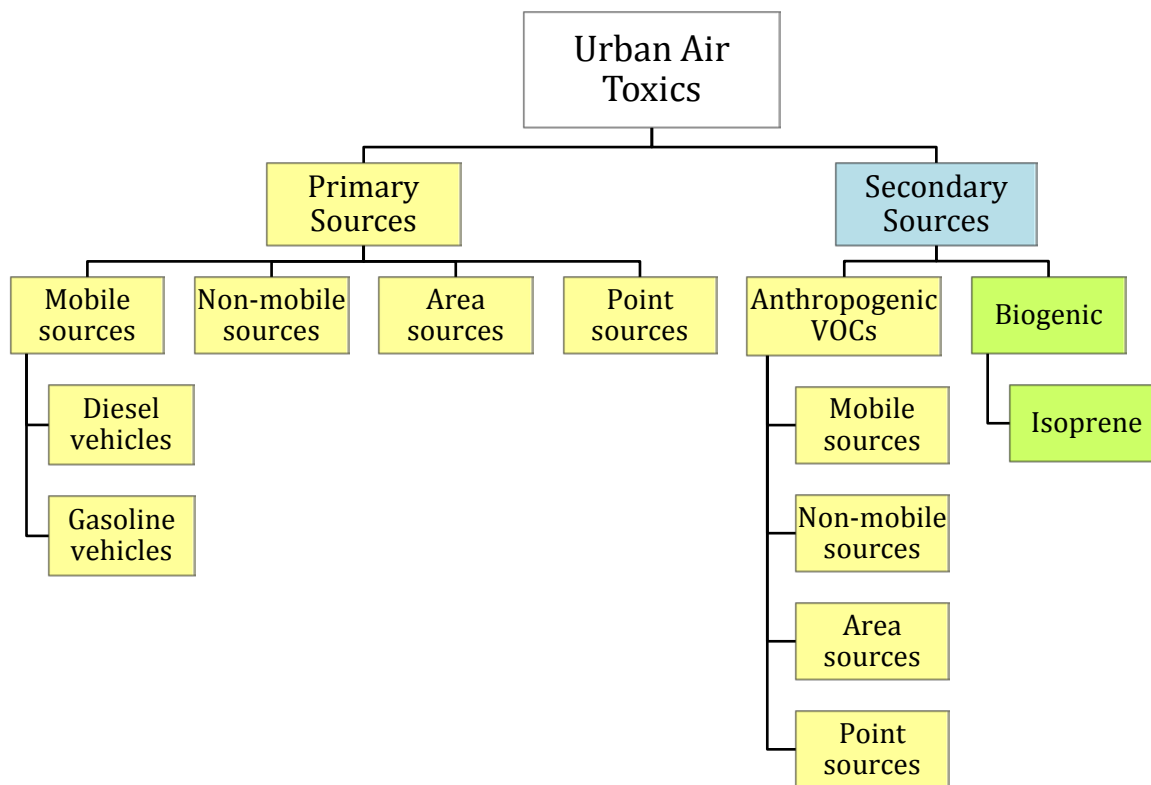


Figure 1.1. Sources of urban air toxics. The yellow boxes represent all anthropogenic and direct emission sources. The green boxes represent BVOC sources.

It is to be noted that there is no secondary production of benzene in the atmosphere. It is directly emitted from various anthropogenic sources. The following subsections describe the nature, health effects, sources and sinks of the three air toxics.

1.2.1. Acetaldehyde

Acetaldehyde (CH_3CHO) is a carbonyl compound commonly found in the ambient environment. It is an intermediate product of plant respiration and is formed as a product

of incomplete wood combustion in fireplaces and wood stoves, coffee roasting, burning of tobacco, vehicle exhaust fumes, and coal refining and waste processing (EPA, 2000b).

Hence, many individuals are exposed to acetaldehyde by breathing ambient air.

Acetaldehyde is reasonably anticipated to be a human carcinogen based on animal studies that have shown nasal tumors in rats and laryngeal tumors in hamsters (NTP, 2011).

Acute effects associated with exposure to acetaldehyde include irritation of the eyes, skin, and respiratory tract.

Acetaldehyde belongs to the carbonyl/aldehyde compounds, which undergo photolysis, reaction with OH radicals and reaction with NO₃ radicals. Reactions with nitrate radical are of minor significance (Seinfeld and Pandis, 2006), leaving the photolysis and OH radical reaction as the major loss process, principally during summer season.

1.2.2. Benzene

Benzene is an aromatic compound commonly found in the environment. The main sources of benzene emission in the air are emissions from burning coal and oil, benzene waste and storage operations, motor vehicle exhaust, and evaporation from gasoline service stations. Tobacco smoke is another source of benzene in air, particularly indoors. Benzene accounts for 3 to 5 percent of mobile source exhaust total organic gases (TOG), which varies depending on control technology (e.g., type of catalyst) and the levels of benzene and aromatics in the fuel (EPA, 2000b).

The major sources of benzene exposure are tobacco smoke, automobile service stations, exhaust from motor vehicles, and industrial emissions. Auto exhaust and industrial

emissions account for about 20% of the total national exposure to benzene (ATSDR, 2007).

Inhaling high levels of benzene can cause drowsiness, dizziness, rapid heart rate, headaches, tremors, confusion, and unconsciousness. Long-term exposure to high levels of benzene in the air can cause leukemia, particularly acute myelogenous leukemia, often referred to as AML, which is a form of cancer that starts inside bone marrow, the soft tissue inside bones that generate blood cells (NTP, 2011). The Department of Health and Human Services (DHHS), the International Agency for Research on Cancer (IARC) and the EPA, all recognizes benzene as a human carcinogen (ATSDR, 2007). Also, for women exposed by inhalation to high levels reproductive effects have been reported; and adverse effects on the developing fetus have been observed in animal tests (ATSDR, 2007).

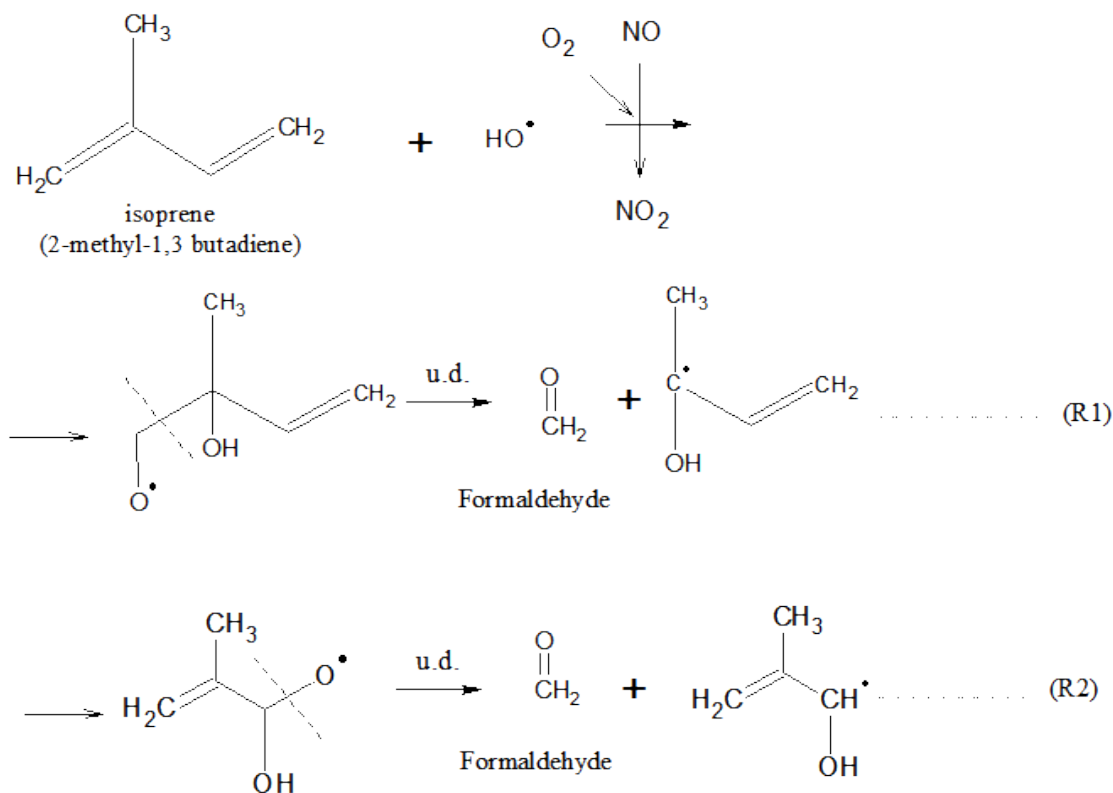
The most significant degradation process for atmospheric benzene is its reaction with atmospheric OH radicals (Seinfeld and Pandis, 2006).

1.2.3. Formaldehyde

Formaldehyde is the simplest form of aldehyde/carbonyl. It is a very common pollutant in the atmosphere. Primary sources of HCHO are mostly anthropogenic emissions from vehicles and biomass burning as an incomplete combustion product. Vehicle exhaust is the dominant source of formaldehyde in urban areas (Anderson et al., 1996; Ban-Weiss et al., 2008; EPA, 2000b; Grosjean, 1982; Grosjean et al., 2001; Grosjean et al., 2002). It is emitted during both gasoline and diesel fuel combustion and accounts for 1 – 4% of total

exhaust TOG emissions, depending on control technology and fuel composition (EPA, 2000b). Primary formaldehyde emissions from mobile sources account for approximately 41% of the emissions in the 1996 National Toxics Inventory (EPA, 2000b).

Formaldehyde can be also created in the atmosphere from other VOCs through photochemical reactions (Altshuller, 1993). These reactions depend on various factors of the atmosphere (e.g. weather, abundance of oxidants, abundance of certain molecules, etc.). Photo oxidation of methane (CH_4) and photo oxidation of isoprene (2-methyl-1,3 butadiene (C_5H_8)), both can contribute to secondary production of HCHO. During summer months, the photochemistry can contribute up to 80 – 90% of the ambient HCHO. This contribution is low (only 30 – 40%) during winter months (Possanzini et al., 2002; Tago et al., 2005). In summer, biogenic emissions such as isoprene dominate compared to anthropogenic sources. Isoprene is emitted from deciduous trees and its emission increase with elevated ambient temperature (Duane et al., 2002). Thus its photo oxidation produces more HCHO during summer. The following reactions (R1 and R2) are responsible for secondary production of formaldehyde from isoprene oxidation. In these reactions, the intermediate products of the oxidation undergo unimolecular dissociation (u.d.) and thus formaldehyde is formed.

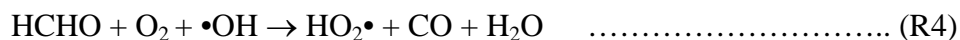


The Department of Health and Human Services (DHHS) states that people can be exposed to formaldehyde primarily from breathing indoor or outdoor air, from tobacco smoke and from use of cosmetic products containing formaldehyde (NTP, 2011).

According to DHHS, the major sources of airborne formaldehyde exposure include combustion sources, emissions from numerous construction and home-furnishing products, and emission from consumer goods. Acute inhalation exposure to formaldehyde in humans can result in respiratory symptoms, and eye, nose, and throat irritation. Other effects seen from exposure to high levels of formaldehyde in humans are coughing, wheezing, chest pains, and bronchitis (EPA, 1988; WHO, 1989). Chronic exposure to formaldehyde by inhalation in humans has been associated with eye, nose, throat irritation, and respiratory symptoms such as asthma (EPA, 1988; WHO, 1989). Based on

sufficient evidence of carcinogenicity from studies in humans and supporting data on mechanisms of carcinogenesis, formaldehyde is known to be a human carcinogen (NTP, 2011).

Formaldehyde is known to be decomposed rapidly by photolysis and react with OH radical and with oxygen radical. Its atmospheric lifetime depends on reactions with OH and photolysis. These two reactions (R3 and R4) are important as formaldehyde contributes to the HO_x (OH + HO₂) budget through its photolysis (McKeen et al., 1997; Starn et al., 1998). Free radical sources like this can eventually contribute to tropospheric ozone (O₃) production.



In a nitrogen oxide rich environment, this hydroperoxy (HO₂•) radical converts into hydroxyl radical (R5).



Thus, HCHO photolysis can be an important source of HO_x radicals in urban environments and have an impact on photochemical ozone production.

1.3. Air toxics in urban areas

Air toxics can pose special threats in urban areas because of the large number of people and the variety of sources of toxic air pollutants. Individually, some of these sources may

not emit large amounts of toxic pollutants. However, all of these pollution sources combined can potentially pose significant health threats, particularly to sensitive subgroups such as children and the elderly.

Population growth in urban areas is responsible for the fast growth of mobile sources which can lead to increased air toxics if the area does not improve the fuels or does not use cleaner vehicle technologies. According to the American Cancer Society (ACS), the cancer of the respiratory system, such as lung cancer, accounts for more deaths than any other cancer in both men and women (29% and 26% respectively) ((ACS)) and exposure to air pollution is an important risk factor. According to their fact sheet, exposure to carcinogenic agents from environmental pollutant account for 2% of all cancer cases. the relationship between such agents and cancer is significant, although the estimated percentage of cancers related to environmental carcinogens is small compared to the cancer burden from acquired factors such as tobacco smoking and poor health choices. Even a small percentage of cancers can represent many deaths: 2% of cancer deaths in the US in 2010 correspond to approximately 11,400 deaths. In the Pacific Northwest region, the state of Washington was estimated to have 4,320 new respiratory cancer cases and the state of Idaho was estimated to have 860 in 2010. For Idaho, the 2002 National-Scale Air Toxics Assessment (NATA) model predicted the cancer risk for Ada County in Idaho to be 32 in a million (EPA, 2010). In the 2005 NATA prediction the risk has increased up to 43 in a million (EPA, 2011), a 34.4% increase from the previous report. In the NATA study, Ada county ranked first in the state of Idaho for cancer risk (IDEQ, 2009).

Another aspect of air toxics in the urban environment is tropospheric ozone (O₃).

Tropospheric ozone is a major component of photochemical smog, frequently found in urban atmospheres. Ozone is considered a major pollutant when found in the lower atmosphere or troposphere. It is one of the criteria pollutants regulated by EPA as discussed in section 1.1. It is a highly reactive gas and exposure to ozone can cause severe respiratory illnesses in human as ozone reacts with biomolecules and breaks them down; thus affecting lung function (Devlin et al., 1997).

Tropospheric ozone is formed from the results of a reaction between atomic oxygen (O) and molecular oxygen (O₂) in the presence of a third molecule (M) (R6). The oxygen atoms are produced primarily from photolysis of NO₂ (R7). NO₂ is a nitrogen oxide, found in the atmosphere from various anthropogenic, biogenic and natural sources. The major source of NO_x (=NO+NO₂) is fossil fuel combustion in high temperature. Ozone and NO further reacts together by converting back to oxygen and NO₂ and thus completing a cycle (R8).



When there are enough VOCs in the atmosphere this cycle is disrupted. As mentioned before, VOCs undergo reactions like R3 and R4 and produce HO₂• radical. Reactions like R5 produces even more •OH radical and NO₂ to create a cycle of oxidation. All these

reactions tied up together can create an endless loop (Figure 1.2) to create more and more tropospheric ozone in the presence of high VOCs and NO_x.

As tropospheric O₃ production depends both on VOCs and NO_x concentrations, it is often useful to determine which one of the pollutants should be reduced to meet the national air quality standards (NAAQS). The relative balance of VOCs and NO_x at a specific place helps to decide whether NO_x tends to contribute to the formation or the destruction of O₃. When the VOC/NO_x ratio is high (VOC is in excess relative to NO_x), NO_x tends to generate ozone. In such cases, the amount of NO_x tends to limit the amount of ozone formed, and the situation is called *NO_x limited*. In recent years as Treasure Valley (Ada county, Idaho) has seen an increase in O₃ levels, which violates the newly revised 8-hr NAAQS of 75 ppbv (Kavouras et al., 2008), it is important to take into account what kind of emission should be reduced to achieve the NAAQS for O₃. In 2007, the VOC/NO_x ratio from an ozone precursor study from this area determined Treasure Valley is mainly NO_x limited area (with few exceptions); which means to reduce O₃ levels the focus should be on reduction of NO_x emissions (Kavouras et al., 2008). The few exceptional sites (including this study site at St Luke's Hospital in Meridian, Idaho) are *VOC limited*. In this case, reducing only NO_x emissions without controlling VOC emissions will not decrease the O₃ level in this area. Treasure valley also has a particulate matter (PM) and secondary organic aerosol (SOA) formation problem (Stockwell et al., 2003). This previous model study has shown that reduction of VOC emission would decrease the formation of secondary aerosol while reduction of NO_x emissions would increase the amount of secondary aerosol in the Treasure Valley. For both of these

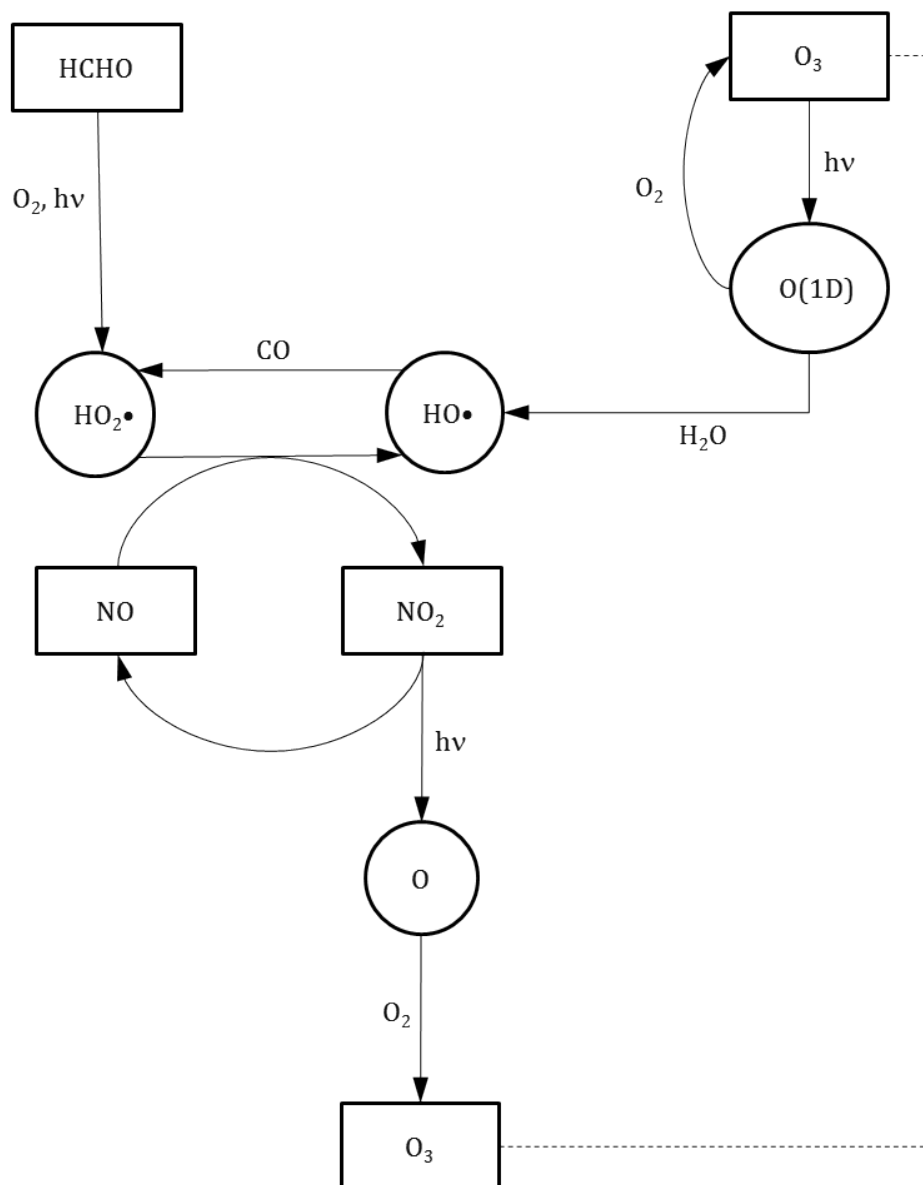


Figure 1.2 Block diagram of O₃ production driven by HCHO, HO_x and NO_x chemistry. Stable compounds are in rectangle shapes; the short lived compounds are in circles.

factors (reduction of O₃ and secondary aerosol formation), VOC emission reduction is essential, hence the knowledge about their sources becomes significant too.

1.4. Modeling air toxics

Modeling air toxic concentrations in urban areas sources possess special challenges because of the various types of toxic sources. Although most HAPs are emitted directly some are produced and destroyed through reactions in the atmosphere. These issues, as well as receptor selection, meteorological data processing, and background concentration selection pose significant technical challenges to the air quality modeler. Air quality models are valuable air quality management tools. They estimate the HAPs concentrations at many locations and the number of the locations in a model far exceeds the number of monitors in a typical ambient monitoring network. A typical air quality model can either use the National Emission Inventory (NEI) data or an EPA-approved model to estimate vehicle emission. For example, an air quality forecast model for the Northwest region AIRPACT-3 (Air Indicator Report for Public Awareness and Community Tracking), a computerized system that runs every day and generates hourly maps of various criteria pollutants, uses the MOBILE6.2 model mobile emissions results. MOBILE6.2 calculates air toxics by applying a “toxics fraction” to the gram per mile (g/mi) total organic gas (TOG) emission rate generated by the model (Heirigs et al., 2004). However, this approach can generate a false real time assessment of the air toxic concentrations in some regions.

Another approach to quantify air toxic emissions from vehicles is comparing it with other vehicle emission tracers such as – carbon monoxide (CO), nitrogen oxides (NO_x), VOCs etc. and calculate their ratios (Rappengluck et al., 2010; Warneke et al., 2007). This ratio,

well known as an emission ratio, is a parameter that can be used to deduce the expected emissions of a certain VOC from a vehicle exhaust tracer, thus quantifying the amount of VOC contributed by mobile sources. As CO and NO₂ are criteria pollutants which are also present in vehicle exhausts, the ambient concentration of these trace gases are readily available from various air quality monitoring sites. To determine an emission ratio, the standard method is to calculate the slope of the linear fit of the scatterplot of two compounds (Warneke et al., 2007). This is a straightforward way to quantify emissions from a certain source e.g. vehicle exhaust. Other parameters found in the regression analysis can also help to understand the nature of the VOC emission with respect to vehicle exhaust. The background concentration of a VOC in the absence of vehicle exhaust can be determined from the intercept of the linear fit.

1.5. Objective

The primary objective of this study is to determine emission ratios for formaldehyde, acetaldehyde, and benzene from roadway vehicles using data collected during the Treasure Valley PM_{2.5} Study conducted in Meridian, Idaho in the winter of 2008-2009. Emission ratios were determined by relating these air toxics concentrations to those of CO and NO_x. The correlation between the targeted VOC and CO was used to quantify relative emission ratios from vehicles. To validate the method's efficacy, it was compared to model output (from MOBILE6.2) and emission inventories used by the regional forecast model AIRPACT-3.

The convenience of the proposed technique is that it can be used as a predictive tool to help air quality policy and decision-making, by using readily available ambient monitoring data. This method can be applied to estimate the emission of any desired VOC from vehicles or from any other major sources of that VOC.

CHAPTER 2: EXPERIMENTAL

The data for this thesis are from the Treasure Valley PM_{2.5} Study that took place in Meridian, Idaho between December 1, 2008 and January 31, 2009. This study was supported by the Idaho Department of Environmental Quality in an effort to better understand PM_{2.5} sources in the Treasure Valley. A report on this study was prepared by the Desert Research Institute (Kavouras et al., 2008)

2.1. Site Description

The Treasure Valley PM_{2.5} Study took place in Meridian, Idaho between December 1, 2008 and January 31, 2009. Meridian is a suburban area located approximately 16 km west of the Boise city center. The measurement site was co-located with a state air monitoring site (St. Luke's) run by the Idaho Department of Environmental Quality (IDEQ) on a large vacant lot behind the St. Luke's hospital at the intersection of Eagle Road and I-84. This has been identified as one of the busiest intersections in Idaho (IDEQ, 2009). The St. Luke's site EPA Air Quality Site system identifier number is 160010010. The site is part of the Speciation Trends Network (PM composition) and a new gas phase criteria air pollutant monitoring site. The site's coordinates are latitude 43.6008 °N, longitude 116.3484 °W, and an elevation of 790 meters. Approximately 375 m north is interstate highway I-84 that runs in an east-west direction. Eagle Road, a major urban arterial road, is about 500 m to the west. An automated traffic reporter (ATR) was located close to this location on I-84. Light duty vehicle (6 ft to 22.9 ft) traffic counts during the morning rush hour (5-9 am) range between 2,000 and 6,000

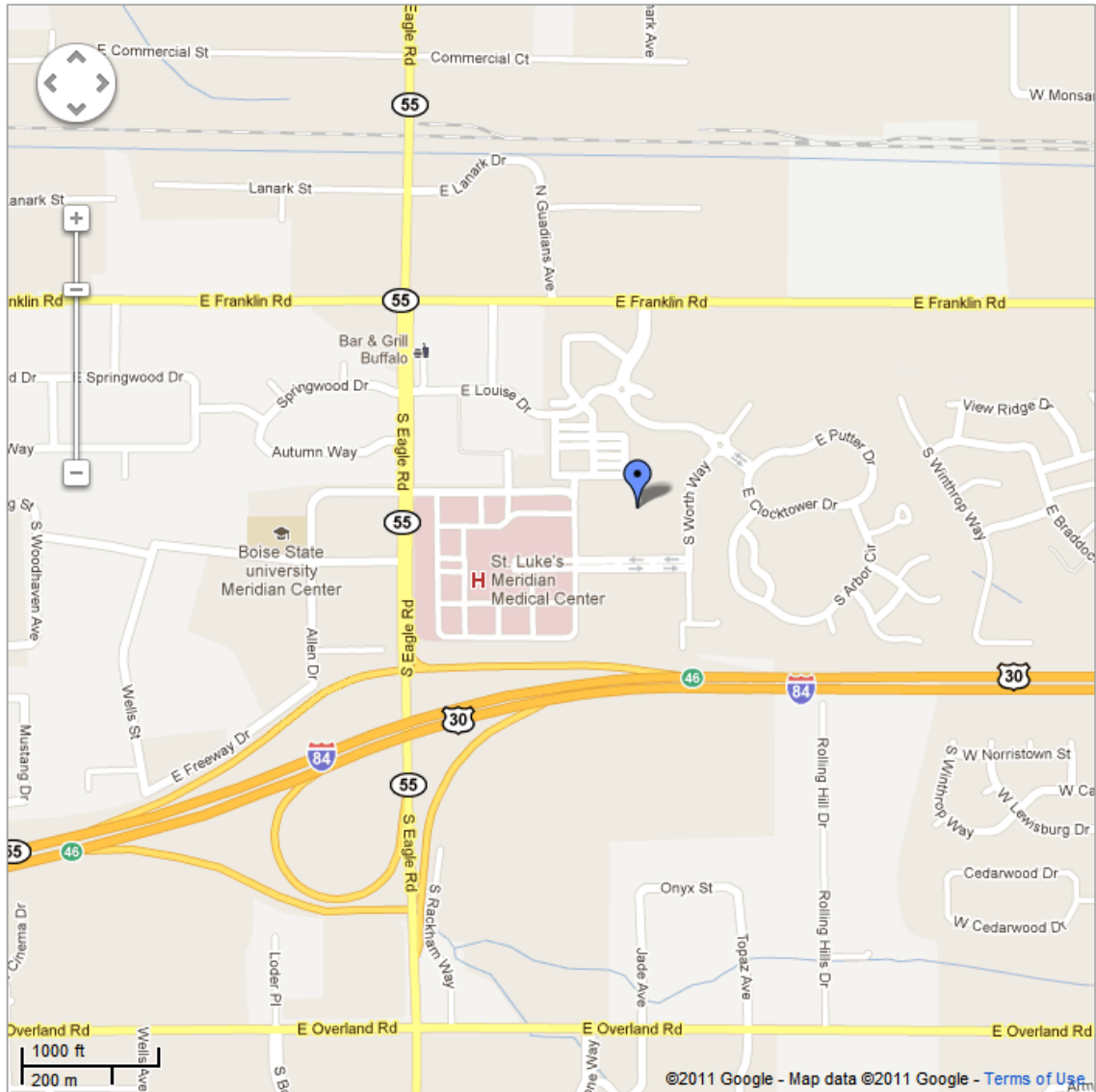


Figure 2.1 Map of the study site in Meridian, Idaho. The blue pointer represents the approximate location of the site, NE to the St. Luke's Hospital. Note the interstate highway (I-84) is on the south of the site. (Source: Google Maps)

vehicles, while those of heavy duty vehicles (> 22.9 feet) range between 400 and 1,000 vehicles per hour. On a daily basis about 100,000 vehicles pass the site along I-84 and about 50,000 vehicles on Eagle Road with vehicle miles travelled (VMT) within 1 km of the site is reported to be 381,400 (IDEQ, 2009). The site was selected by IDEQ to reflect

regional conditions in the valley being situated mid-point between the high population areas of Boise in Ada County to the east and the smaller cities of Nampa and Caldwell in Canyon County to the west. The 2010 US census reports the Ada County population to be 392,365 and Canyon County to be 188,923. The population of Meridian is reported to be 75,092. The monitoring site is surrounded by a mix of light industrial and commercial spaces with limited residential development in the immediate area. The fetches to the west northwest and southeast, the dominant air flow directions, include mixed commercial and residential areas. Air flow through the valley is impacted by drainage flows. The Treasure Valley slopes towards the northwest as part of the general topography of the Snake River Plain depression. The Boise River flows through the city of Boise and the city's emissions get transported in stable drainage flows to the northwest during early morning and evening. To the immediate east of Boise rise the Boise Front Range Mountains to an elevation of over 2,300 m. The valley is frequently impacted by severe wintertime stagnation events.

2.2. Measurements

The Laboratory for Atmospheric Research outfitted a 50 foot portable office trailer rented for the study with a suite of instruments to measure gas phase species (O_3 , CO, CO_2 , NO, NO_2 , NO_y , VOCs), particulate matter composition and size distribution, and surface meteorological measurements. An aerosol LIDAR was also deployed to provide boundary layer heights and aerosol optical depth. This was the first deployment of newly acquired instrumentation for the Mobile Atmospheric Chemistry Lab (MACL).

Meteorological data were acquired with a Vaisala WXT 510 sensor to measure temperature, pressure, humidity, precipitation, and wind speed and wind direction. The



Figure 2.2. Close-up of the measurement trailer equipped with the instruments.

sensor was mounted on a portable meteorological tower at a 10-m height. The tower was located next to the trailer and also provided a support for gas inlets, radiation sensor, and a sonic anemometer. A gas inlet line consisting of ½” PFA tubing ran from the top of the tower (~ 10 m) inside the trailer through a window. A pump pulled air at a nominal flow rate of 30 L/min as measured by an inline flow meter (TSI). The various gas phase instruments sub-sampled from this flow. The exception was the NO_x / NO_y instrument

which has its own dedicated inlet / converter box mounted on the tower at about 6-m height.

NO, NO₂, and NO_y (NO_{xy}) were measured using a two channel chemiluminescence NO detector (Air Quality Design). NO_y was measured on one channel by conversion to NO with a molybdenum oxide catalytic converter. NO₂ and NO were measured on the other channel. NO₂ was converted to NO using a blue light photolytic converter. Calibrations were performed every 23 hours, and zeros were performed every 120 seconds. A NIST traceable NO calibration standard of 5.03 ppmv \pm 1% (Scott-Marrin Inc) was diluted in dry zero air to provide a $25 \pm 5.4\%$ ppbv NO calibration level. Calibration of the NO₂ converter efficiency was performed using gas phase titration of NO to NO₂. A nitric acid perm tube (KinTek Laboratories) was used to calibrate the conversion efficiency of HNO₃ by the molybdenum oxide catalytic converter, which remained steady at between 96 and 98% throughout the campaign. Data were recorded at 1 Hz and 2 minute averages reported.

CO was measured with a VUV fluorescence instrument (Aerolaser GmbH). Standard addition calibrations were performed every 4 hours using a NIST Traceable 10.01 ppmv standard cal gas \pm 1% (Scott- Marrin). The CO instrument response time was on the order of 1 second with detection limits of \sim 10 ppbv for a 1 second integration time. The CO data were recorded at 1 Hz and averaged to 1 minute for archiving. O₃ was measured by a Dasibi 1003 UV absorption analyzer and 1 minute averages reported for data archiving.

Volatile organic compounds (VOCs) were measured with a Proton Transfer Reaction Mass Spectrometer (PTR-MS, Ionicon Analytik GmbH). The instrument was operated at 120 Td drift field condition (2 mbar drift pressure, 60 °C drift temperature, and a drift voltage of 535 volts). Twenty-five organic ions were monitored with dwell times ranging from 1 to 5 seconds resulting in a 1 minute measurement cycle. The PTR-MS was calibrated and zeroed on an automated, regular schedule using a 14 VOC component compressed gas standard with a stated accuracy of $\pm 5\%$ (Scott- Marrin, USA). The standard was diluted to 19.8 ppbv with humid zero air produced by scrubbing ambient air with a Pt catalyst (1% Pt on alumina spheres) at 260 °C. The sensitivity to formaldehyde was determined in the field using an HCHO permeation device (Kintek Laboratories) diluted with humid zero air to 40 ppbv. The PTR-MS displays a humidity dependent sensitivity to HCHO (Jobson and McCoskey, 2010). The humidity dependence was determined in the lab prior to the field experiment and verified with post field experiment calibrations. The ion $m/z=39$ corresponding to the proton bound cluster $H+(H_2O)_2$ is linearly proportional to ambient water vapor and allows for HCHO sensitivity to be accurately determined.

CHAPTER 3: RESULTS AND DISCUSSION

3.1. Data Description

Continuous measurements of formaldehyde, acetaldehyde and benzene along with other VOCs and trace gases were made from December 2008 to January 2009. During this time period, 15 VOCs were measured using the PTR-MS. These measurements were averaged over 5 minutes to improve signal-to-noise ratios for some species. Table 3.1 shows a summary of the statistics of these measured 15 VOCs. It is noted the average mixing ratios over this time period for formaldehyde, acetaldehyde and benzene were

Table 3.1. Summary of statistics of measured volatile organic compounds (VOCs) and carbon monoxide and nitrogen oxides (5 - minute averages)

Species	m/z	Max. (ppbv)	Min. (ppbv)	Median (ppbv)	Mean (ppbv)
Acetaldehyde	45	11.8	BDL*	0.533	0.735
Acetone	59	18.2	0.305	1.36	1.61
Acetonitrile	42	1.24	0.009	0.071	0.078
Benzene	79	3.53	0.024	0.185	0.273
C2-Benzenes	107	5.02	BDL	0.202	0.346
C3-Benzenes	121	4.41	BDL	0.101	0.171
C4-Benzenes	135	0.281	BDL	0.008	0.012
Formaldehyde	31	9.58	BDL	1.06	1.30
Methanol	33	67.8	BDL	2.31	3.50
Naphthalene	129	0.398	BDL	0.024	0.033
Pentenes	71	21.2	BDL	0.168	0.276
Phenol	97	0.800	BDL	0.029	0.050
Toluene	93	5.55	0.016	0.235	0.411
unkown#1	69	2.36	BDL	0.091	0.151
unkown#2	137	2.82	BDL	0.071	0.123
Carbon monoxide		1456.16	78.00	168.55	221.93
Nitrogen oxides		421.02	0.48	13.09	24.70

*BDL = Below detection limit

respectively 1.30, 0.74 and 0.27 ppbv. For formaldehyde and acetaldehyde, these mixing ratios are consistent with the mixing ratios found in big cities during winter (Anderson et al., 1996; Ho et al., 2002; Possanzini et al., 1996; Tago et al., 2005).

Figures 3.1.1 – 3.1.5 illustrate the entire time series of the temperature and humidity, mixing ratios of 15 VOCs, Carbon Monoxide (CO) and Nitrogen Oxides (NO_x).

Although it is hardly visible in these figures, the ups and downs in the mixing ratios in the VOCs coincide with those of CO. During the two months of the study period, there were some days with significant low levels of VOCs and trace gases. During this time, the temperature and relative humidity also remained almost constant without any major fluctuations. This time (January 13 – 20, 2009) was known to be a stagnation period when meteorology strongly influenced the dispersion of the pollutants. Wind rose plots for this period (Figure 3.3) also supports the theory of change in wind direction.

However, the actual reason behind the low levels of trace gases remains a mystery.

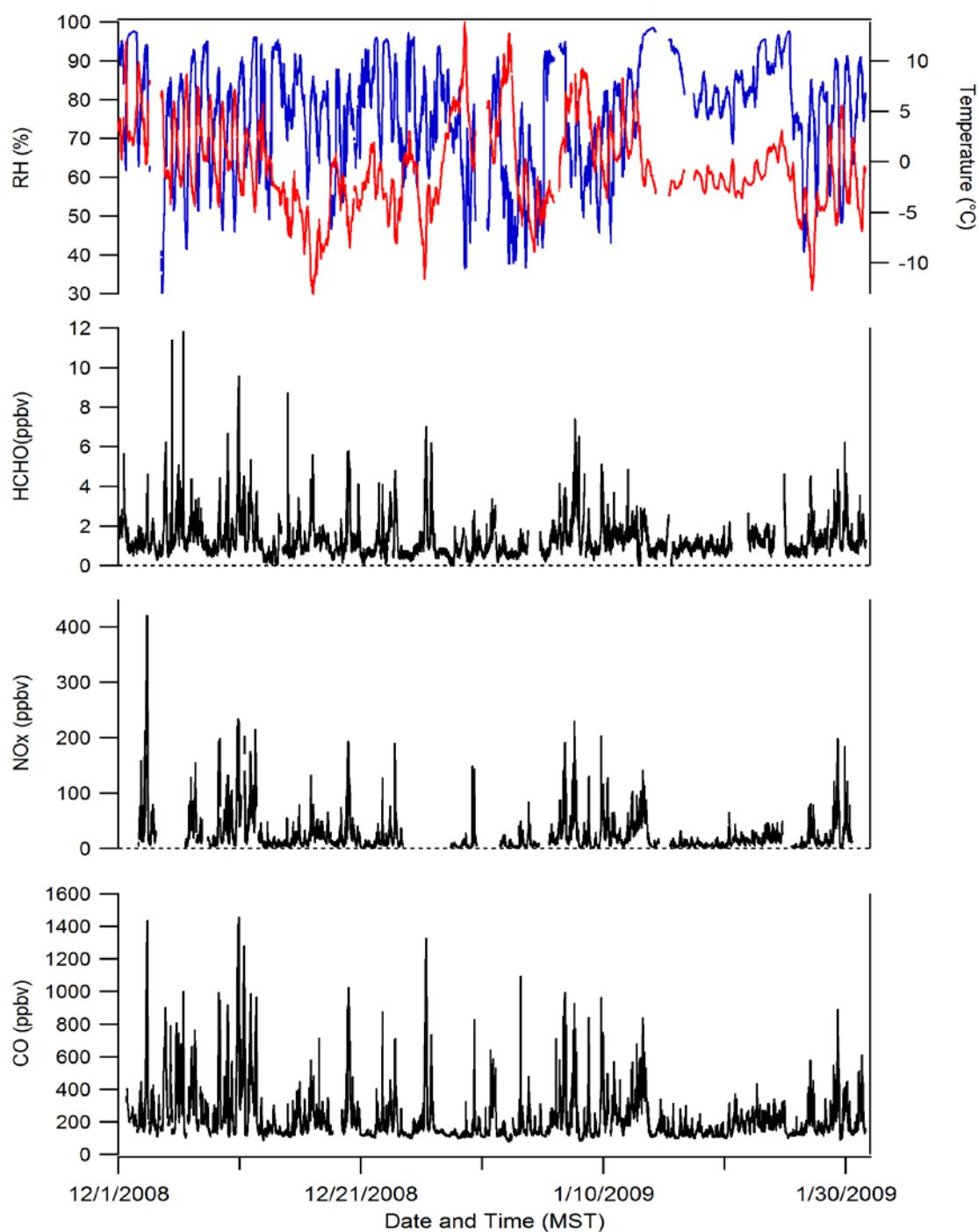


Figure 3.1.1 Plots of 5 - minute averaged data of temperature, relative humidity, formaldehyde (HCHO), nitrogen oxides (NO_x) and carbon monoxide (CO) mixing ratios in Meridian, Idaho, from 1 December, 2008 to 31 January, 2009.

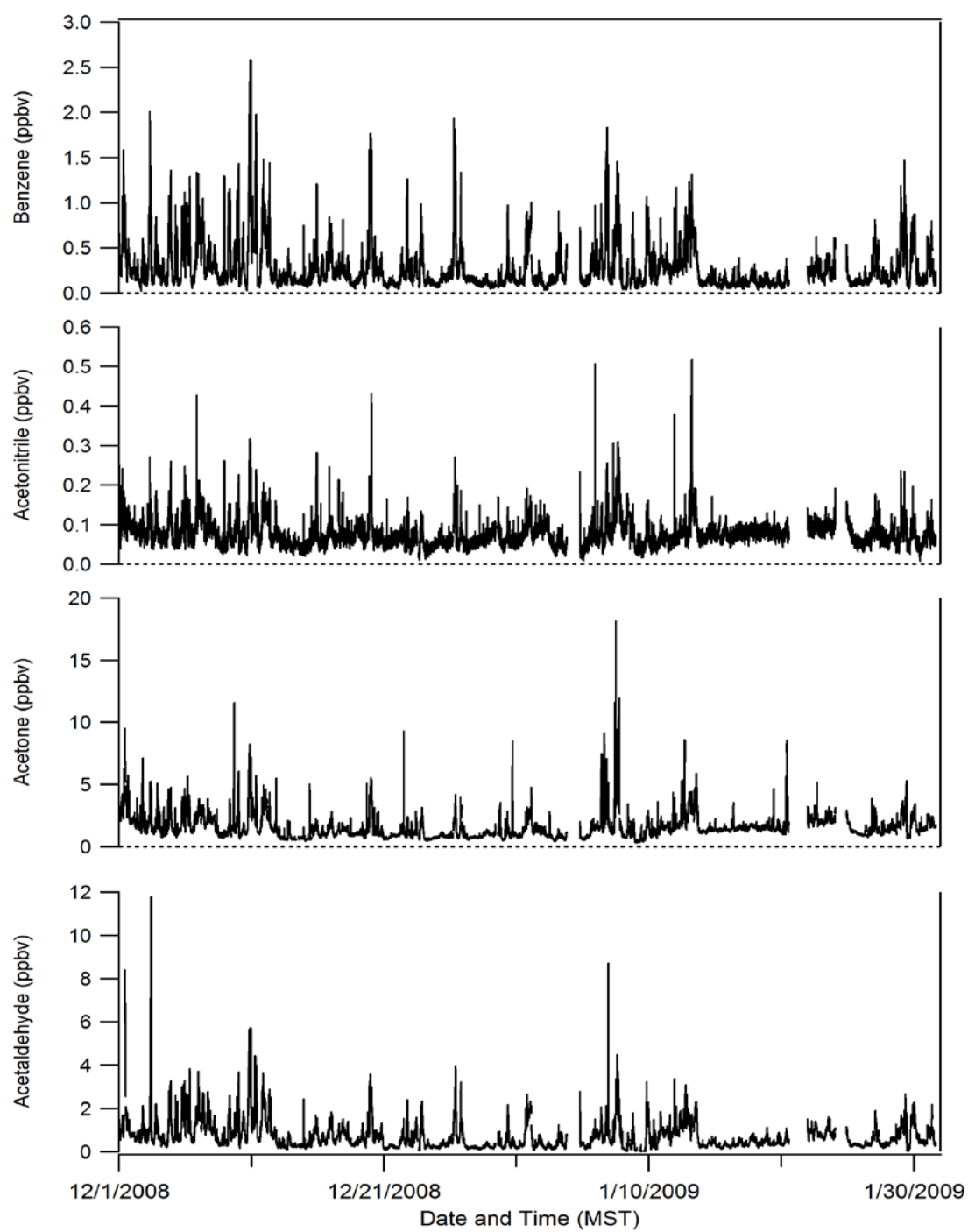


Figure 3.1.2 Plots of 5 - minute averaged data of acetaldehyde, acetone, acetonitrile and benzene mixing ratios in Meridian, Idaho, from 1 December, 2008 to 31 January, 2009.

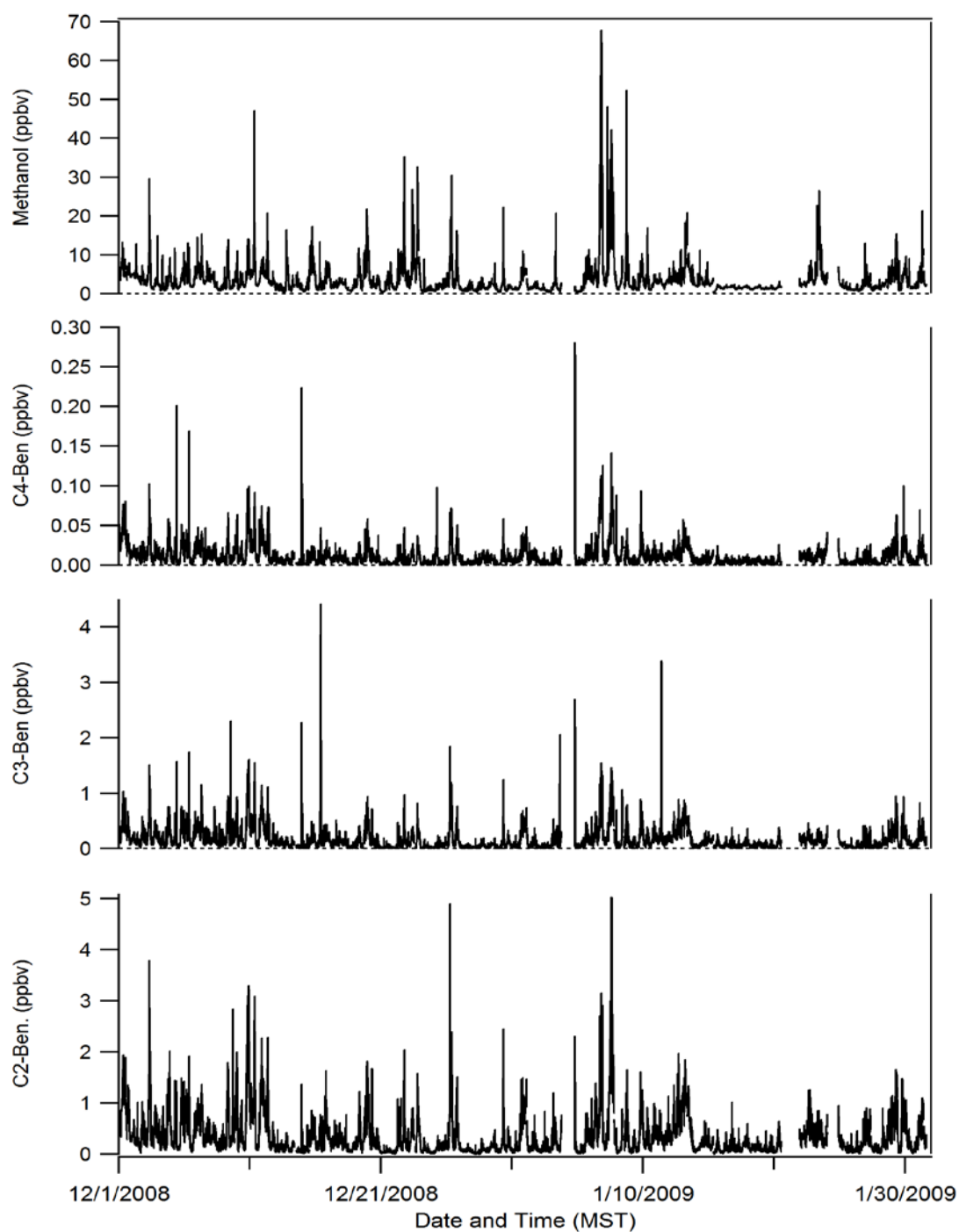


Figure 3.1.3 Plots of 5 - minute averaged data of C2-benzene, C3-benzene, C3-benzene and methanol mixing ratios in Meridian, Idaho, from 1 December, 2008 to 31 January, 2009.

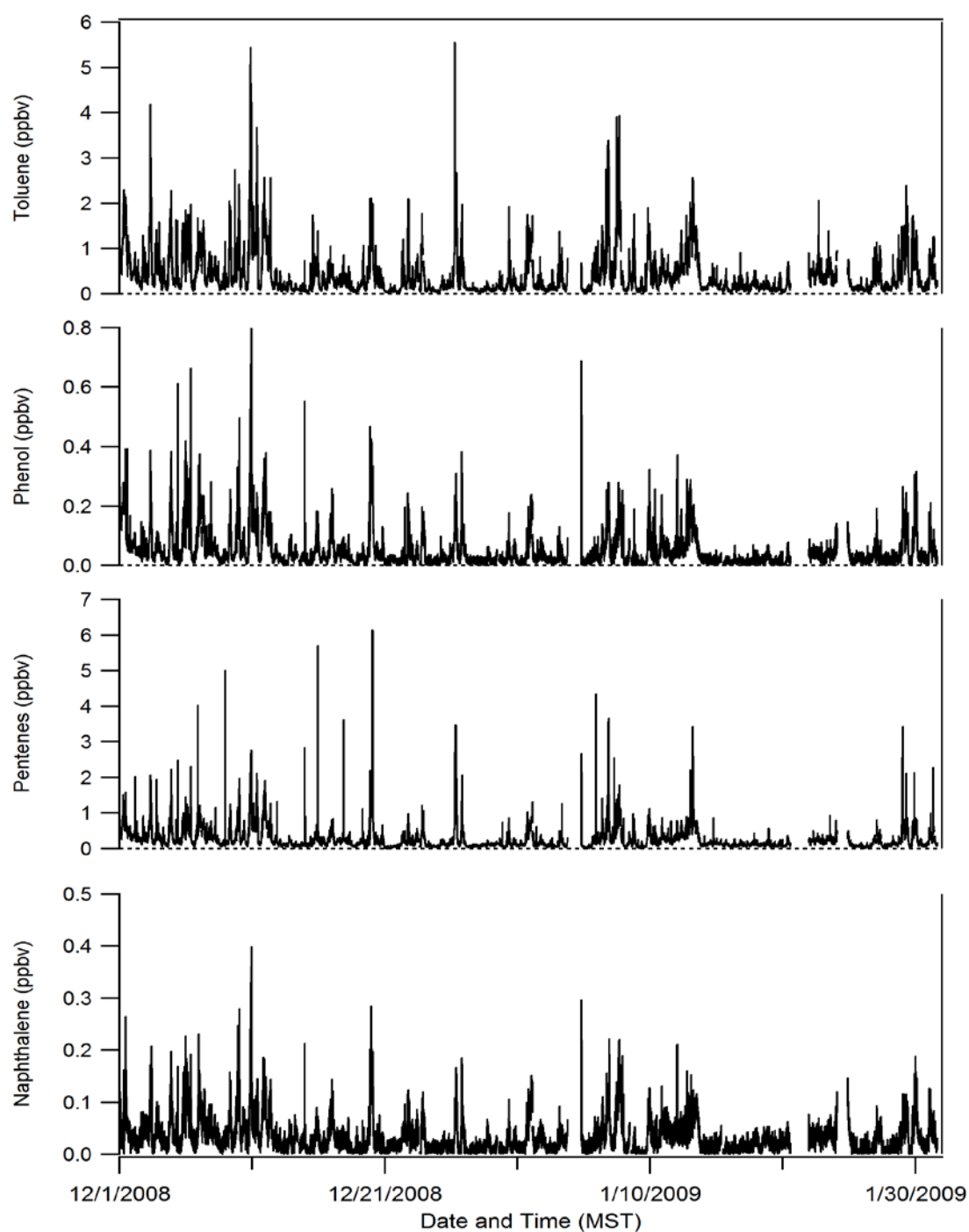


Figure 3.1.4 Plots of 5 - minute averaged data of naphthalene, pentenes, phenol and toluene mixing ratios in Meridian, Idaho, from 1 December, 2008 to 31 January, 2009.

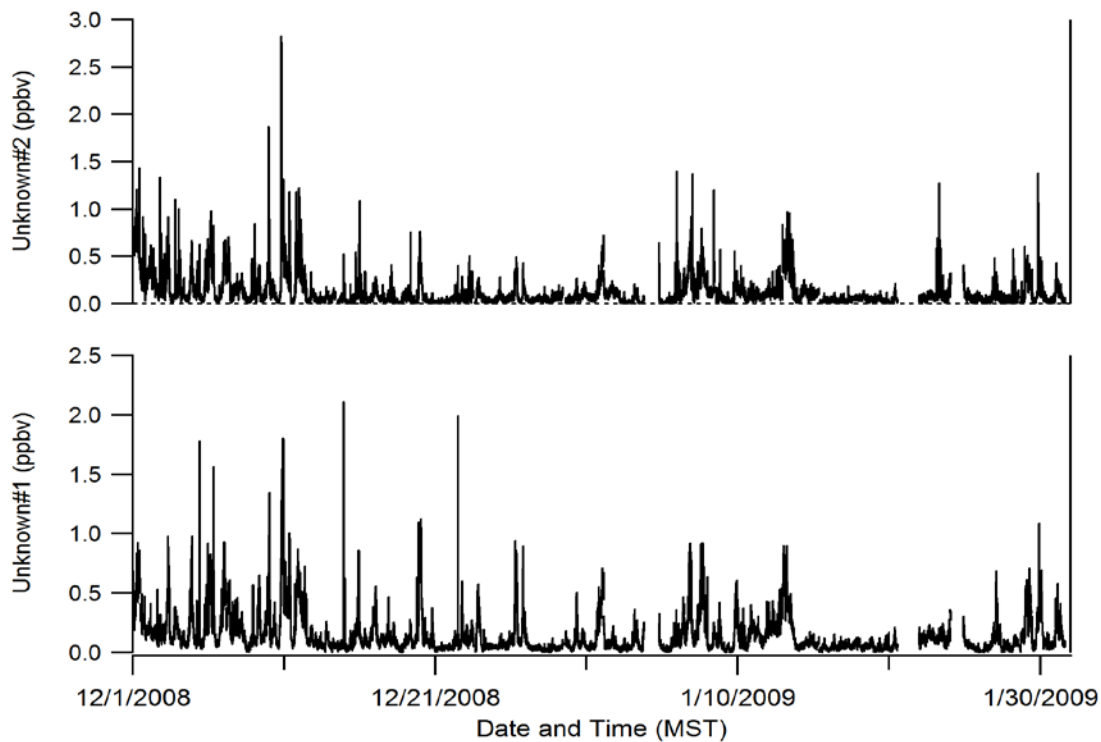


Figure 3.1.5 Plots of 5 - minute averaged data of unknown #1 (m69) and unknown #2 (m137) mixing ratios in Meridian, Idaho, from 1 December, 2008 to 31 January, 2009.

A diurnal representation of the air toxics measurements are shown in Figure 3.2. In this figure, the 5 minute averaged air toxics (formaldehyde, acetaldehyde and benzene) and CO mixing ratios are averaged over half hour periods and plotted against the time of day. The grey shaded area is the weekday vehicle-miles travelled (VMT). As we can see, the mixing ratios of CO and other VOCs, all follow the same diurnal pattern with coinciding peaks. The number of on-road vehicles significantly increased during the morning and evening rush hour period. At the same time, the mixing ratios of CO and VOCs also increased rapidly forming two distinct peaks during these time periods.

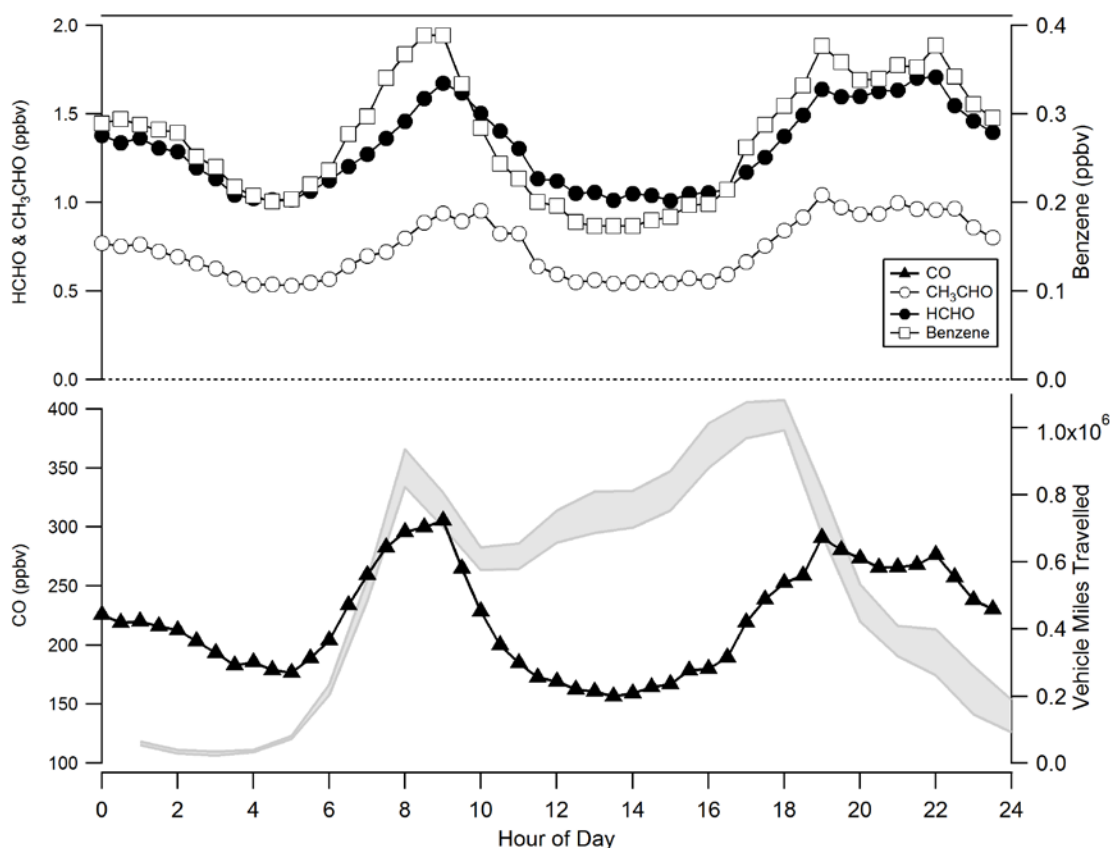


Figure 3.2. Diel profiles of formaldehyde, acetaldehyde, benzene and CO mixing ratio as half hour averages. Grey shading indicates weekday VMT

For the entire campaign, the wind flow to the measurement site was mostly from S and SE direction. Figure 3.3 shows the wind rose plot for the entire campaign period, subdivided into day (defined as 05:00 – 17:00 h) and night (17:00 - 5:00 h). Here, the figure shows 44 – 49.5% of the wind comes from the S and SE directions, both night and days. Another significant wind direction is from W and WNW. Almost 25 – 27% wind was from this particular direction. During stagnation period, the wind direction changed to ESE (17%) during day. During night, wind speed was very low and was not from any particular direction.

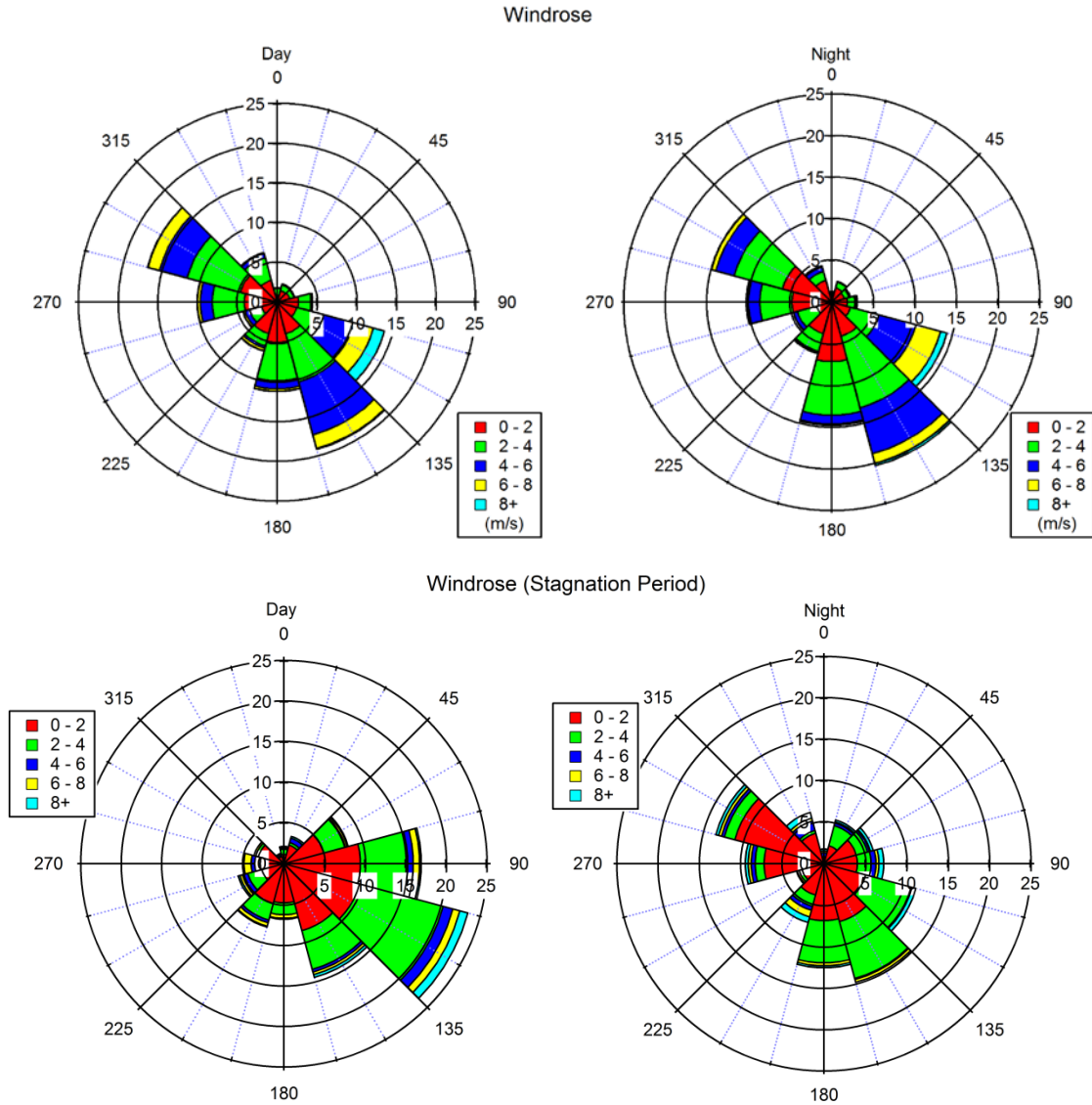


Figure 3.3 Wind rose plots showing wind speed and fractional occurrence of wind flow direction in 30° increment bins for day and night during the entire campaign and the stagnation period.

Figure 3.4.1 – 3.4.2 are plots of 5 minute averaged mixing ratios of CO and the air toxics as a function of wind direction. All the VOCs and CO mixing ratios were higher during night. All the species had higher mixing ratios in S-SE wind. Due to the site's location,

this finding is quite reasonable, as one of the interstate highways is on the south side of the site as mentioned before (Refer to § 2.1.).

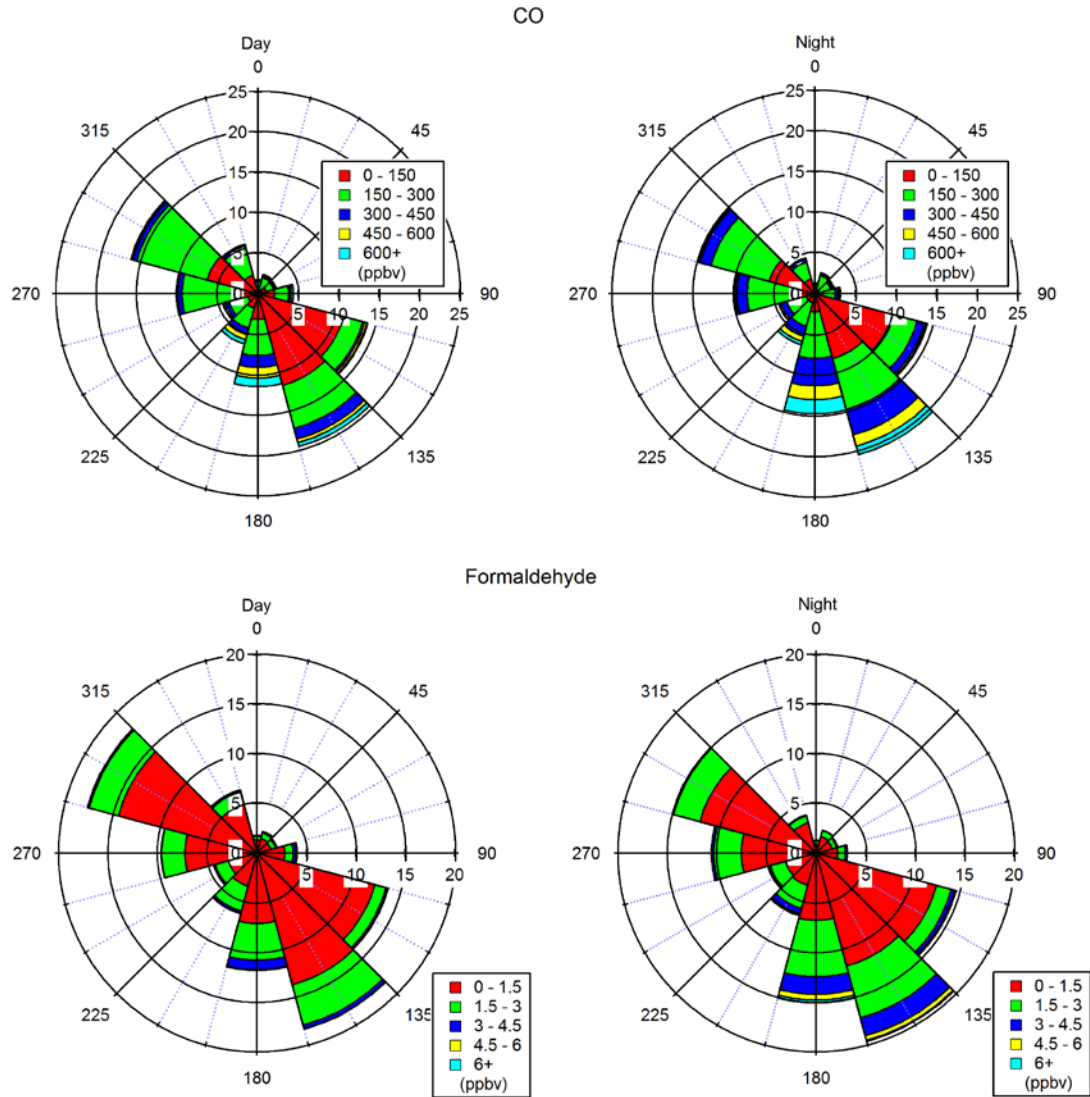


Figure 3.4.1 Plots of 5 minute averaged mixing ratios of CO and formaldehyde as a function of wind direction in 30° increment bins. Wind from S and SE direction contributes to the highest mixing ratios.

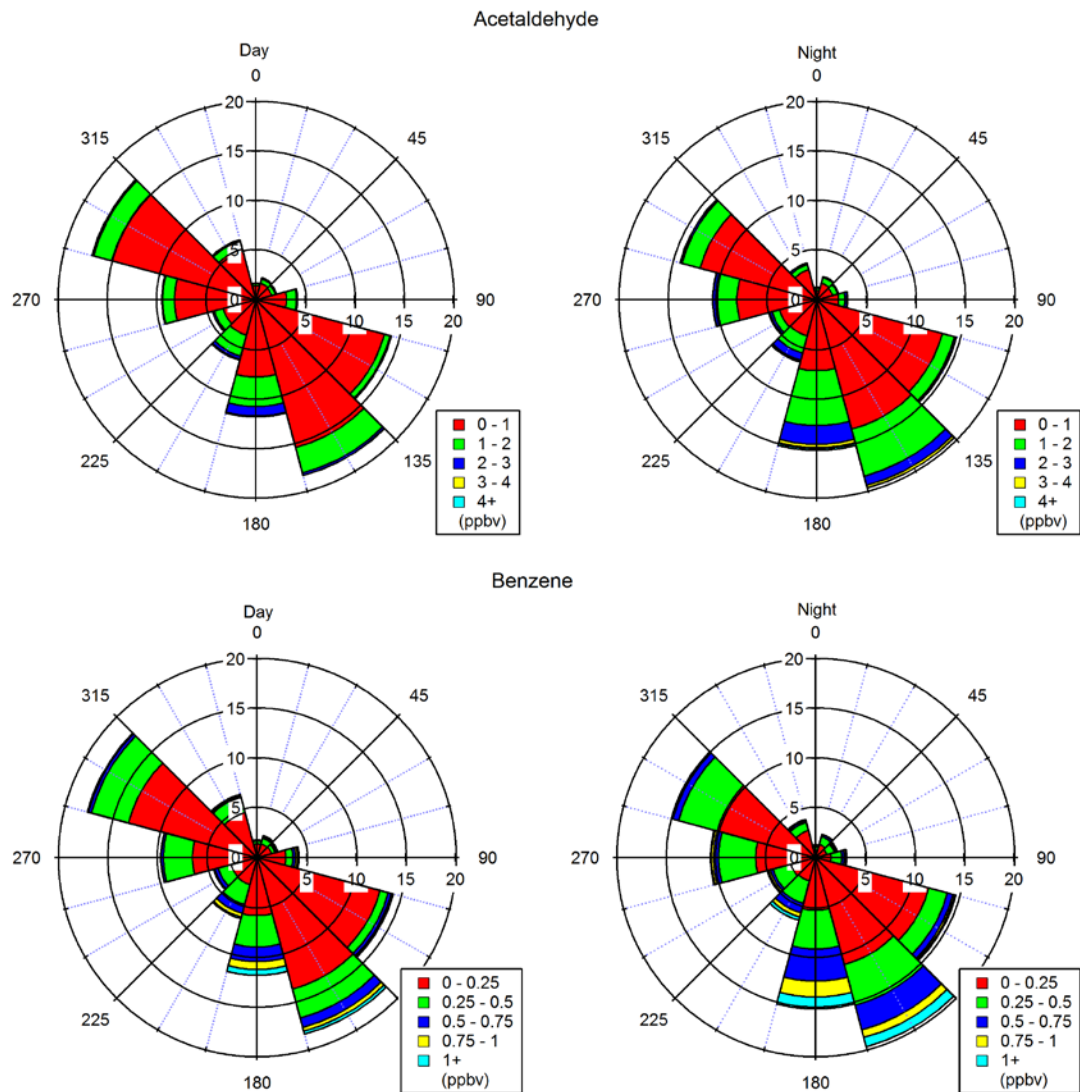


Figure 3.4.2 Plots of 5 minute averaged mixing ratios of Acetaldehyde and Benzene as a function of wind direction in 30° increment bins. Wind from S and SE direction contributes to the highest mixing ratios.

3.2. Morning Rush hour Analysis

To analyze HCHO and its relationship to vehicle emissions, carbon monoxide (CO) was chosen as the main vehicle emission tracer similar to previous studies (Anderson et al., 1996; Friedfeld et al., 2002; Possanzini et al., 1996; Rappengluck et al., 2010). Carbon monoxide can act as an excellent tracer because the main source of CO is incomplete combustion of fossil fuel e.g. from automobiles, etc. A direct connection of atmospheric CO mixing ratio and vehicle exhaust is found from the analysis of vehicle-miles travelled (VMT) plots. Vehicle-miles travelled (VMT) is the total number of miles driven by all vehicles within a given time period and geographic area. It is a useful planning tool used by regional transportation and environmental agencies. A daily VMT plot depicts increase of vehicles on the road during a specific time of the day. A typical day has two significant spikes in VMT, shown in Figure 3.2, the morning rush hour period and the evening rush hour period. Figure 3.2 also shows how atmospheric CO mixing ratio corresponds to VMT. The plot shows CO mixing ratios follow a similar pattern as VMT with two significant increases during the morning and evening rush hour. As discussed before the mixing ratios of the air toxics also follow this same pattern. This suggests that vehicle exhaust is one of the main sources of atmospheric CO and air toxics. So this gas can be used as a valid tracer for vehicle exhaust.

Another important point to remember when discussing tracers, all vehicles does not emit CO equally. The combustion processes of different fueled vehicles are different. For example- the exhaust from a spark ignition (SI) vehicle will contain more CO than a

compression ignition (CI) vehicle. In an SI engine, the combustion process goes through at a lower temperature than a CI engine. This lower temperature can burn the fuel (usually gasoline) inefficiently causing more CO in the exhaust. On the other hand, a very high temperature in the combustion chamber of a CI engine results a little CO in the exhaust. However, the high temperature can cause more nitrogen oxides ($\text{NO}_x = \text{NO} + \text{NO}_2$) than an SI engine. So CO might not be a useful tracer for CI or diesel engines. In this case, NO_x could be a more suitable choice.

Different type of vehicle can show different patterned VMT plot. Figure 3.5 and 3.6 show VMT plots for gasoline and diesel fueled vehicles respectively. From the two plots it is evident that the amount of gasoline fueled vehicles outnumber their diesel counterparts by two orders of magnitude. Figure 3.5 shows that the VMT by gasoline fueled vehicles have a pattern consisting two distinct rush hour peak. But the VMT plot (Figure 3.6) for diesel fueled vehicles, is rather different. They do increase significantly during the morning rush hour period, but remain high throughout the day and decreases only after 5:00 PM. This implies the emissions from these vehicles also remain consistently high.

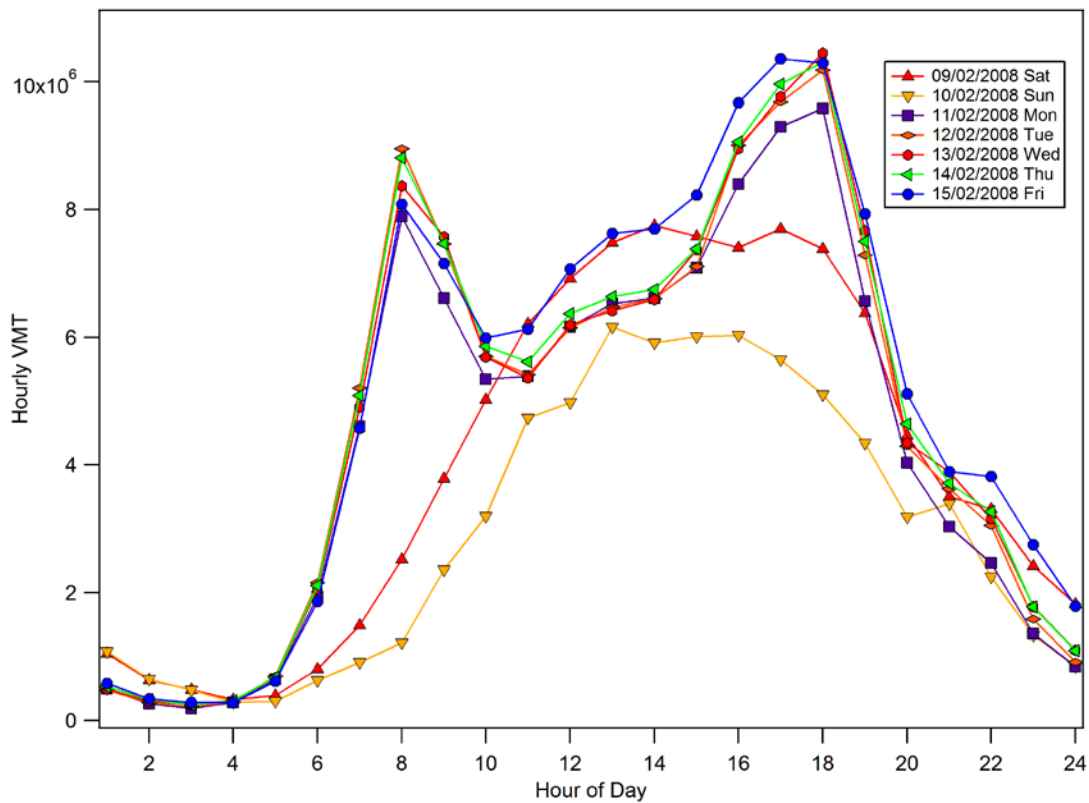


Figure 3.5 Hourly vehicle miles travelled (VMT) of gasoline vehicles over a week
(Source: IDEQ)

A fuel specific tracer, either for gasoline or diesel, could determine which VOCs are emitted more from which types of fuel. One way to do this is to associate CO as a tracer for gasoline fueled or SI vehicles. For diesel (or CI engines) one can use NO_x as a tracer. The preliminary hypothesis was benzene is emitted more from gasoline fueled vehicles, whereas the aldehydes are emitted more from diesel vehicles.

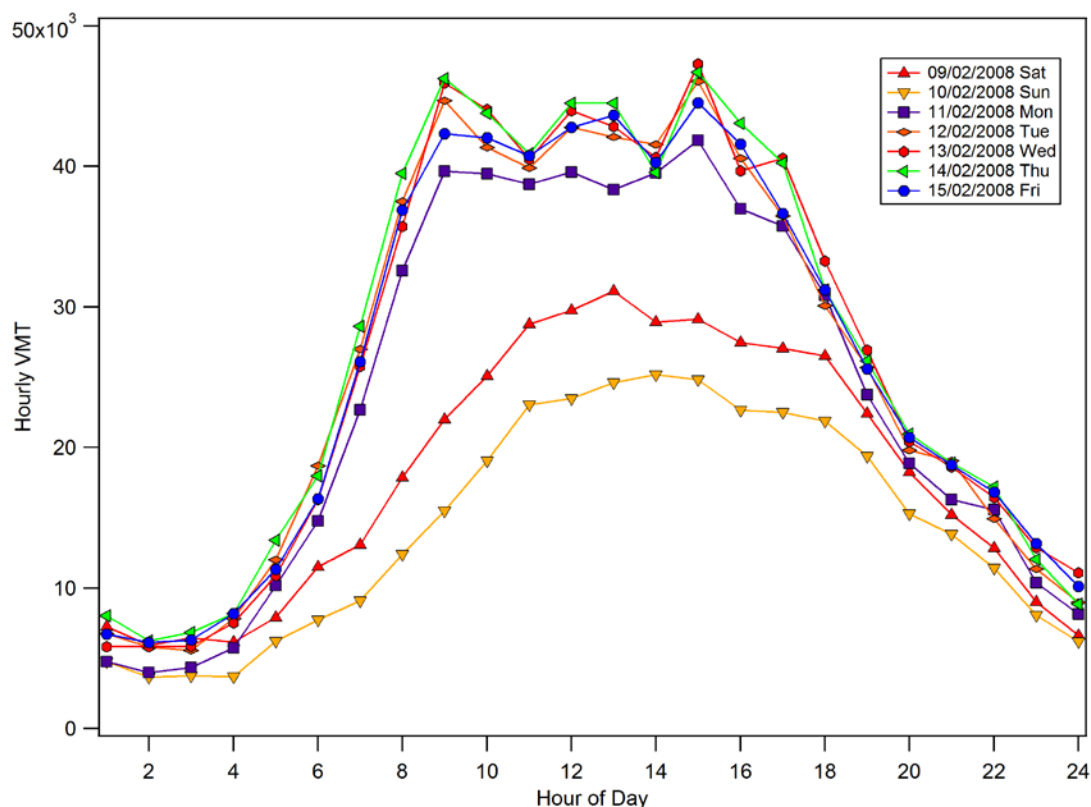


Figure 3.6 Hourly vehicle miles travelled (VMT) of diesel vehicles over a week (Source: IDEQ)

The diel profiles of the atmospheric VOCs (Figure 3.2) clearly suggest that they have similar diurnal patterns of gasoline vehicles VMT. So our primary interest is to examine vehicle exhaust originated from gasoline and use CO as a tracer. The VOCs were also analyzed, using NO_x as a tracer to further examine our hypothesis.

3.3. Selection criteria for morning rush hour periods

Formaldehyde and acetaldehyde can be generated photochemically in the atmosphere.

The absence of sunlight can assure there is no secondary formation of these VOCs in the atmosphere. As the primary goal was to assess VOC emissions from vehicles, a time of

the day was selected when there was almost no sunlight to limit the possibility of HCHO and CH₃CHO formation from other VOCs emitted in the exhaust.

During the two winter months, the average sunrise in Meridian was after 8:00 AM. So the morning rush hour period, defined as 5:00 AM – 8:00 AM, was chosen to analyze VOCs and their relation to vehicle emissions. Also, the limited solar radiation during this period contributed to limited turbulence and convective mixing in the atmosphere; so the atmospheric mixing layer height was low and was consistent over this period.

We chose days with clear signature rush hour profiles of CO and VOCs, as illustrated in Figure 3.2. The signature rush hour profile was defined as those periods where CO mixing ratios increased by 200 ppbv at least. Days with no significant rush hour period or unusual rush hour profiles, e.g. on weekends and holidays, were excluded from the analysis. After checking these factors, five days (Table-3.2) were chosen from the 2 months of data.

3.4. Air Toxics Correlation Analysis for Rush Hour periods

3.4.1. Correlation with CO

3.4.1.1. Formaldehyde

The HCHO-CO relationships for the chosen five days are shown in Figure 3.7. The regression parameters are also tabulated in Table 3.2. Among the five days we have chosen for the analysis, the best correlation was seen on January 29, 2009 ($R^2 = 0.845$).

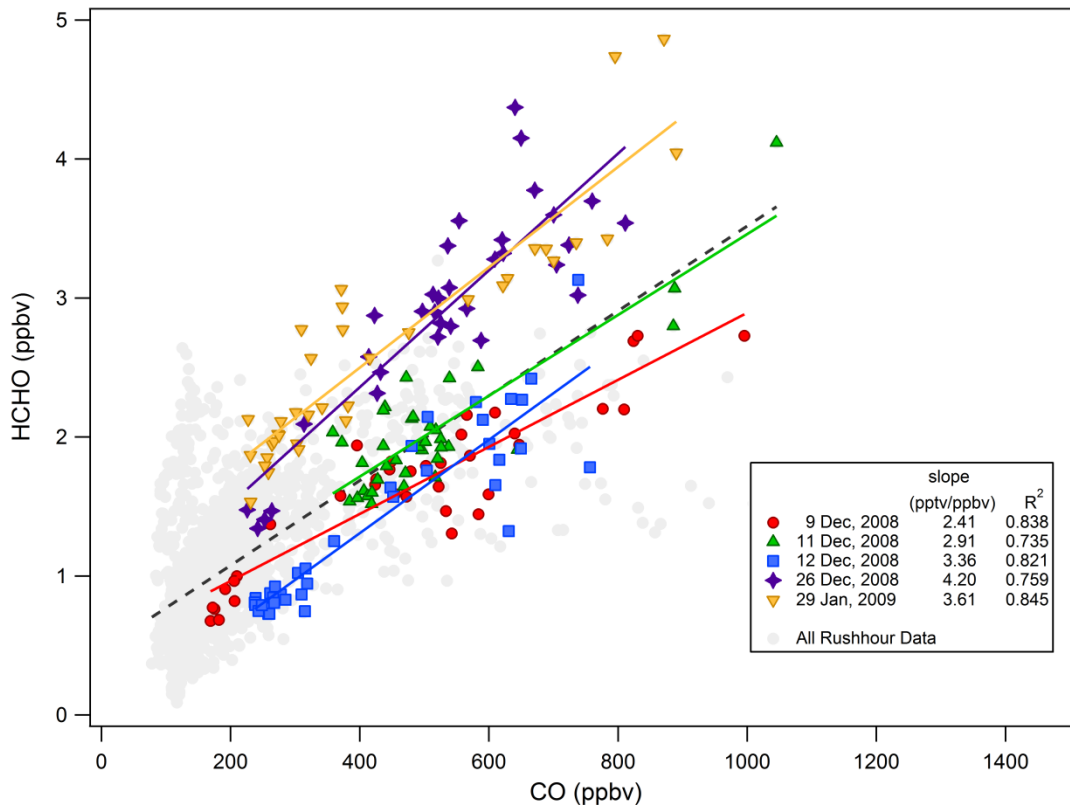


Figure 3.7 Relationships between HCHO and CO mixing ratios in Meridian, Idaho. Gray points include all morning rush hour data during the 2 month period. The color coded data points represent each day's morning rush hour period. The solid colored lines indicate the linear, least-squares fit to the respective color-coded data. The dotted black line indicates the linear, least-squares fit to all the morning rush hour data

The slope was highest on December 26, 2008 (4.2 pptv HCHO/ ppbv CO) but the regression parameter was much lower ($R^2 = 0.759$). For the five chosen days the average HCHO-CO slope was 3.30 ± 0.29 pptv HCHO/ppbv CO which is slightly higher than the slope (3.0 pptv HCHO/ ppbv CO) when we include all the rush hour data for 60 days. All of these ratios are consistent with the results from previous studies (Anderson et al., 1996; Possanzini et al., 1996; Rappengluck et al., 2010).

Table 3.2. Parameters for linear regressions of HCHO vs. CO for the selected morning rush hour periods. The average temperature and relative humidity are included

Month	Date	Day	Temp. (°C)	RH (%)	Slope (pptv/ppbv)		Intercept (ppbv)		R ²
December	9	Tuesday	-3.82	85.6	2.41	± 0.18	0.48	± 0.10	0.838
	11	Thursday	-2.65	86.7	2.91	± 0.30	0.55	± 0.16	0.735
	12	Friday	-4.27	95.8	3.36	± 0.27	-0.03	± 0.12	0.821
	26	Friday	-10.58	86.3	4.20	± 0.43	0.68	± 0.24	0.759
January	29	Thursday	-5.60	88.7	3.61	± 0.27	1.05	± 0.13	0.845
average					3.30	± 0.29	0.55	± 0.15	

Using these linear regression parameters from Table 3.2 an equation (Eq. 1) was derived which could be used to predict HCHO mixing ratios from CO emission from vehicle sources, which could be obtained in national emission inventories (NEI).

$$[HCHO_{predicted}] \text{ ppbv} = 3.30 \times [CO] \text{ ppbv}/1000 + 0.55 \dots \dots \dots (1)$$

Using this equation, we calculated the amount of HCHO from the CO ambient data.

Figure 3.8 illustrates the agreement between the observed and calculated HCHO for a random three day period in December. In general there was reasonable agreement between predicted HCHO based on rush hour correlation with CO and ambient levels

observed throughout the study period.

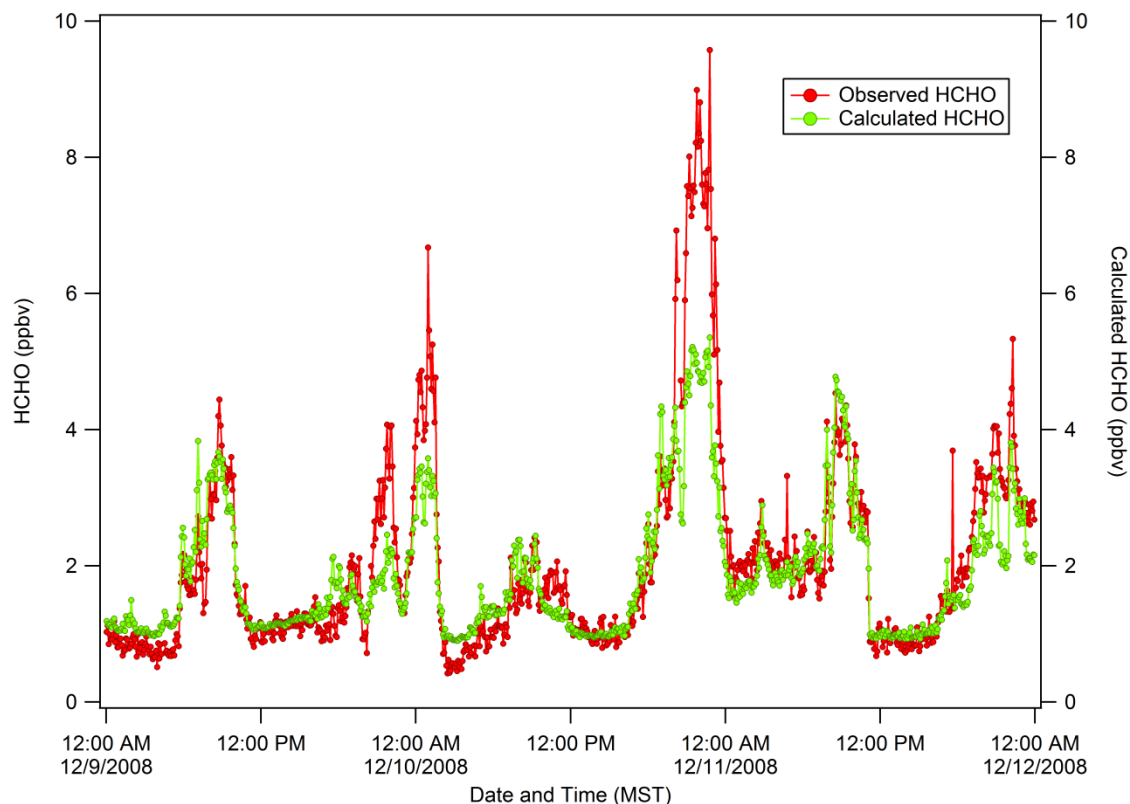


Figure 3.8 Measured and calculated (using HCHO/CO ratio) HCHO mixing ratios. The green points are the calculated HCHO from CO ambient data

To quantify how well the predicted formaldehyde mixing ratios correlated with the observations, we calculated the ratio between these values. Then the ratio was plotted as a log histogram. In the ideal case, the ratio should be equal to 1. Figure 3.9 shows the histograms of the ratios. The ratios are subdivided into day and night time as defined before. As we can see, for both times, the ratios are almost normally distributed. For day and night, the average values were 0.93 ± 0.36 and 0.98 ± 0.39 respectively. This suggests that our predicted mixing ratio are within 38% error for 64% of the time.

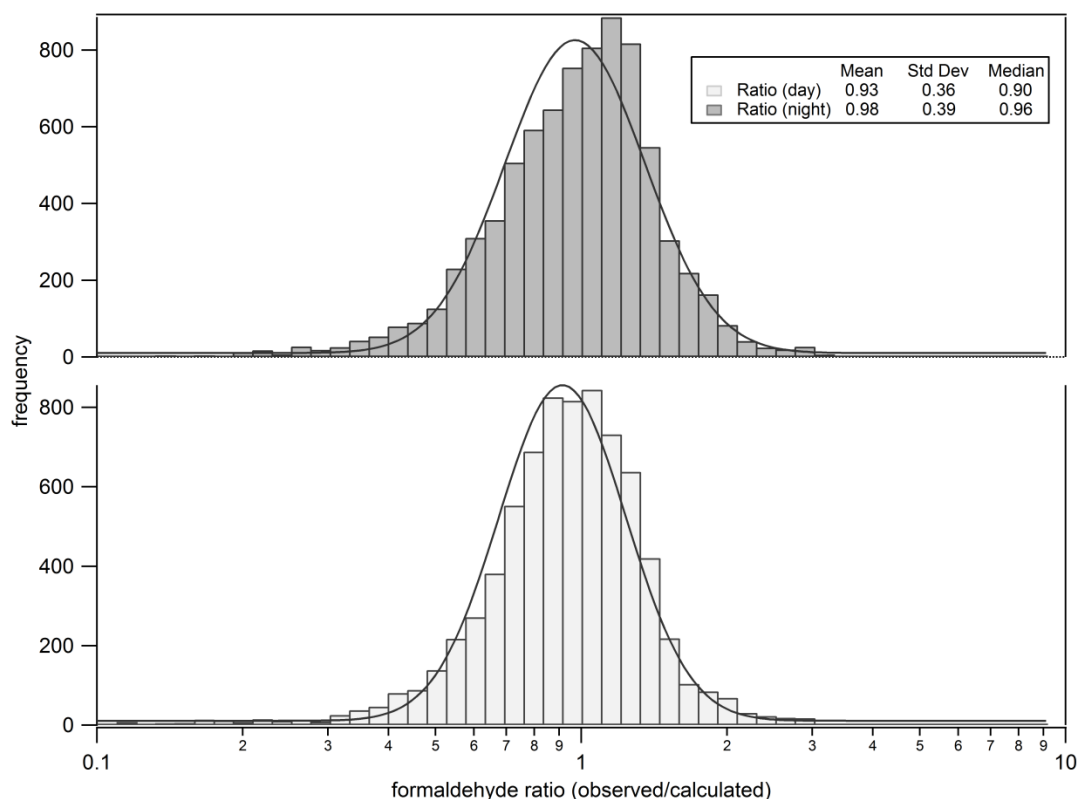


Figure 3.9 Histogram plots of the ratio of observed and predicted (using HCHO/CO ratio) formaldehyde mixing ratios.

Atmospheric formaldehyde and acetaldehyde often come from similar sources. The ratio between these two can depict what type of source is dominant. We found that the average formaldehyde/acetaldehyde (FA/AA) ratio was 1.50 (Table 3.4). This confirms that the carbonyl emissions in this study were mainly from vehicles. Previous studies show, FA/AA ratio varies from 1-2 in urban setting, dominated by vehicle emissions; it is much higher (~10) where there is biogenic emissions (Anderson et al., 1996; Ho et al., 2002; Possanzini et al., 1996; Viskari et al., 2000). Their relationship is shown in Figure 3.10.

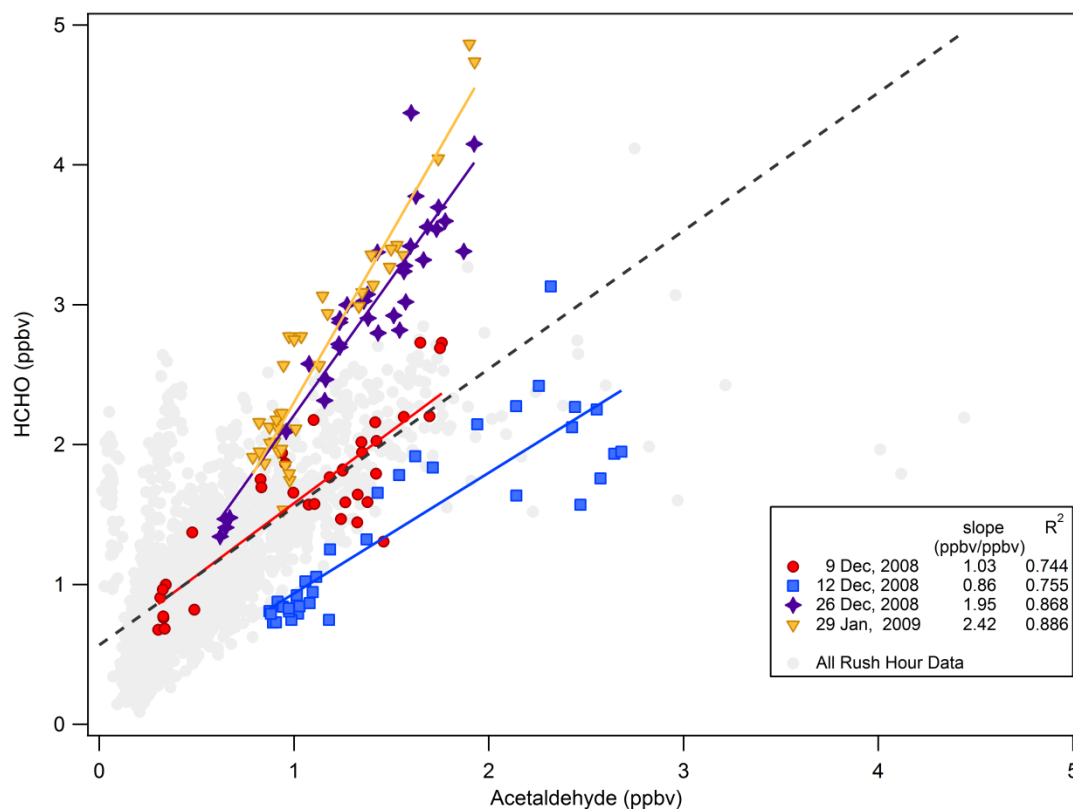


Figure 3.10. Relationships between formaldehyde and acetaldehyde mixing ratios

Table 3.3. Parameters for linear regressions of HCHO vs. Acetaldehyde for the selected morning rush hour periods

Month	Date	Day	Slope (ppbv/ppbv)		Intercept (ppbv)		R ²
December	9	Tuesday	1.03	± 0.10	0.55	± 0.12	0.744
	11	Thursday	--		--		--
	12	Friday	0.86	± 0.08	0.07	± 0.14	0.755
	26	Friday	1.95	± 0.14	0.26	± 0.19	0.868
January	29	Thursday	2.42	± 0.15	-0.12	± 0.18	0.886
average			1.50	± 0.11	0.21	± 0.14	

3.4.1.2. Acetaldehyde

The acetaldehyde (CH_3CHO)-CO relationships are shown in Figure 3.11. The regression parameters are also tabulated in Table 3.5. The highest slope was seen on December 12, 2008, 2.84 ± 0.42 pptv CH_3CHO /ppbv CO. For the five chosen days the average slope was 2.11 ± 0.20 pptv CH_3CHO /ppbv CO. This slope is a little lower than that of HCHO/CO , which is expected according to some previous studies (Anderson et al., 1996; Possanzini et al., 1996), as CH_3CHO is less abundant in the atmosphere than HCHO .

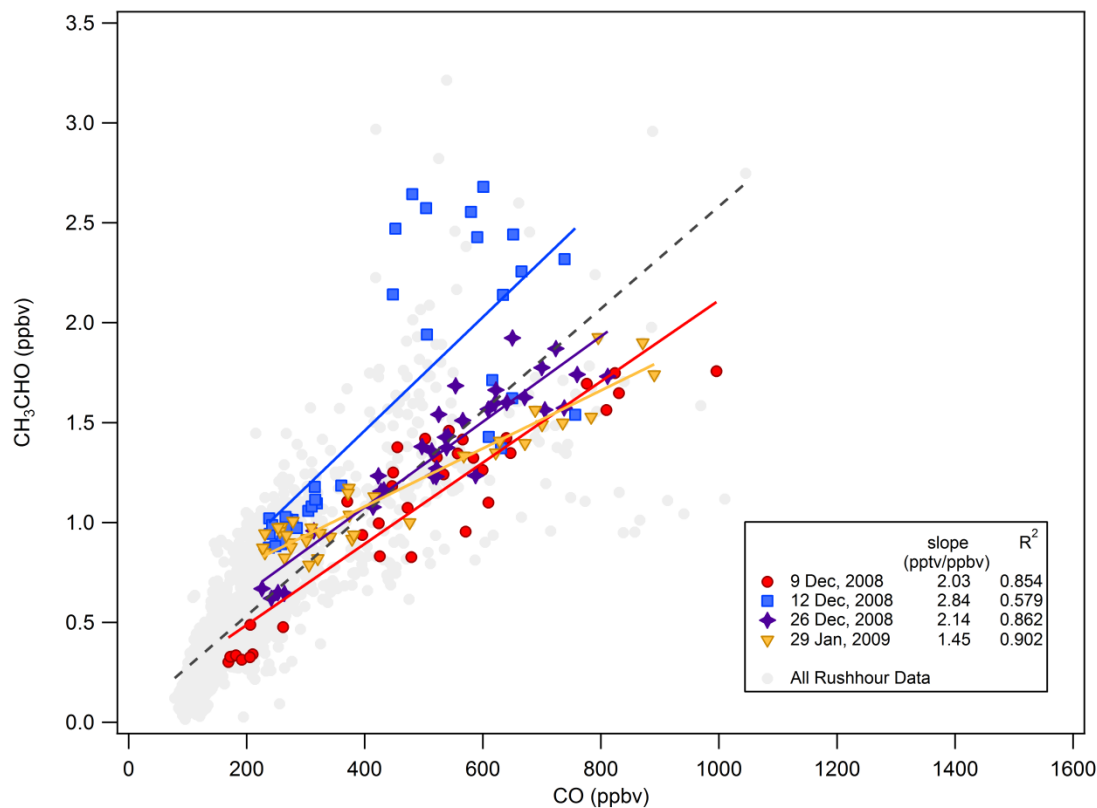


Figure 3.11. Relationships between acetaldehyde and carbon monoxide mixing ratios in Meridian, Idaho.

The linear regression parameters were then used (Eq. 2) to predict CH₃CHO emission from CO emission from vehicle sources, like before.

$$[CH_3CHO_{predicted}] \text{ ppbv} = 2.11 \times [CO] \text{ ppbv}/1000 + 0.28 \dots \dots \dots (2)$$

Figure 3.12 shows the agreement between the observed and calculated CH₃CHO for the same three day period depicted in Figure 3.8.

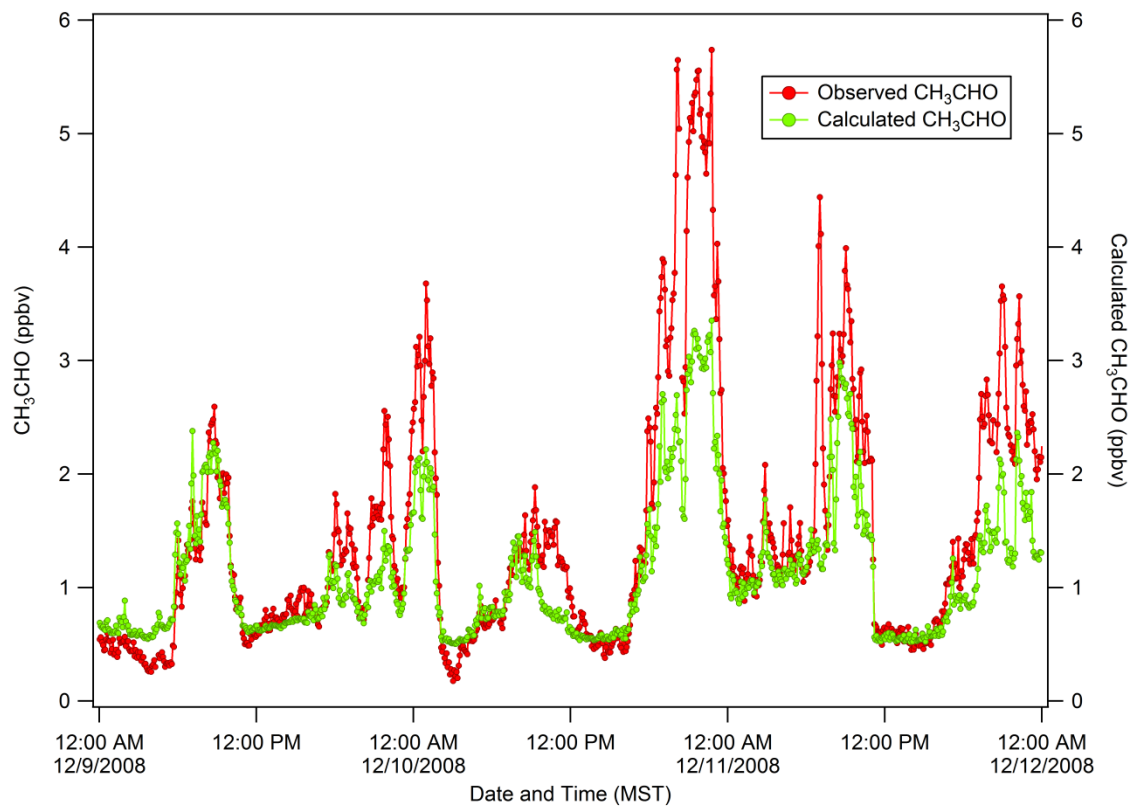


Figure 3.12. Measured and calculated (using CH₃CHO/CO ratio) CH₃CHO mixing ratios using. The green points are the calculated CH₃CHO from CO ambient data

Table 3.4. Parameters for linear regressions of Acetaldehyde vs. CO for the selected morning rush hour periods

Month	Date	Day	Slope (pptv/ppbv)	Intercept (ppbv)	R ²
December	9	Tuesday	2.03 ± 0.14	0.08 ± 0.08	0.854
	11	Thursday	--	--	--
	12	Friday	2.84 ± 0.42	0.33 ± 0.19	0.579
	26	Friday	2.14 ± 0.15	0.22 ± 0.09	0.862
January	29	Thursday	1.45 ± 0.08	0.50 ± 0.04	0.904
average			2.11 ± 0.20	0.28 ± 0.10	

A similar check was done for the calculated acetaldehyde mixing ratios as formaldehyde. The histograms of the ratios are shown in Figure 3.13. For acetaldehyde, the distribution of the ratios had a positive skew. For day and night, the average values were 0.80 ± 0.40 and 0.92 ± 0.46 respectively. The median values of these distributions were 0.74 and 0.89 respectively for day and night. During day, the acetaldehyde mixing ratios were both under and over predicted. But during night, the calculated acetaldehyde mixing ratios are mostly under predicted, as we can see some higher values of ratio dominates the distribution. The error for the predicted values for both time of the day is 43% in average.

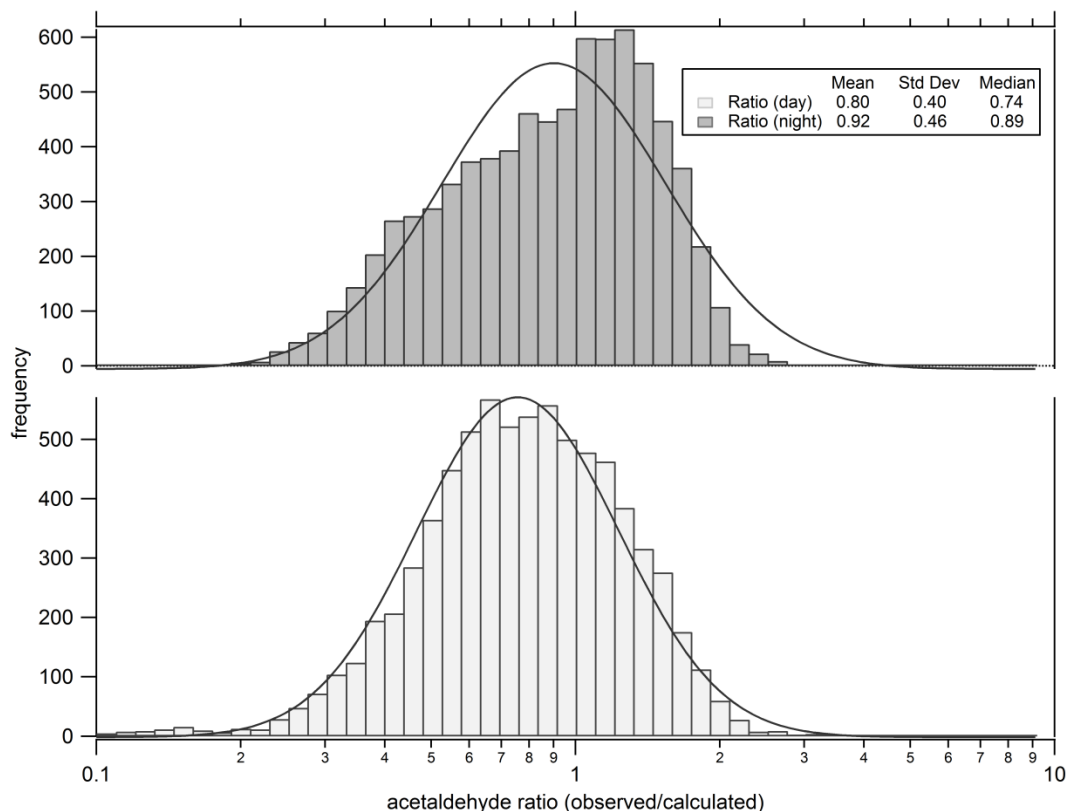


Figure 3.13. Histogram plots of the ratio of observed and prediction (using $\text{CH}_3\text{CHO}/\text{CO}$ ratio) acetaldehyde mixing ratios.

3.4.1.3. Benzene

The benzene-CO relationships are shown in Figure 3.14. The regression parameters are also tabulated in Table 3.6. The highest slope was seen on January 29, 2009, 1.43 pptv benzene /ppbv CO. For the five chosen days the average slope was 1.3 ± 0.07 pptv benzene /ppbv CO. Unlike the aldehydes, the benzene/CO slope was very consistent throughout the study period. For all five days R^2 values were more than 0.88. The linear regression parameters were then used (Eq. 3) to predict benzene emission from CO emission from vehicle sources, like before.

$$[\text{Benzene}_{\text{predicted}}] \text{ ppbv} = 1.30 \times [\text{CO}] \text{ ppbv}/1000 - 0.02 \dots\dots\dots (3)$$

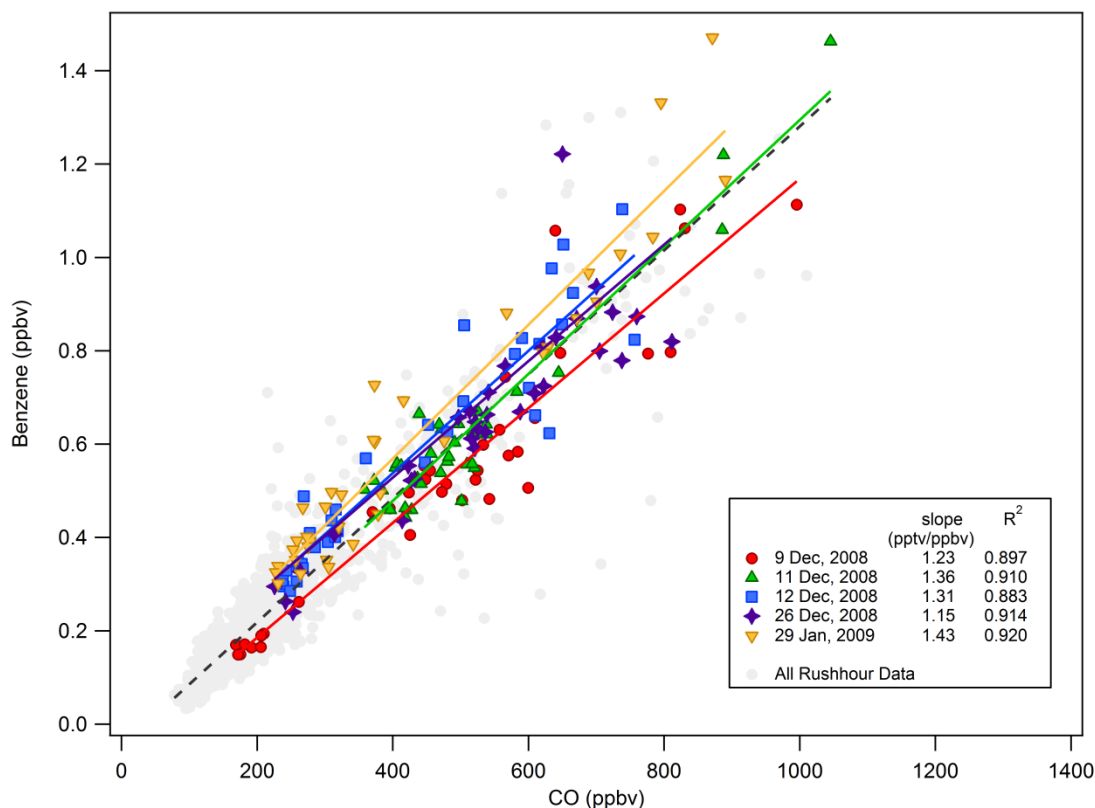


Figure 3.14. Relationships between benzene and carbon monoxide mixing ratios in Meridian, Idaho.

Table 3.5. Parameters for linear regressions of benzene vs. CO for the selected morning rush hour periods

Month	Date	Day	Slope (pptv/ppbv)	Intercept (ppbv)	R ²
December	9	Tuesday	1.23 ± 0.07	-0.06 ± 0.04	0.897
	11	Thursday	1.36 ± 0.07	-0.06 ± 0.04	0.910
	12	Friday	1.31 ± 0.08	0.01 ± 0.04	0.883
	26	Friday	1.15 ± 0.07	0.03 ± 0.04	0.914
January	29	Thursday	1.43 ± 0.07	0.00 ± 0.03	0.920
average			1.30 ± 0.07	-0.02 ± 0.04	

Figure 3.15 shows the agreement between the observed and calculated benzene. Among all the air toxics, benzene was predicted the best using the linear regression parameters

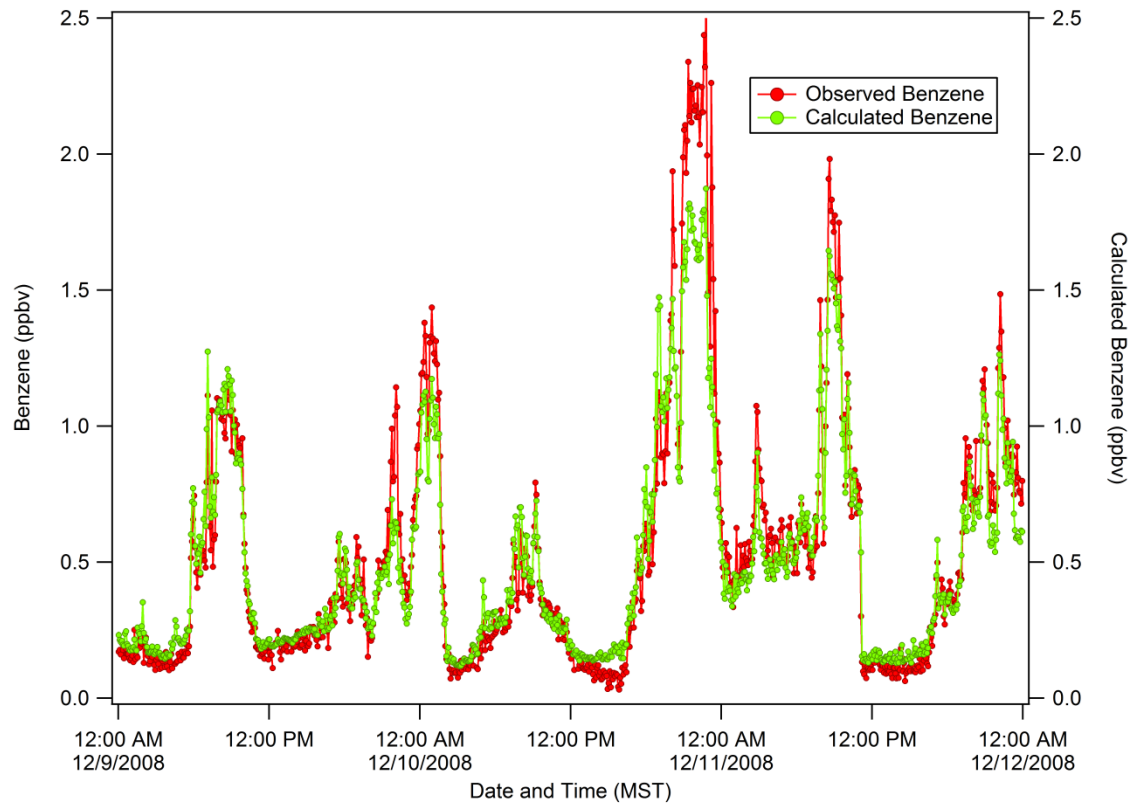


Figure 3.15. Measured and calculated (using benzene/CO ratio) benzene mixing ratios. The green points are the calculated benzene from CO ambient data

and CO emission. A check for the predicted emissions also supports this theory. For benzene, the observation/prediction ratios show a normally distributed histogram in Figure 3.16. The average ratios for day and night were 0.90 ± 0.20 and 0.98 ± 0.30 respectively. The calculated benzene mixing ratios for day had the narrowest distribution among all the toxics.

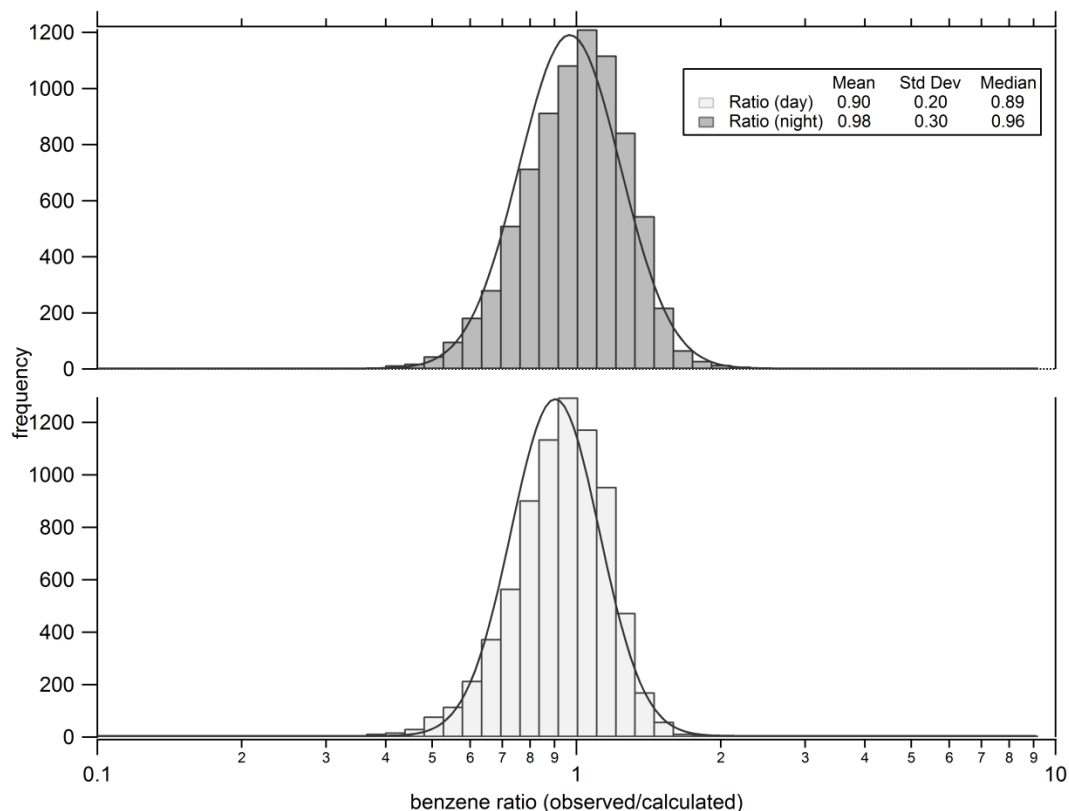


Figure 3.16. Histogram plots of the ratio of observed and predicted (using benzene/CO ratio) benzene mixing ratios.

3.4.1.4. Other species

Among the 15 VOCs measured in the study, there were two unknowns. The two ions are $m/z = 69$ and $m/z = 137$. Usually these two ions are attributed to isoprene (C_5H_8) and monoterpenes ($C_{10}H_{15}$) respectively. Isoprene and monoterpenes are biogenic VOCs emitted from trees. However, this study was carried out in winter and biogenic emissions of isoprene would be expected to be zero since deciduous trees have lost their leaves and little photosynthesis is occurring at this time of year in evergreens. Cold winter temperatures also imply emissions of monoterpenes will be low since emission rates for

monoterpenes are temperature dependent. These two factors lead us to a hypothesis that these species are of non-biogenic sources and possibly ion fragments from larger organic compounds found in exhaust. Analysis of gasoline by PTR-MS shows the presence of an $m/z = 69$ ion. Analysis of diesel fuel shows the presence of an $m/z = 137$ ion but no $m/z = 69$ ion. These ions may be useful winter time tracers for gasoline exhaust ($m/z = 69$) and diesel exhaust ($m/z = 137$) respectively. Here, two VOCs were analyzed expecting to find fuel specific tracers for gasoline and diesel vehicle exhaust other than CO and NO_x.

3.4.1.4.1. $m/z = 69$

We used CO as a tracer of the vehicle exhaust as before and carried out similar analysis for unknown #1 ($m/z = 69$). Figure 3.17 shows the relationships between $m/z = 69$ and CO. Although the slopes for the five chosen days, are not quite high as benzene-CO slopes (§ 3.3.3.), $m/z = 69$ has good correlation ($R^2 > 0.7$) to CO for most of the days. This suggests that $m/z = 69$ shares common sources with CO. The highest R^2 ($=0.858$) was observed on December 12, 2008. The highest slope was 0.632 pptv $m/z = 69$ /ppbv CO and was observed on December 26, 2008 although R^2 was 0.789 for that day.

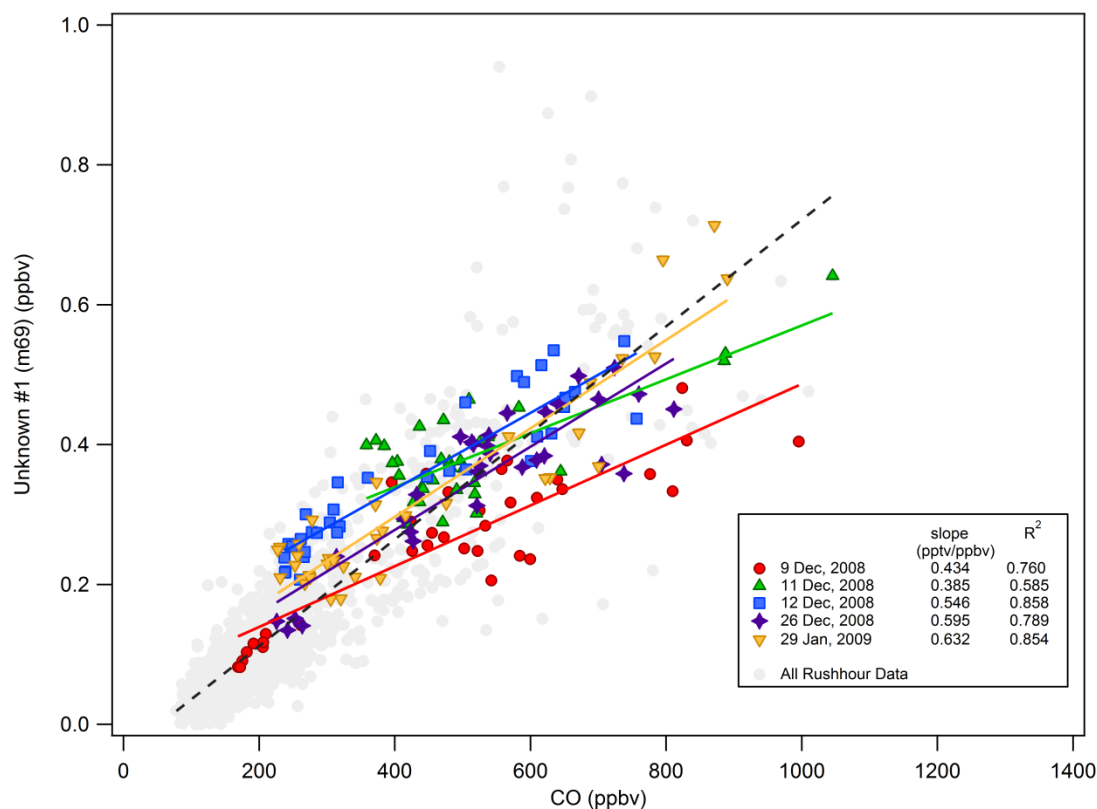


Figure 3.17. Relationships between unknown #1 ($m/z = 69$) and carbon monoxide mixing ratios in Meridian, Idaho.

3.4.1.4.2. $m/z = 137$

Figure 3.18 shows the relationship between unknown #2 ($m/z = 137$) and CO. Unlike, $m/z = 69$, $m/z = 137$ shows a rather erratic relationship with CO. The regression parameter R^2 was quite low (<0.6) for most of the days. The highest slope was 0.383 pptv/ppbv CO with an R^2 of 0.578 on December, 26, 2008. This suggests $m/z = 137$ and CO are not from the same source after all.

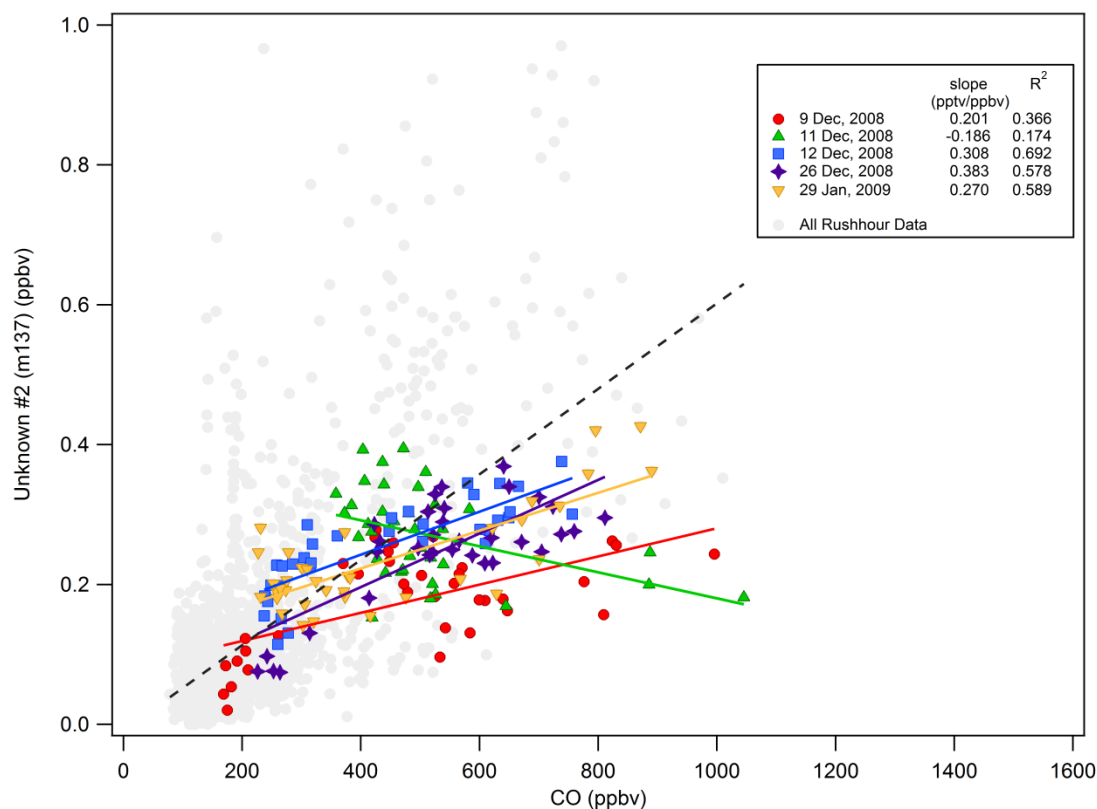


Figure 3.18. Relationships between unknown #2 (m/z =137) and carbon monoxide mixing ratios in Meridian, Idaho.

3.4.1.4.3. Aromatics

Toluene, C₂-alkylbenzene, and C₃-alkylbenzene data were summed to provide an overall total alkyl aromatic level. Figure 3.19 shows the relationship between the total alkyl aromatics and CO. As the figure shows these aromatics show a very strong ($R^2 > 0.8$) correlation to CO during the rush hour analysis for most of the days. This strong correlation suggests that these aromatics indeed come from vehicle exhausts. The regression parameters of this analysis are shown in Table 3.7.

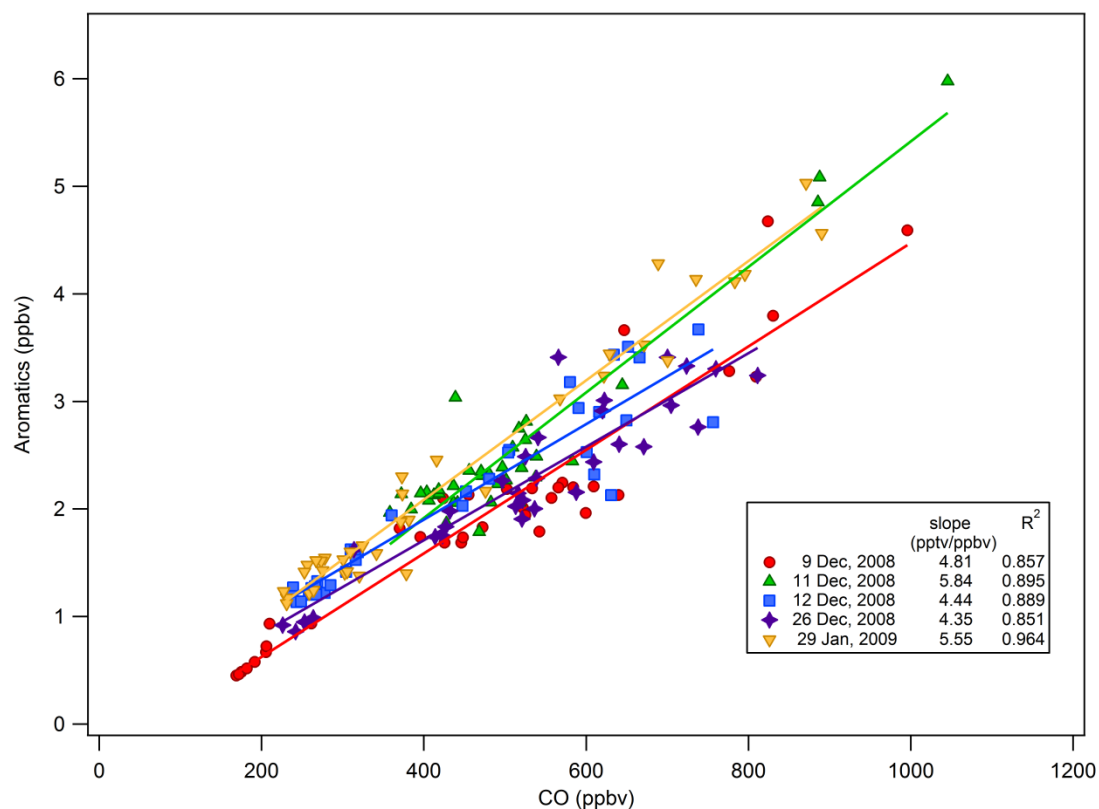


Figure 3.19 Relationships between aromatics and carbon monoxide mixing ratios in Meridian, Idaho.

Table 3.6. Parameters for linear regressions of aromatics vs. CO for the selected morning rush hour periods

Month	Date	Day	Slope (pptv/ppbv)	Intercept (ppbv)	R ²
December	9	Tuesday	4.81 ± 0.27	-0.34 ± 0.14	0.900
	11	Thursday	5.84 ± 0.34	-0.42 ± 0.18	0.895
	12	Friday	4.44 ± 0.27	0.12 ± 0.12	0.889
	26	Friday	4.35 ± 0.34	-0.03 ± 0.19	0.851
	29	Thursday	5.55 ± 0.18	-0.13 ± 0.09	0.964
average			5.00 ± 0.28	-0.03 ± 0.15	

3.4.2. Correlation with NO_x

3.4.2.1. Formaldehyde

NO_x could be used as a tracer for diesel fueled vehicles as they emit more NO_x than gasoline fueled vehicles. Regression analyses with NO_x with the various VOCs can showcase the contribution of the diesel exhausts to their emissions. Figure 3.20 shows the relationship between HCHO and NO_x. Here HCHO-NO_x is shown for only three days because there was not sufficient data for NO_x on 11 December and 26 December, 2008.

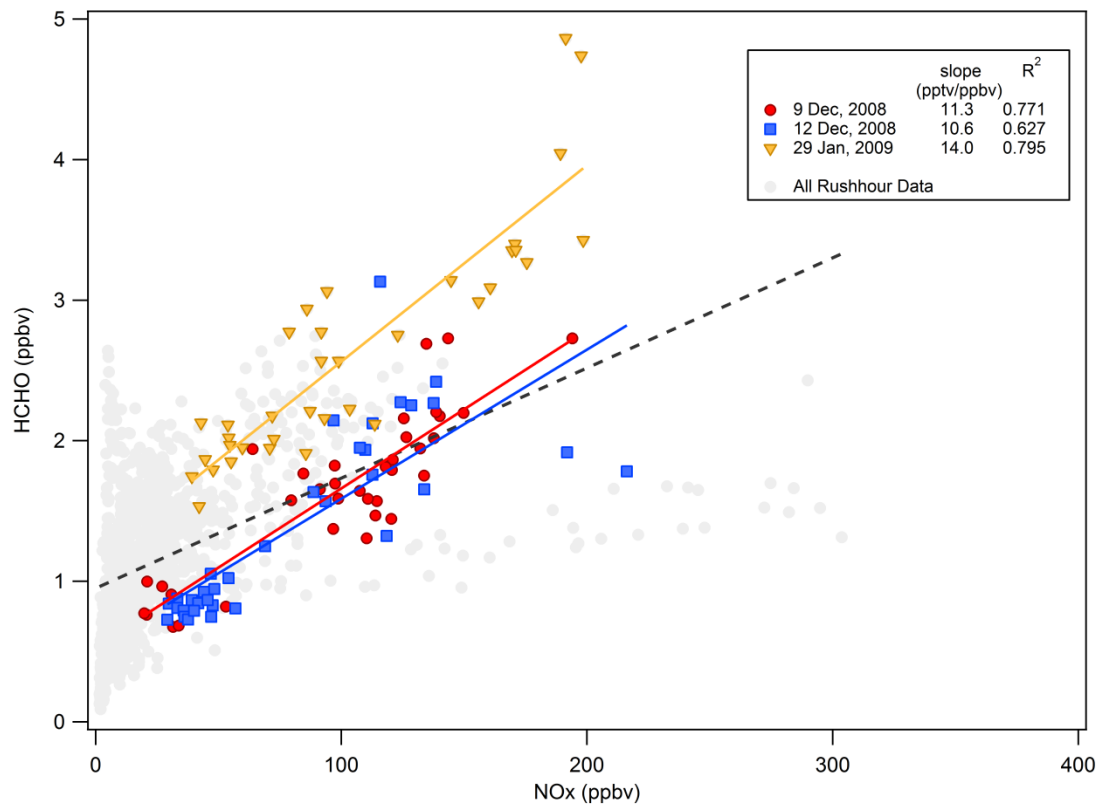


Figure 3.20. Relationships between HCHO and NO_x mixing ratios in Meridian, Idaho.

The regression parameters for this analysis are shown in Table 3.3. As we can see, the best correlation was seen on January 29, 2009 ($R^2 = 0.795$) with the highest HCHO-NO_x

ratio (14 pptv HCHO/ ppbv NO_x). The average slope from the four days was 11.9 ± 1.0 pptv HCHO/ppbv NO_x.

Table 3.7. Parameters for linear regressions of HCHO vs. NO_x for the selected morning rush hour periods. The average temperature and relative humidity are included

Month	Date	Day	Temp. (°C)	RH (%)	Slope (pptv/ppbv)	Intercept (ppbv)	R ²
December	9	Tuesday	-3.82	85.60	11.3 ± 1.1	0.54 ± 0.11	0.771
	11	Thursday	-2.65	86.70	--	--	--
	12	Friday	-4.27	95.80	10.6 ± 1.4	0.53 ± 0.13	0.627
	26	Friday	-10.58	86.30	--	--	--
January	29	Thursday	-5.60	88.70	14.0 ± 1.2	1.17 ± 0.14	0.795
average					11.9 ± 1.2	0.74 ± 0.13	

Using the average linear regression parameters from the table above, an equation was derived (Eq. 4), similar to Eq. 1. In this case, the prediction of HCHO would depend on the ambient NO_x mixing ratio.

$$[HCHO_{predicted}] \text{ ppbv} = 11.9 \times [NO_x] \text{ ppbv}/1000 + 0.74 \dots \dots \dots (4)$$

Using this equation, we calculated the amount of HCHO from the measured NO_x mixing ratio. Figure 3.21 illustrates the comparison between the observed and calculated HCHO for the same random three day period in December as before. The predicted HCHO mixing ratios agree reasonably with the observed levels of HCHO during the rush hour period. However it failed to capture the high levels of HCHO during night.

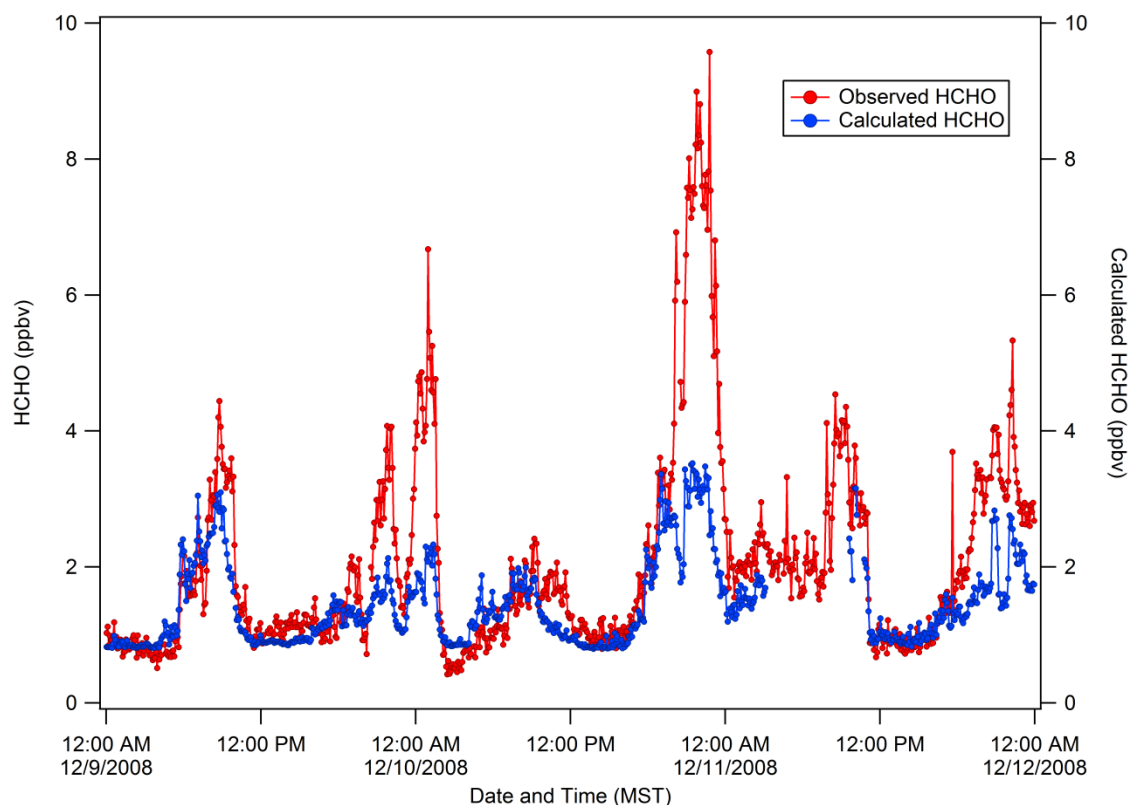


Figure 3.21. Measured and calculated (using HCHO/NO_x ratio) HCHO mixing ratios. The blue points are the calculated HCHO from NO_x ambient data

The ratios between the predicted and observed levels of HCHO were plotted into histograms as shown in Figure 3.22. The ratios were subdivided into day and night time as defined before. For both night and day, the histograms show wider spreads than the histograms in Figure 3.9. During both times, we see high values of the ratio, suggesting under predicted HCHO mixing ratios. The distributions had average values 1.17 ± 0.46 and 1.27 ± 0.55 . However, the nighttime histogram clearly showed a positive skew with a median of 1.23. This suggests that the HCHO emissions were under-predicted within 55% of the error during night.

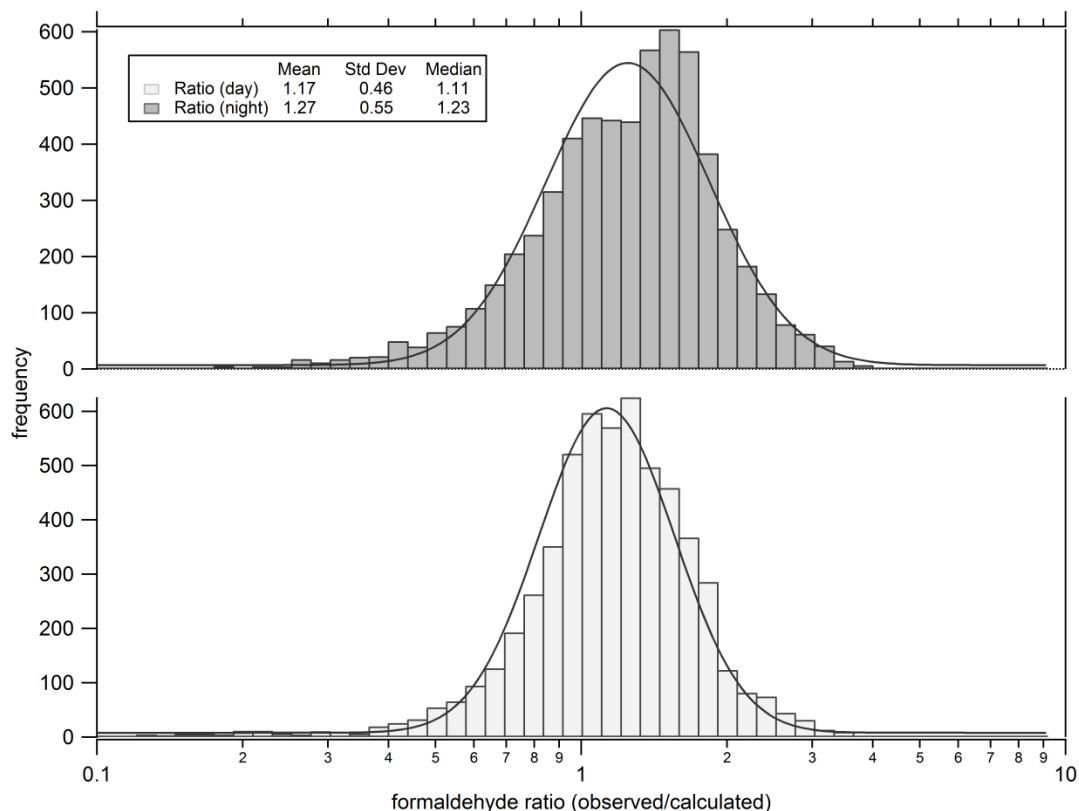


Figure 3.22. Histogram plots of the ratio of observed and predicted (using HCHO/NO_x ratio) formaldehyde mixing ratios.

3.4.2.2. Acetaldehyde

The acetaldehyde (CH₃CHO) –NO_x relationships are shown in Figure 3.23. The regression parameters are also tabulated in Table 3.5. The highest slope was seen on December 9, 2008, 9.42 ± 0.87 pptv CH₃CHO /ppbv NO_x. From the regression analyses of three days the average slope was found to be 7.99 ± 1.03 pptv CH₃CHO /ppbv NO_x.

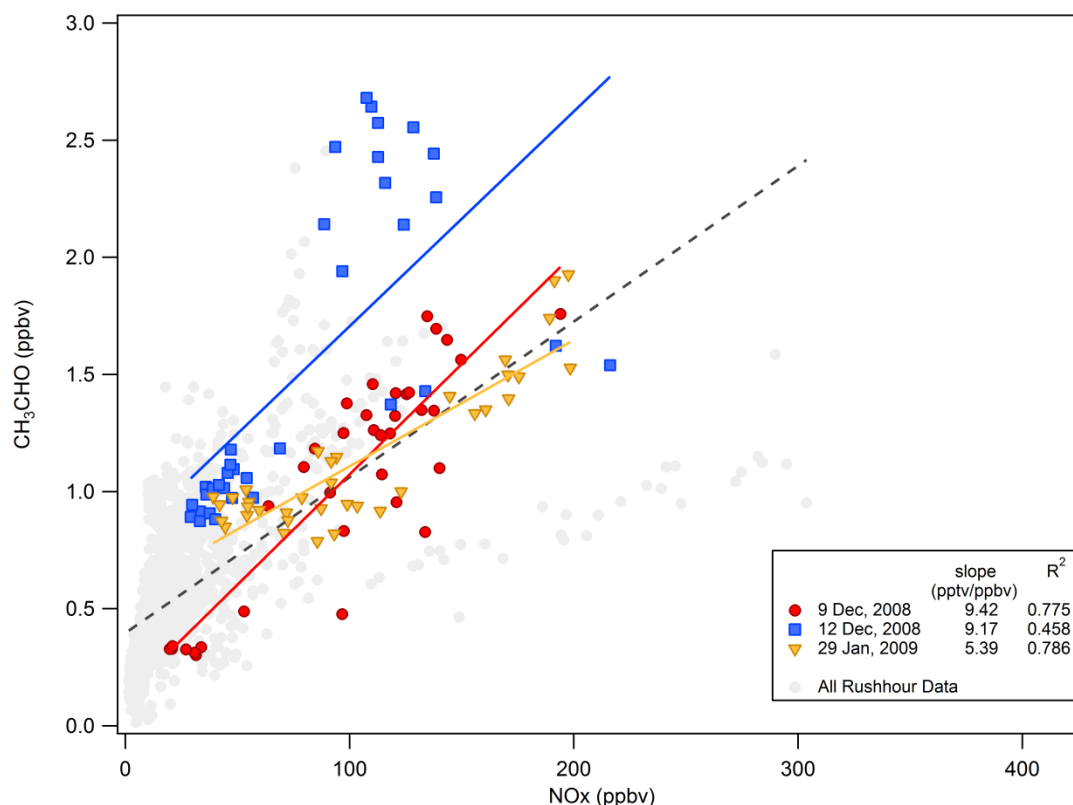


Figure 3.23. Relationships between acetaldehyde and NO_x mixing ratios in Meridian, Idaho.

The linear regression parameters were then used (Eq. 5) to predict CH₃CHO emission from NO_x emission from vehicle sources, like before.

$$[CH_3CHO_{predicted}] \text{ ppbv} = 7.99 \times [NO_x] \text{ ppbv}/1000 + 0.50 \dots \dots \dots (5)$$

Figure 3.24 shows the comparison between the observed and calculated CH₃CHO for the same three day period depicted in Figure 3.8.

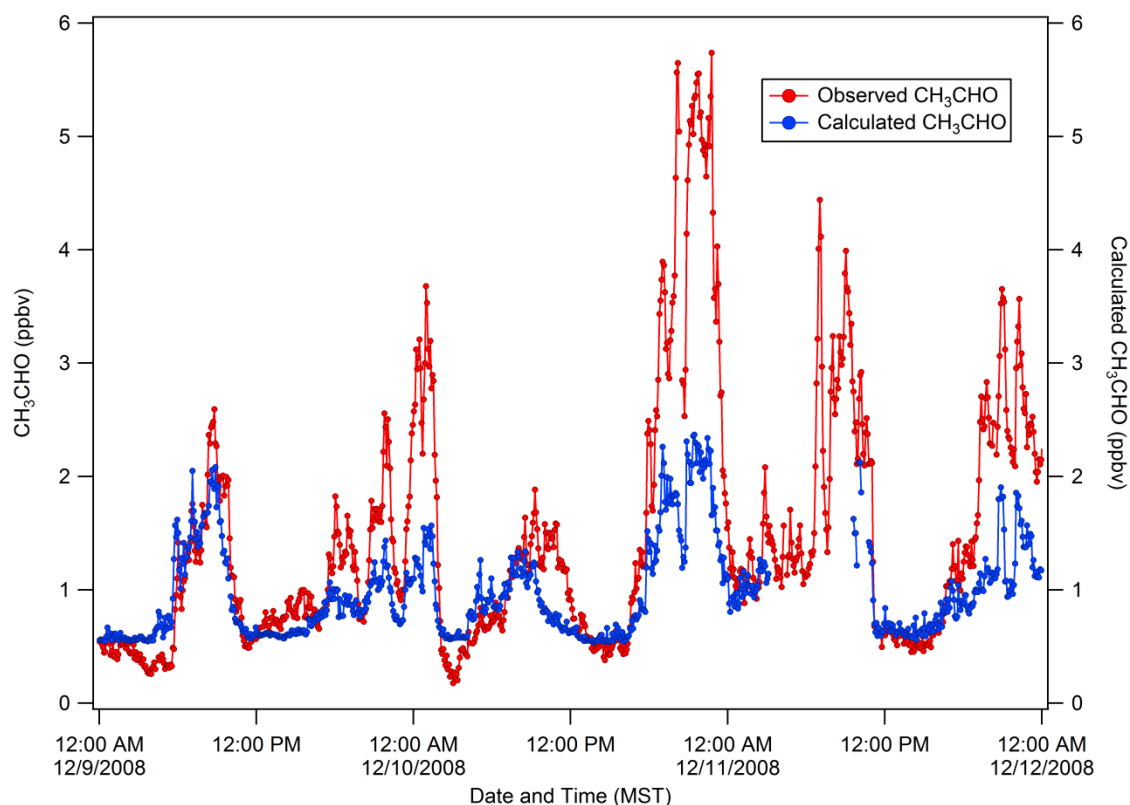


Figure 3.24. Measured and calculated (using $\text{CH}_3\text{CHO} / \text{NO}_x$ ratio) CH_3CHO mixing ratios. The blue points are the calculated CH_3CHO from NO_x ambient data

Table 3.8. Parameters for linear regressions of CH_3CHO vs. NO_x for the selected morning rush hour periods

Month	Date	Day	Slope (pptv/ppbv)	Intercept (ppbv)	R^2
December	9	Tuesday	9.42 ± 0.87	0.13 ± 0.09	0.775
	11	Thursday	--	--	--
	12	Friday	9.17 ± 1.74	0.79 ± 0.16	0.458
	26	Friday			
January	29	Thursday	5.39 ± 0.48	0.57 ± 0.06	0.786
average			7.99 ± 1.03	0.50 ± 0.10	

The calculated CH_3CHO levels were quite similar to the calculated HCHO from NO_x emissions. Both of aldehydes were under-predicted during night. However, the CH_3CHO levels were over predicted during day by equation 5. The histograms of the ratios are shown in Figure 3.25.

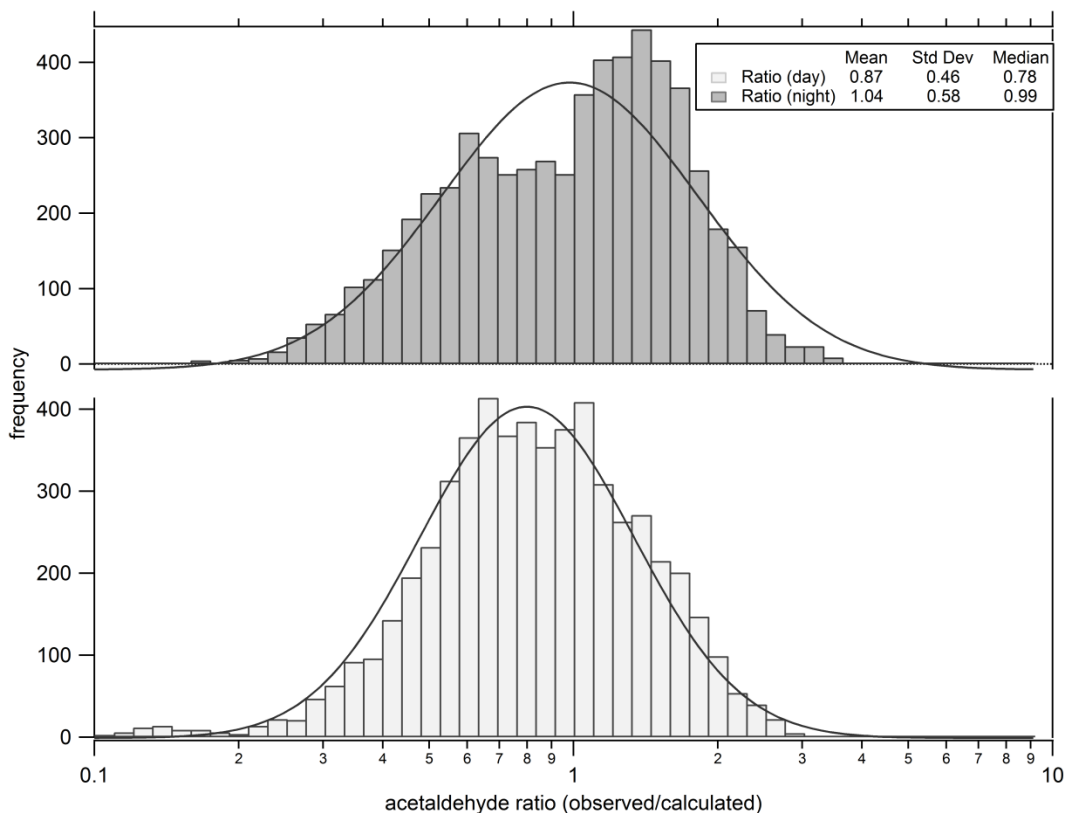


Figure 3.25. Histogram plots of the ratio of observed and predicted (using $\text{CH}_3\text{CHO}/\text{NO}_x$ ratio) acetaldehyde mixing ratios.

For night, the distribution of the ratios had a significant positive skew. The ratios were mostly between 1 and 2. The average and median of this distribution were 1.04 ± 0.58 and 0.99 respectively. The day time distribution had a lesser skew than the night time distribution. The average and median values of this distribution were 1.04 ± 0.46 and

0.78 respectively. These two distributions imply, predicting CH_3CHO from NO_x emissions might produce false results during night.

3.4.2.3. Benzene

The benzene – NO_x relationships are shown in Figure 3.26. The regression parameters are also tabulated in Table 3.9.

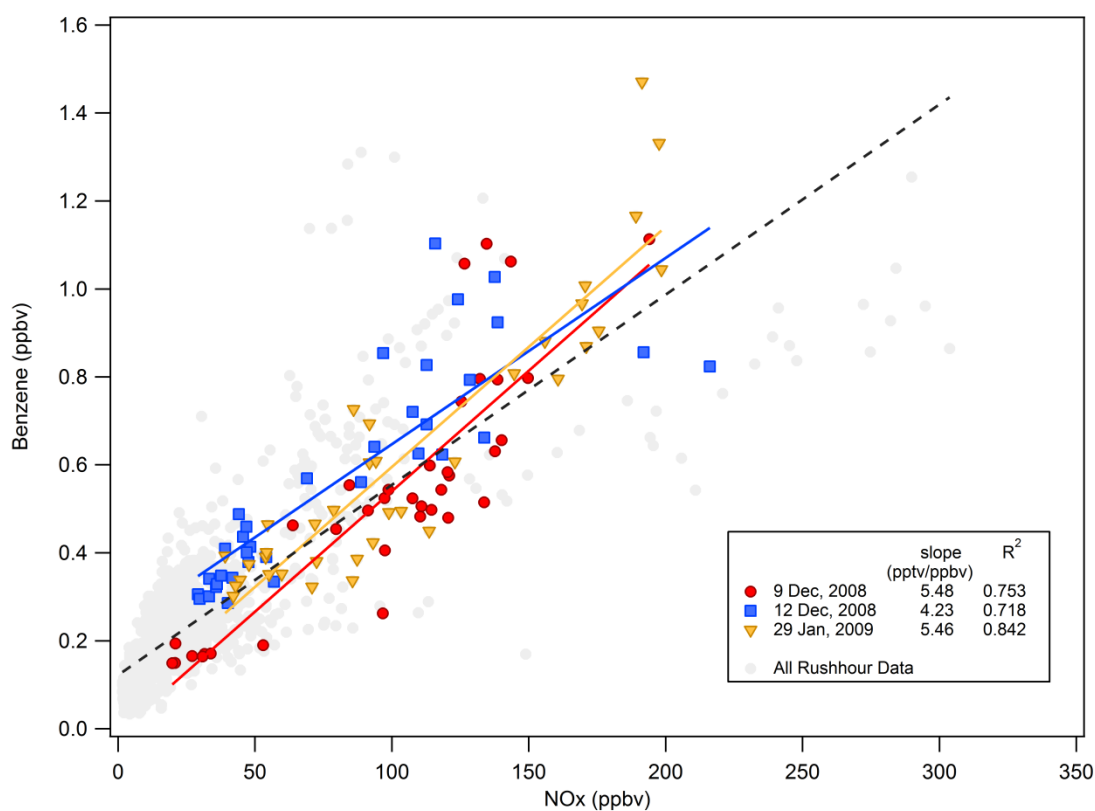


Figure 3.26. Relationships between benzene and NO_x mixing ratios in Meridian, Idaho.

The highest slope was seen on December 9, 2008, 5.48 pptv benzene /ppbv NO_x . For the three chosen days the average slope was 5.06 ± 0.47 pptv benzene /ppbv NO_x .

Table 3.9. Parameters for linear regressions of benzene vs. NO_x for the selected morning rush hour periods

Month	Date	Day	Slope (pptv/ppbv)	Intercept (ppbv)	R ²
December	9	Tuesday	5.48 ± 0.54	-0.01 ± 0.06	0.753
	11	Thursday	--	--	--
	12	Friday	4.23 ± 0.46	0.22 ± 0.04	0.718
	26	Friday	--	--	--
January	29	Thursday	5.46 ± 0.41	0.05 ± 0.05	0.842
average			5.06 ± 0.47	0.09 ± 0.05	

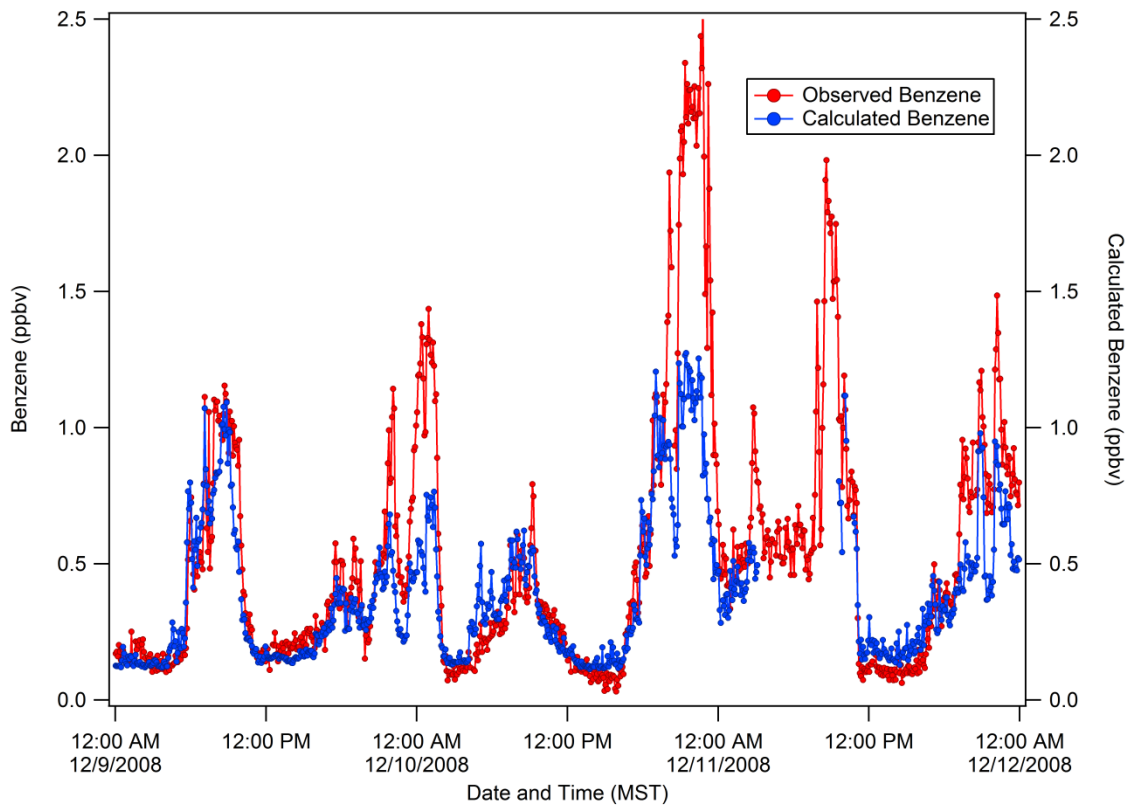


Figure 3.27 Measured and calculated (using benzene/NO_x ratio) benzene mixing ratios. The blue points are the calculated benzene from NO_x ambient data

The linear regression parameters were then used (Eq. 6) to predict benzene emission from ambient NO_x concentrations, like before.

$$[Benzene_{predicted}] ppbv = 5.06 \times [NO_x] ppbv/1000 + 0.09 \dots \dots \dots (6)$$

Figure 3.27 shows the comparison between the observed levels of benzene to the predicted based on NO_x emission. To further inspect the quality of the prediction, a statistical analysis was performed by calculating the ratio between observation/prediction and binning them to create histograms. Figure 3.28 represents the histograms of the ratio divided into day and night. According to this figure, we can see the average values of the histograms are 1.10 ± 0.34 and 1.30 ± 0.53 for day and night time respectively. The median of these distributions were 1.06 and 1.23 respectively for day and night. For both time of the day, we see higher values of the ratio suggesting the benzene mixing ratios were under predicted. This was more obvious during night when most of the ratios were greater than 1.

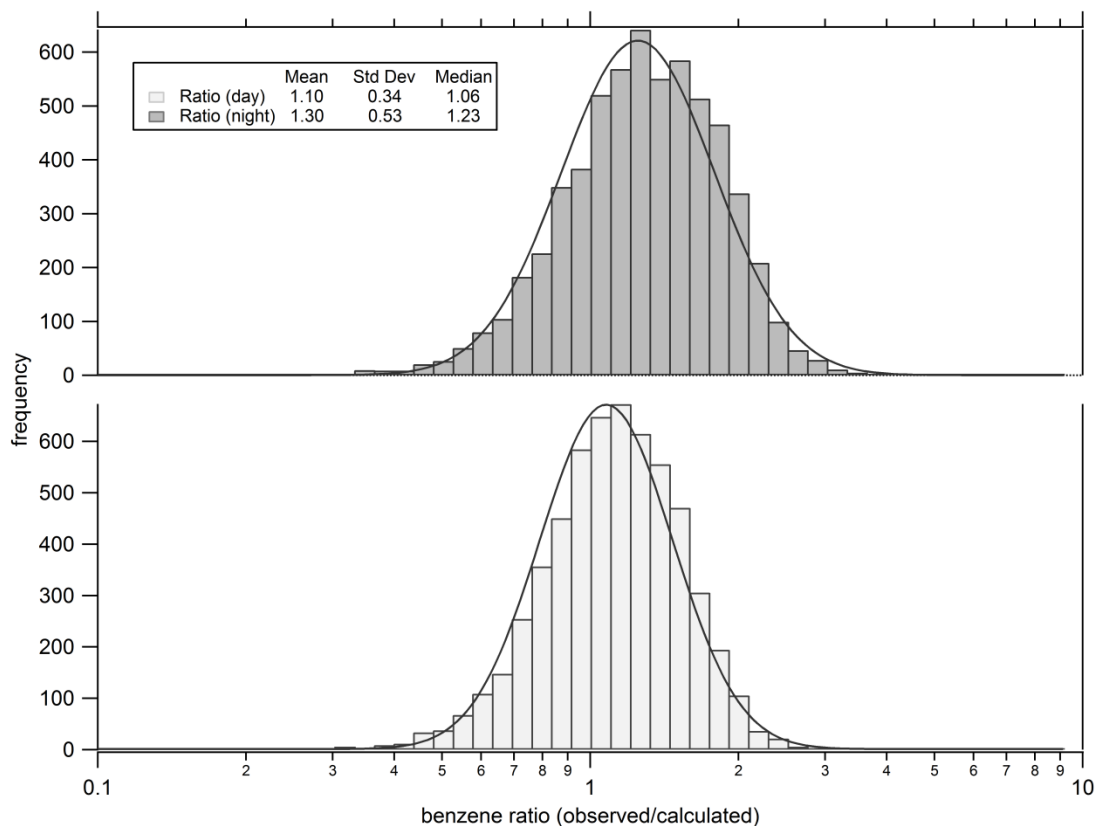


Figure 3.28. Histogram plots of the ratio of observed and predicted (using benzene/NO_x ratio) of benzene mixing ratios

3.4.2.4. Other species

For the two ions, $m/z = 69$ and $m/z = 137$, regression analyses were done by correlating them with NO_x emissions. The hypothesis behind these analyses was that these ions were not from biogenic sources, rather fragmented ions from larger organic compounds.

Another interest was to use these ions as a tracer for either gasoline or diesel exhaust.

Their correlations with CO (refer to § 3.4.1.4.) led us to believe, $m/z = 69$, usually recognized as isoprene, shared a common source as CO. As for $m/z = 137$, the regression

analysis led us to the opposite conclusion that they do not share the same source. In this section, their relations with NO_x emission are analyzed to ensure if they are exclusive to one type of exhaust or not.

3.4.2.4.1. m/z = 69

Figure 3.29 shows the slopes between unknown #1 (m/z =69) and NO_x mixing ratios are higher than the slopes between m/z=69 and CO. This was expected because of the relation between CO and NO_x emissions. The highest R² (=0.719) was observed on

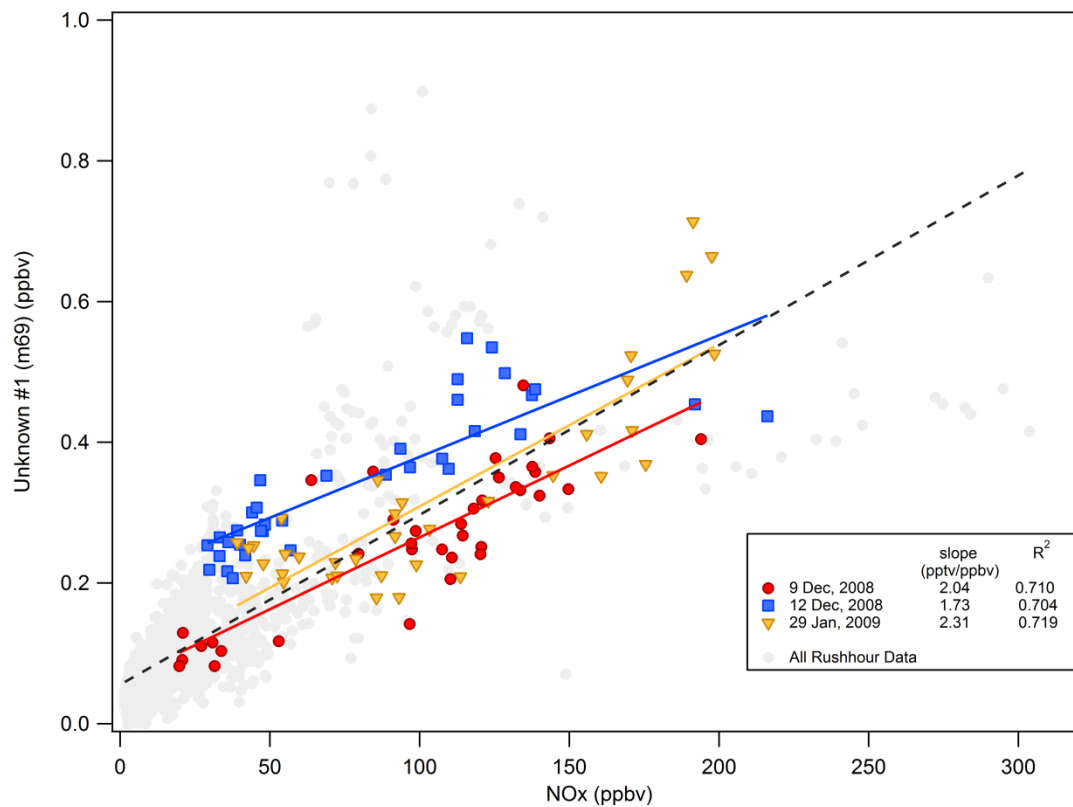


Figure 3.29 Relationships between unknown #1 (m/z =69) and NO_x mixing ratios in Meridian, Idaho.

January 29, 2009 with the highest slope of 2.31 pptv m/z 69 /ppbv NO_x. In general, m/z=69 had good correlation ($R^2 > 0.7$) to NO_x for most of the days. This suggests that m/z =69 shares common sources with NO_x too. As m/z=69 is not found in diesel fuel, we can conclude that the NO_x emission related to m/z =69 might come from gasoline exhaust rather than diesel exhaust.

3.4.2.4.2. m/z = 137

It was expected the relationship between unknown #2 (m/z = 137) and NO_x to be better than that with CO emissions. Figure 3.30 shows that the hypothesis was incorrect. Although the relationship with NO_x was not as erratic as that with CO, m/z =137 was poorly correlated with NO_x emissions too. The regression parameter R^2 was quite low (<0.6) for most of the days. The highest slope was 1.02 pptv/ppbv CO with an R^2 of 0.399 on December, 9, 2008. The regression parameters are shown in Table 3.10.

Table 3.10. Parameters for linear regressions of unknown #2 (m/z =137) vs. NO_x for the selected morning rush hour periods

Month	Date	Day	Slope (pptv/ppbv)	Intercept (ppbv)	R^2
December	9	Tuesday	1.02 ± 0.22	0.08 ± 0.02	0.399
	11	Thursday	--	--	--
	12	Friday	1.00 ± 0.16	0.17 ± 0.01	0.554
	26	Friday	--	--	--
January	29	Thursday	0.99 ± 0.17	0.13 ± 0.02	0.499
average			1.00 ± 0.18	0.12 ± 0.02	

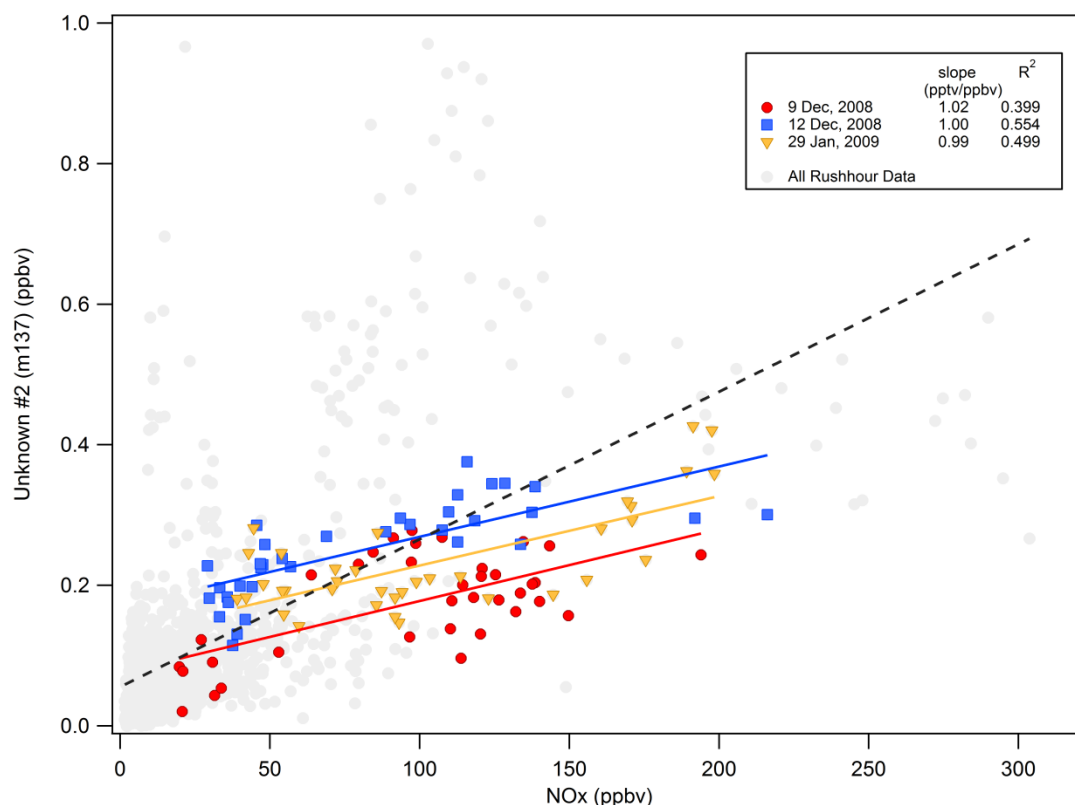


Figure 3.30 Relationships between unknown #2 ($m/z = 137$) and NO_x mixing ratios in Meridian, Idaho.

The regression parameters suggest that the $m/z = 137$ and NO_x emissions are not from the same source. However, the intercepts were consistent and had positive values which suggest that there were ambient $m/z = 137$ not related to NO_x emissions. Determining the actual source of this ion is beyond the scope of this study.

3.4.2.4.3. Aromatics

Figure 3.31 shows the relationship between the total alkyl aromatics and NO_x mixing ratios. As observed here these aromatics show good ($R^2 > 0.7$) correlation to NO_x during the rush hour analysis for most of the days. Comparing these to the previous analyses

with CO we can conclude that aromatics are not exclusive to CO emissions. The regression parameters for this analysis are shown in table 3.11.

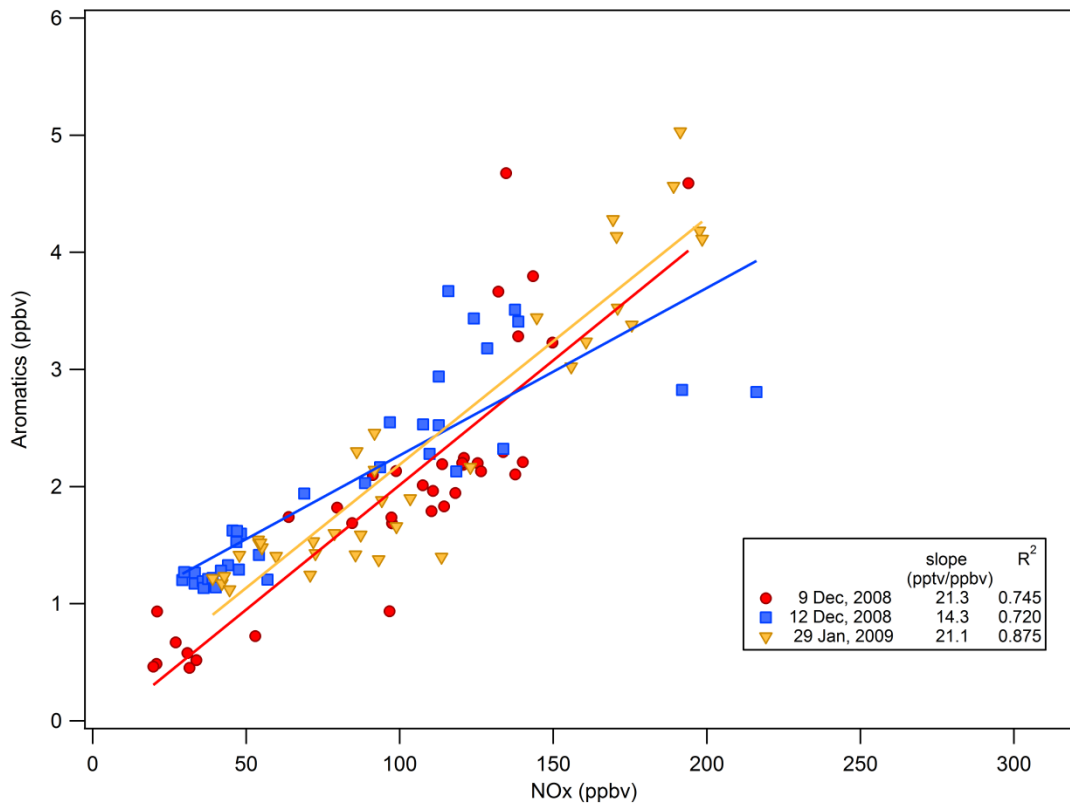


Figure 3.31 Relationships between aromatics and NO_x mixing ratios in Meridian, Idaho.

Table 3.11. Parameters for linear regressions of aromatics vs. NO_x for the selected morning rush hour periods

Month	Date	Day	Slope (pptv/ppbv)	Intercept (ppbv)	R ²
Decemeber	9	Tuesday	21.3 ± 2.1	-0.11 ± 0.23	0.745
	11	Thursday	--	--	--
	12	Friday	14.3 ± 1.6	0.84 ± 0.15	0.720
	26	Friday	--	--	--
January	29	Thursday	21.1 ± 1.4	0.08 ± 0.16	0.875
average			18.9 ± 1.7	0.25 ± 0.19	

3.5. Comparison to AIRPACT-3

The measurements were compared to mobile emissions simulated for input to an air quality forecast model, AIRPACT-3 (Air Indicator Report for Public Awareness and Community Tracking v.3) is a computerized system for air quality forecasting in the Pacific Northwest region. The system runs nightly, producing detailed hourly maps of ozone and other pollutant concentrations for a forecast period of ~ three days in the immediate future. The domain (shown in Figure 3.32) of AIRPACT covers three Northwest states – Idaho, Oregon and Washington. The domain is treated as a three

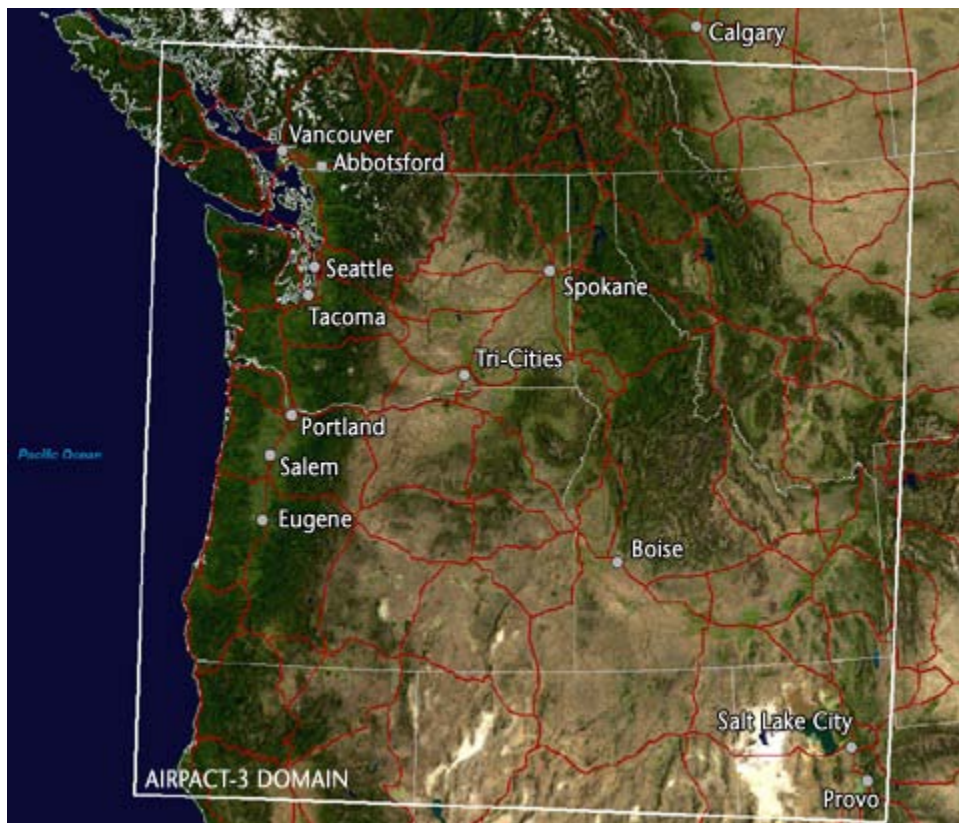


Figure 3.32. AIRPACT-3 domain. Satellite image of AIRPACT-3 domain showing major cities and interstate highways (red lines)

dimensional space of 95 (N-S) by 95 (E-W) grid cells ($12\text{km} \times 12\text{ km}$ each) in 21 vertical layers (Herron-Thorpe et al., 2010). AIRPACT is based on EPA's chemical transport model CMAQ. This model uses the vehicle emissions from MOBILE6.2 to calculate mobile emissions and a detailed atmospheric kinetic mechanism (SAPRC99) to account for the gas phase chemical reactions responsible for photochemical production of ozone and other VOCs (Chen et al., 2008).

Mixing ratios were generated by AIRPACT for the two month study period (December, 2008 to January, 2009) and were extracted for the study location (Meridian, Idaho). Only the first vertical layer was taken into account to represent the atmospheric boundary layer receiving mobile emissions. The AIRPACT results were hourly specified in contrast to the measurements which were averaged over 5 minutes. The measured air toxics emission ratios with respect to CO and NO_x emissions were then compared to the emission ratios found from AIRPACT emissions. The following sub-sections describe the comparison of these emission ratios for different VOCs.

3.5.1. Formaldehyde

Figure 3.33 shows the relationship between primary emission of formaldehyde and CO for the chosen rush hour period. As we can see, the slope from the model data is 0.47 pptv HCHO/ppbv CO. The figure also shows the slope for the observed data. For the ease of comparison we have used the same intercept as the model data. The observed intercept is shown in parenthesis in the figure. As stated before our observations show HCHO/CO slope to be 3.30 pptv/ppbv. These two slopes differ by a factor 7.0.

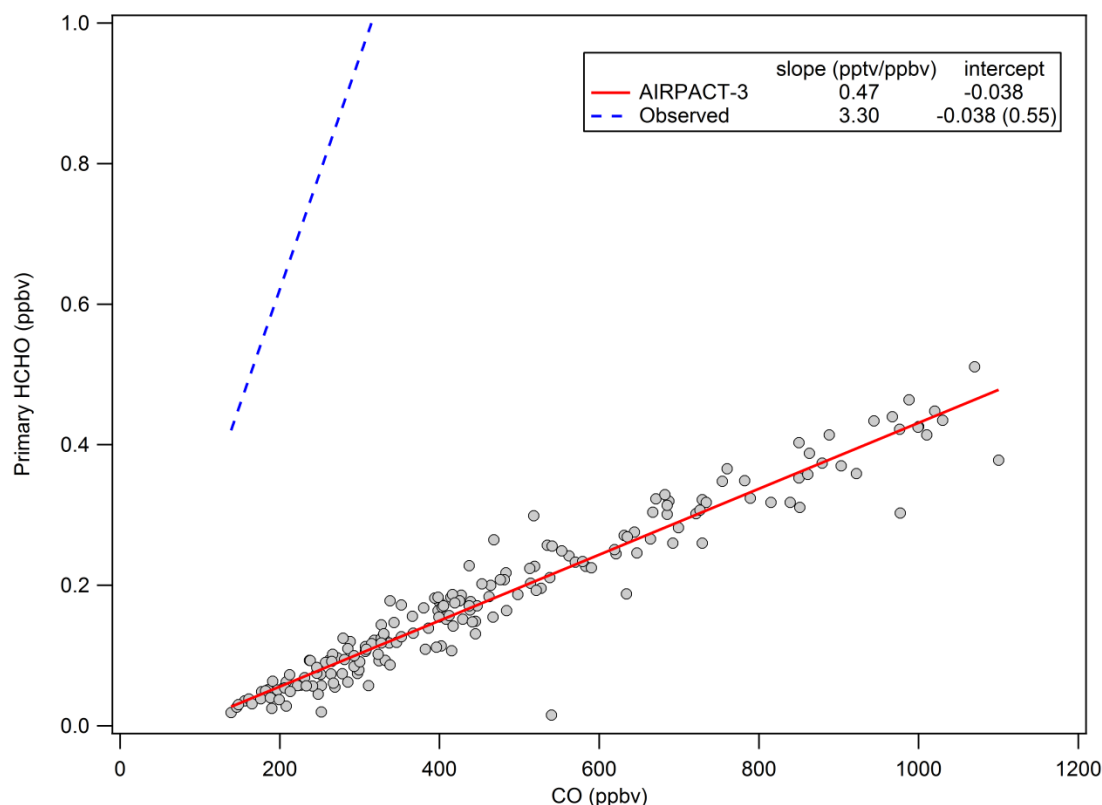


Figure 3.33 Comparison of HCHO/CO slopes from AIRPACT-3 model and measurements. The solid red line represents the least-squares fit for the AIRPACT-3 model. The blue dashed line is the fit for the observed data.

HCHO and NO_x relationships modeled emissions were also examined and a similar comparison was done with observations. Figure 3.34 shows their relationship. Unlike HCHO-CO relationship, HCHO-NO_x slope for modeled data was very similar to the observation. The model yielded a slope of 8.00 pptv HCHO/ppbv NO_x. The average slope from our observation for HCHO-NO_x was 11.9 pptv HCHO/ppbv NO_x, higher than the model slope by a factor of 1.5. The good agreement for AIRPACT versus observations and HCHO versus NO_x correlation compared to those with CO suggests that CO emissions from AIRPACT might be overestimated.

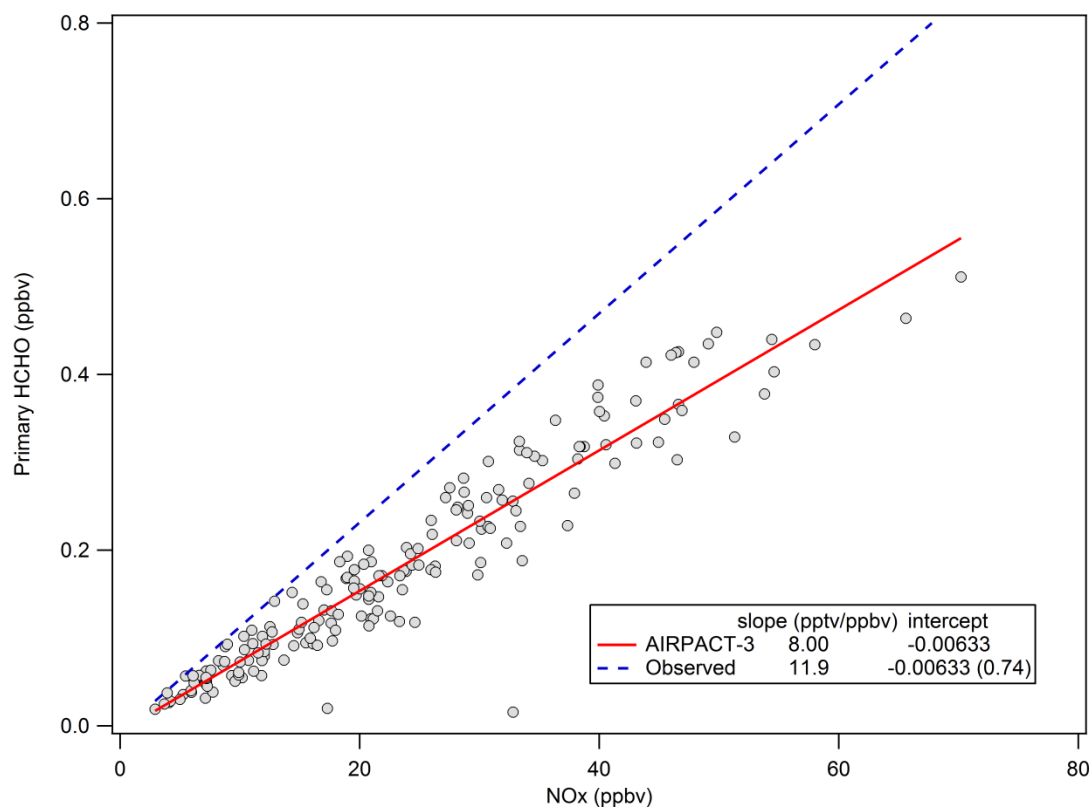


Figure 3.34 Comparison of HCHO/NO_x slopes from AIRPACT-3 model and measurements. The solid red line represents the least-squares fit for the AIRPACT-3 model. The blue dashed line is the fit for the observed data.

3.5.2. Acetaldehyde

Figure 3.35 shows the relationship between primary emission of acetaldehyde and CO for model data. The slope from the model data is 0.136 pptv CH₃CHO/ppbv CO. The average slope from our observation for acetaldehyde-CO was 2.11 pptv CH₃CHO/ppbv CO. The slopes differ by a factor of 15.5. The poor level of agreement is similar to that observed for HCHO versus CO, and suggests again that AIRPACT CO emissions may be overestimated.

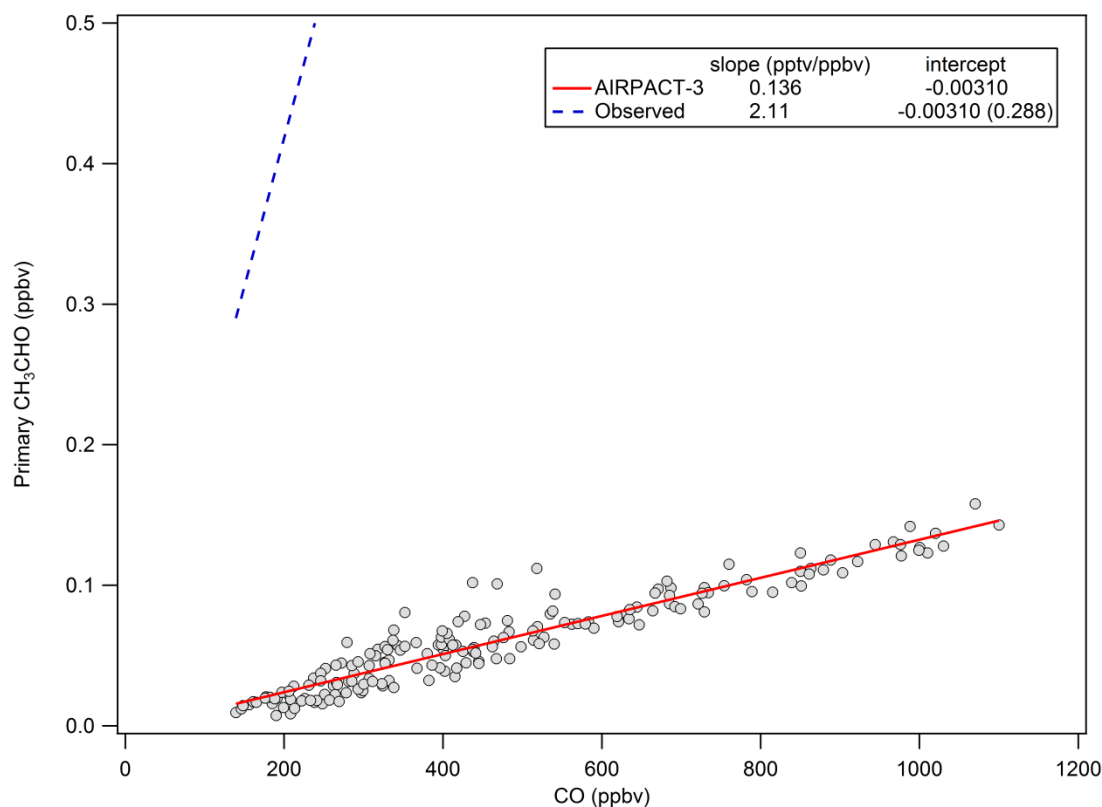


Figure 3.35 Comparison of CH₃CHO /CO slopes from AIRPACT-3 model and measurements. The solid red line represents the least-squares fit for the AIRPACT-3 model. The blue dashed line is the fit for the observed data.

Comparing emission ratios of CH₃CHO with respect to NO_x gave an opposite result of that with CO. Figure 3.36 shows that the two slopes obtained from the measurement and the model agree relatively well. The slope found from the model data was 3.31 pptv/ppbv NO_x. The average slope from the measurements was 7.99 pptv/ppbv, which is larger than the modeled slope by a factor of 2.4. This result is very similar to that of HCHO-NO_x relationship, suggesting again that AIRPACT represents the ambient NO_x levels better than CO levels.

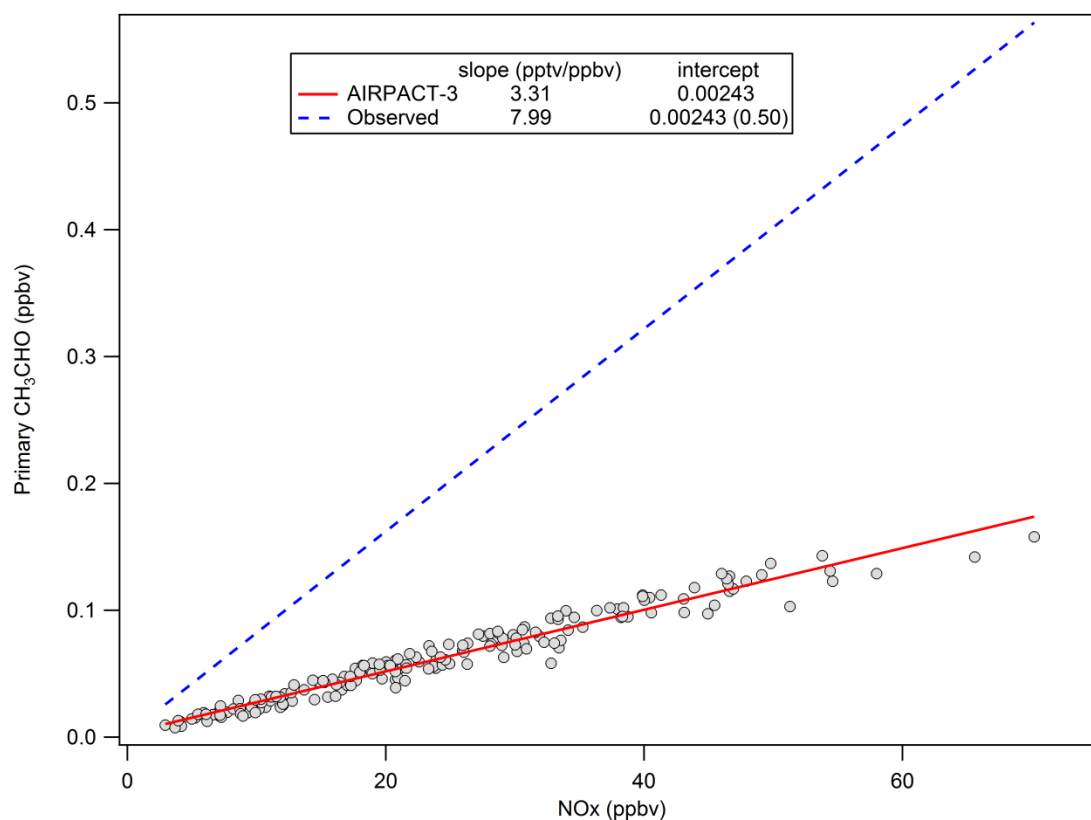


Figure 3.36 Comparison of $\text{CH}_3\text{CHO} / \text{NO}_x$ slopes from AIRPACT-3 model and measurements. The solid red line represents the least-squares fit for the AIRPACT-3 model. The blue dashed line is the fit for the observed data.

3.5.3. Benzene

Unlike HCHO-CO or CH₃CHO –CO relationships, the relationship of benzene-CO for modeled data and observed data agreed quite well (Figure 3.37).

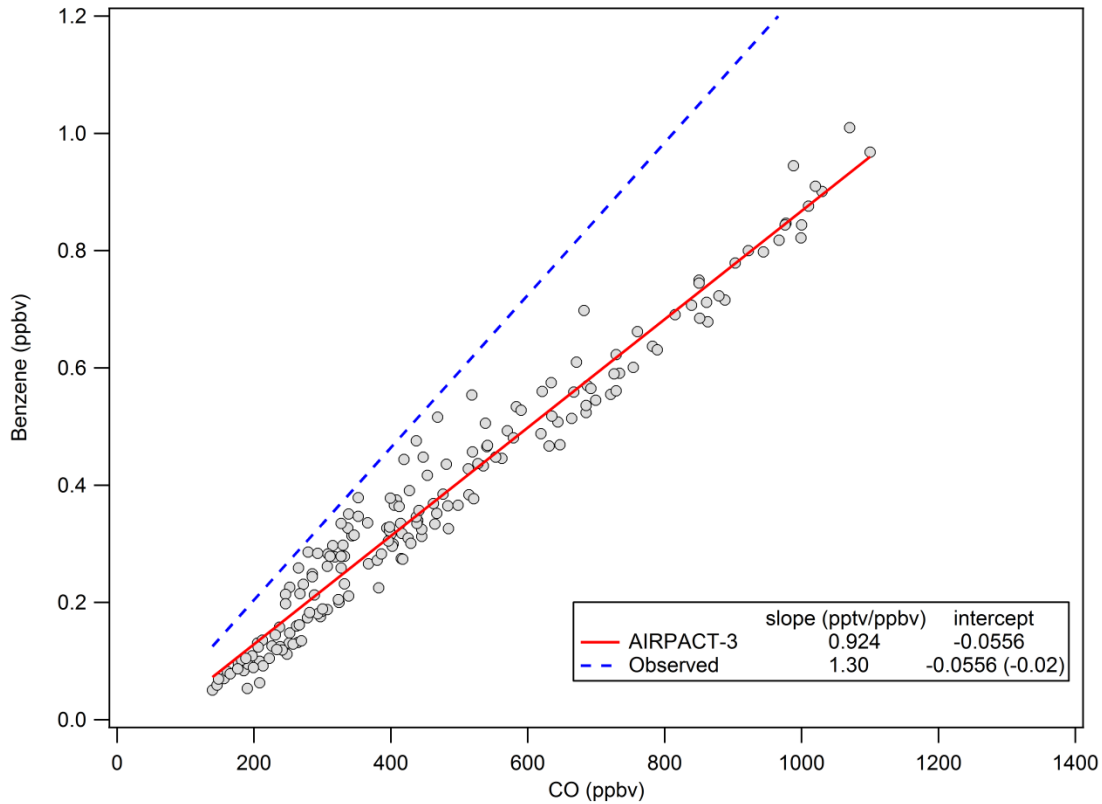


Figure 3.37 Comparison of benzene /CO slopes from AIRPACT-3 model and measurements. The solid red line represents the least-squares fit for the AIRPACT-3 model data shown as grey circles. The blue dashed line is the fit for the observed data.

The slope for the model benzene-CO was 0.924 pptv benzene/ ppbv CO. The average slope from our observation was 1.30 pptv benzene/ ppbv CO, which is higher than the model value by a factor of 1.4. However, for benzene and NO_x relationship (Figure 3.38), the model predicted that benzene emissions were higher relative to NO_x emissions. The emission ratio obtained from the model was 15.8 pptv benzene/ppbv NO_x. But the

emission ratio from the observations was only 5.06 pptv benzene/ppbv NO_x. In this case, the modeled emission ratio was higher by a factor of 3.1.

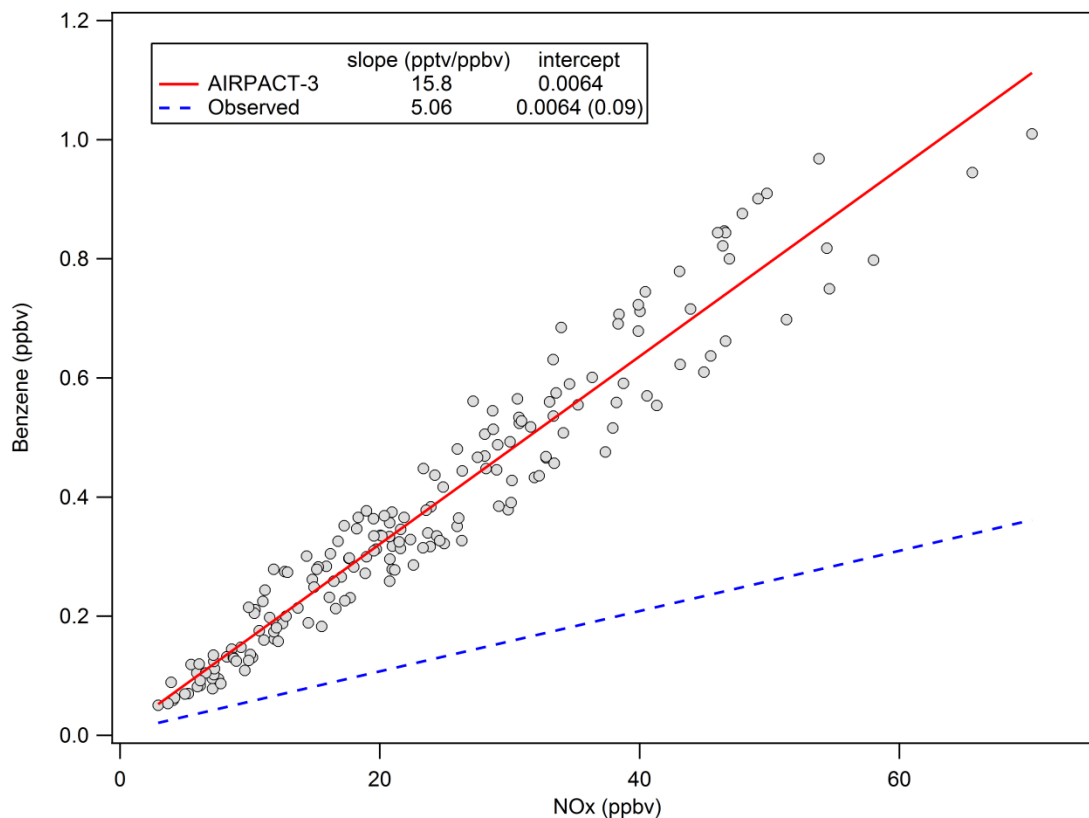


Figure 3.38 Comparison of benzene /NO_x slopes from AIRPACT-3 model and measurements. The solid red line represents the least-squares fit for the AIRPACT-3 model data shown as grey circles. The blue dashed line is the fit for the observed data.

3.5.4. Aromatics

The emissions of aromatic VOCs (refer to § 3.4.2.4.3) were compared to the aromatics from the model data. The model uses a SAPRC99 chemical mechanism lumping scheme (Chen et al., 2008). In this mechanism the groups ARO1 and ARO2 represent most of the

alkyl monoaromatic species measured by the PTR-MS as total alkyl aromatics. We summed these two groups and compared it to the aromatics from our observation.

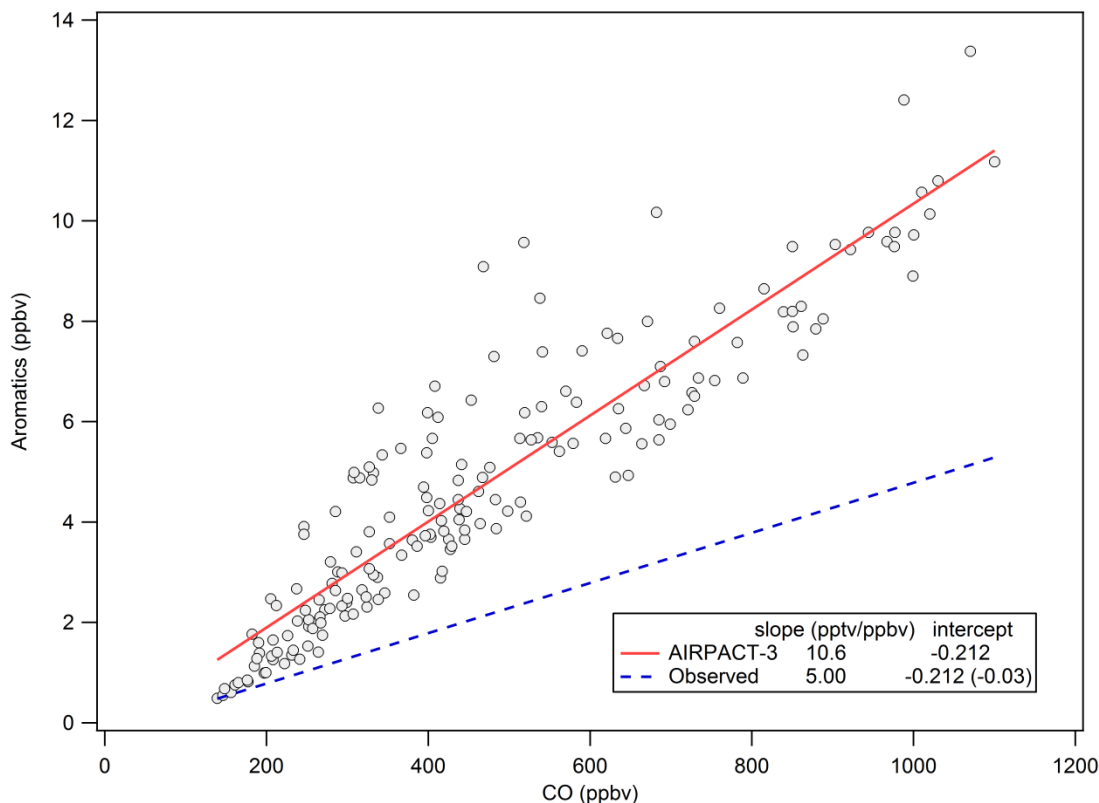


Figure 3.39 Comparison of mono aromatics/CO slopes from AIRPACT-3 model and measurements. The solid red line represents the least-squares fit for the AIRPACT-3 model. The blue dashed line is the fit for the observed data.

As we can see from the comparison in Figure 3.39, the slope for the model aromatics-CO was 10.6 pptv / ppbv CO. The average slope from our observation was 5.00 pptv / ppbv CO. In this case, the slope from the model data is higher than the observations, by a factor of 2.1. The emission ratio of aromatics with respect to NO_x from observation and model showed that the observation ratio was at tenth of the model value. Figure 3.40 shows the comparison of these two emission ratios.

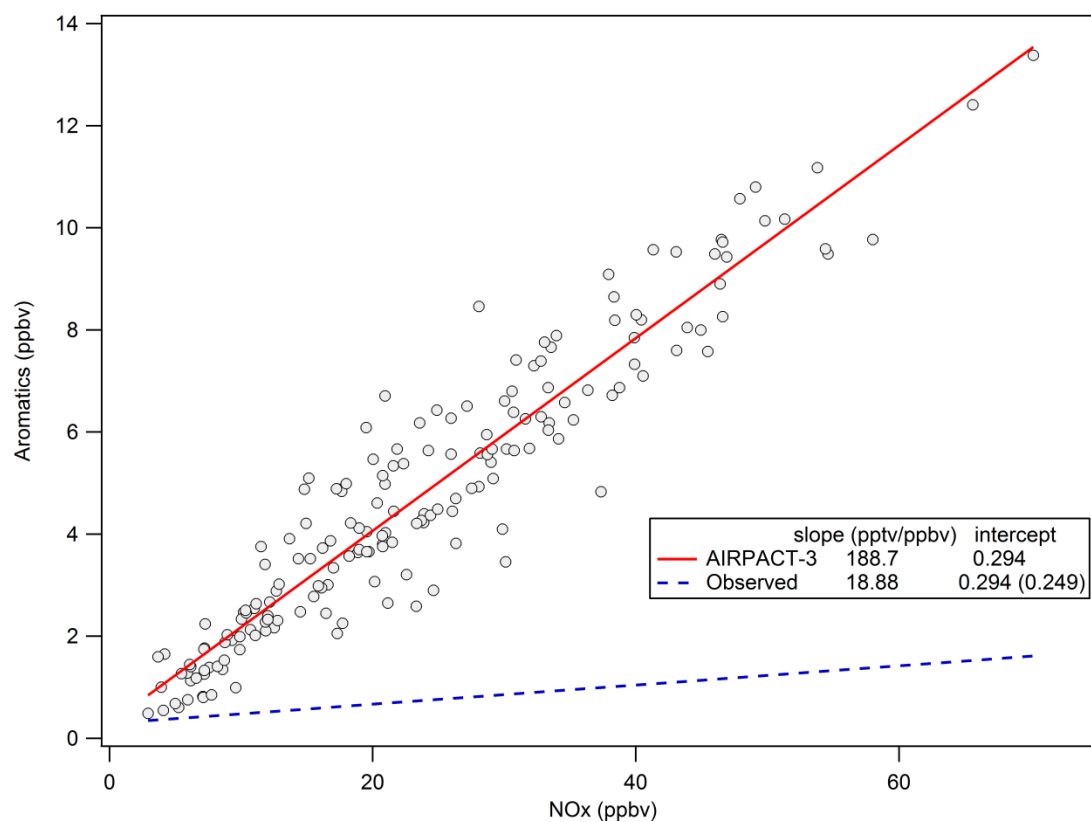


Figure 3.40 Comparison of mono aromatics/CO slopes from AIRPACT-3 model and measurements. The solid red line represents the least-squares fit for the AIRPACT-3 model. The blue dashed line is the fit for the observed data.

The model data yielded an emission ratio of 188.7 pptv/ppbv NO_x. In contrast, the average emission ratio from the measurement was only 18.9 pptv/ppbv NO_x.

3.6. Summary and discussion

Emission ratios with respect to CO and NO_x were calculated for priority mobile toxics, formaldehyde, acetaldehyde and benzene, and some other VOCs of interest from measurements in an urban environment of Meridian, Idaho during winter. Morning rush hour during winter, in northern mid-latitudes, is an excellent time to capture the influence of vehicle emissions on air toxics without conducting intensive tunnel studies as have been done previously for various urban locations (Ban-Weiss et al., 2008; Grosjean et al., 2001). We used two trace gases CO and NO_x as our vehicle exhaust tracer. Our initial hypothesis was that CO was better tracer for gasoline fueled vehicles in contrast to NO_x for diesel fueled vehicles. Unfortunately, we did not see any trend where the toxics were more closely linked to either of the tracers. The predicted air toxic mixing ratios from emission ratios prove that CO did better than NO_x as a vehicle exhaust tracer in general. The reasons behind the poor performance of NO_x as a tracer, are related to the chemistry of these trace gases. NO_x is highly reactive. It can photolyze in the atmosphere in the presence of sunlight. It can also be removed from the atmosphere through various processes, especially at night. On the contrary CO has a longer atmospheric lifetime and it is conserved throughout the day. These factors make CO a more reliable vehicle exhaust tracer than NO_x.

Emission ratios were also calculated from modeled data generated by AIRPACT. These were compared with the measured emission ratios. According to our analyses, the emission ratios were comparable between aldehyde –NO_x and benzene-CO relationships.

However, the modeled ratios for aldehyde-CO relationships were significantly lower than measured values. The lower slopes from the modeled output could be a result of underestimating primary aldehydes (mainly HCHO) or overestimating CO in the emission inventories.

Research conducted by Air Improvement Resource on the emission inventory model MOBILE6.2, suggests the simulator over predicts CO emissions at colder temperatures for some types of vehicles (Air Improvement Resource, 2005). One possible reason is that MOBILE6.2 is unable to capture the nature of CO emissions. Recently, EPA has developed a new mobile emission predictor known as MOBILE Vehicle Emission Simulator (MOVES). Comparison between these two models (MOBILE 6.2 and MOVES) reveals that the 80% of the wintertime ambient CO emissions come from startup (cold start) of the vehicles. As MOBILE 6.2 cannot separate these two factors (on-road vs. off network vehicles), it can predict higher emissions from on-road vehicles which might not be emitting the same level of CO. This report also discusses that MOBILE6.2 neglects the effect of vehicle fleet age on CO emissions. The prediction of CO is reliable for vehicle fleet before the year 2000. But for the subsequent years it over-predicts CO emissions as these vehicles are less sensitive to temperature, hence CO emission due to cold start is significantly reduced.

Another weak point about the MOBILE6.2 model is that the air toxic emissions are predicted through toxic fraction approach. In this approach, a toxic ratio is applied to the total organic gas (TOG) emission rate to get the toxic emission factor. These ratios and

factors depend on various properties of the vehicle (type, catalytic technology used, fuel type and characteristics, etc.). However, on an evaluation report of this model, it is further revealed the toxic-TOG ratios for all vehicles since 1981, are calculated by a complex model relationship which is based on emissions data prior to mid-1990s model years (Heirigs et al., 2004). Since 1994 there has been more stringent emission standard which are implemented for newer vehicles. These facts can greatly influence the VOC emissions from the model itself.

Table 3.12 summarizes the emission ratios of the three air toxics with respect to CO and NO_x found in this study.

Table 3.12. Emission ratios of VOCs with respect to CO and NO_x for Meridian, Idaho from measurements and from AIRPACT-3

Compounds	ER_{measured} (pptv/ppbv CO)	ER_{AIRPACT} (pptv/ppbv CO)	ER_{measured} (pptv/ppbv NO _x)	ER_{AIRPACT} (pptv/ppbv NO _x)
acetaldehyde	2.11	0.136	7.99	3.31
aromatics	5.00	10.6	18.9	188.7
benzene	1.30	0.92	5.06	15.8
formaldehyde	3.30	0.47	11.9	8.00
unknown #1 (m/z 69)	0.519	--	2.03	--
unknown #2 (m/z 137)	0.195	--	1.00	--

The comparable results between the measured emission ratios and the ones from MOBILE6.2, for NO_x, suggest that the prediction of NO_x emission from the model is correct. Using this finding along with the calculated emission ratios, we can correct the emissions of these air toxics in the model. In this case, the mixing ratios of formaldehyde,

acetaldehyde and benzene should be corrected by a factor of 1.5, 2.4 and 0.3 respectively. We also used this finding to further correct the CO emission from the model. In this case, we used the corrected toxics from NO_x emission ratios and calculated the corrected emission ratio with respect to CO for the model. We found that on average CO levels were predicted 5.2 times higher by the model.

These emission ratios were also compared to the ones found in previous studies, performed in various urban locations. Table 3.13 shows the emission ratios found in some of the previous studies along with the measured ones from this study. As we can see from Table 3.13, all of studies were not conducted in winter. For formaldehyde, the emission ratio falls into the range of 0.47 – 6.0. The high emission ratio corresponds to Houston, TX, where it is assumed the primary formaldehyde emissions might be influenced by industrial sources in addition to vehicle exhaust (Rappengluck et al., 2010). On the other hand the lowest emission ratio was from AIRPACT simulation, done in this study. For acetaldehyde, the range is narrower, from 0.13 – 2.11. The highest one is from our observed mixing ratios. Benzene had the narrowest range (0.6 – 1.24) of emission ratios. The observed emission ratio from this study is the highest for benzene: 1.30.

No emission ratios with respect to NO_x emissions were reported in any literature.

Table 3.13. Emission ratios of air toxics with respect to CO from Meridian, Idaho (from this study) and other cities. Units are in pptv/ppbv CO

<i>Ambient Measurement</i>					
Place/Time	by	Season	HCHO	CH₃CHO	C₆H₆
Mexico City, Mexico, 2006	(Bon et al., 2011)	spring	--	1.0	1.2
Boston, MA, 1999	(Baker et al., 2008)	late summer - fall	--	--	0.9
New York City, NY 1999	(Baker et al., 2008)	late summer - fall	--	--	0.6
Salt Lake City, UT, 1999	(Baker et al., 2008)	late summer - fall	--	--	1.0
Houston, TX, 2006	(Rappengluck et al., 2010)	late summer - fall	6.0	--	--
Denver, CO, 1990-1991	(Anderson et al., 1996)	winter	1.30	0.5	--
Rome, Italy, 1995	(Possanzini et al., 1996)	winter	2.43	1.0	--
Meridian, ID, 2008-2009	Measured	winter	3.30	2.11	1.30
	AIRPACT	winter	0.47	0.14	0.92
Los Angeles, CA, 2002	(Warneke et al., 2007)		--	--	0.95
<i>Tunnel Studies</i>					
Place/Time	by	Season	HCHO	CH₃CHO	C₆H₆
San Francisco, CA, 1999	(Ban-Weiss et al., 2008)	summer	0.77	0.13	--
San Francisco, CA, 2001	(Ban-Weiss et al., 2008)	summer	0.91	0.13	--
San Francisco, CA, 2006	(Ban-Weiss et al., 2008)	summer	0.62	0.19	

CHAPTER 4: CONCLUSION

The motivation for this study was to develop a better understanding of air toxics from mobile sources. The US EPA has labeled six air toxics to be the most hazardous to human health, including formaldehyde, acetaldehyde and benzene, and all of them are mainly emitted by vehicles when low temperatures inhibit biogenic emissions. This study, conducted in Meridian, Idaho during two winter months, has given us an opportunity to observe the relationships between these toxics and well known vehicle exhaust tracer such as CO and NO_x in urban environment. The emission ratios of these toxics were calculated from the slope of the linear fit of scatter plots between two compounds. We found that the emission ratios for HCHO with respect to CO and NO_x respectively to be 3.30 ± 0.29 pptv/ppbv and 11.9 ± 1.2 pptv/ppbv. As expected, the emission ratios for acetaldehyde were a little lower, 2.11 ± 0.20 pptv/ppbv CO and 7.99 ± 1.03 pptv/ppbv NO_x. Emission ratios for benzene were 1.30 ± 0.07 pptv/ppbv CO and 5.06 ± 0.47 pptv/ppbv NO_x. Although there were a few studies where the relationship of air toxics and vehicle exhaust is examined, these emission ratios were found to be in the range of results from previous studies that were done in various cities across the globe.

Air toxics can pose a special threat in urban areas by affecting the health millions of people. Some of these air toxics like aldehydes play an important role in atmospheric chemistry by contributing to radical budget of a certain area. For example - formaldehyde can also contribute to formation of ground level ozone, which is a criteria pollutant that can cause respiratory illnesses in human. US EPA has been trying to regulate these air

toxics by implementing hazardous pollutant control standards (NESHAPS) where maximum achievable control strategies are often applied to reduce the emission of these toxics. Estimating toxics from various sources is an important step in this process. For this purpose, EPA can rely on emission predictor models e.g. MOBILE 6.2. This particular model was developed a long time ago and relies on outdated information on vehicle emissions. This can mislead the current situation of certain pollutant by either over-predicting or under-predicting some of the pollutants.

This study also compared the found emission ratios to modeled emission ratios.

AIRPACT-3 is a regional air quality forecast system for the Northwestern region of the US. This system predicts direct emissions of acetaldehyde, benzene and formaldehyde from vehicle source along with CO and NO_x emissions. The emission ratios were calculated by a method similar to that used for the measurements. Measured emission ratios of aldehydes-NO_x and benzene - CO compared well to the modeled data. However, the aldehyde – CO relationship of the model resulted in emission ratios significantly lower than those measured, by a factor of 7 - 15. This implies that the emission factor model (MOBILE6.2) predicts erroneous emissions for the aldehydes and CO from vehicle exhausts. Previous evaluations and criticisms of MOBILE6.2 suggest that this error could be a result of the model's dependence on outdated information on vehicle emissions. Most of the algorithms developed for this model heavily rely on vehicle fleet from mid-1990s. As technology for reduction of hydrocarbon emissions have been deployed over the past decade, new vehicles produce lower VOCs and CO emissions. The wide range in formaldehyde – CO emission ratios (refer to § 3.6 and Table 3.13)

observed in different studies suggest that the emission rates and ratios of some of these VOCs (formaldehyde, acetaldehyde and benzene) are not well understood and demonstrate a crucial need to incorporate these factors in future models.

The method used in this study to calculate the emission ratios of the desired VOCs was developed through similar approaches following previous studies. The simplicity of this method makes it a great tool to get a snapshot of air quality at a local scale. Levels of VOCs can be measured by using the emission ratios and ambient mixing ratios of CO or NO_x available from air quality monitoring network. This can also be used as an evaluation tool for air quality models. The emission ratios could guide modelers to see if any of the pollutants are either under or over predicted. Comparing the emission ratios found in this study, for NO_x, to the ones from MOBILE6.2, suggest that the CO emissions were over predicted by the model by a factor of 5.2.

One of the limitations of this analysis technique is that it was used for a very specific time. Emission ratios found this way might not be suitable for other timeframes. During summer months, the ambient concentration of some of the air toxics, e.g. –formaldehyde, highly depend on their photochemical production in the atmosphere. As the study was conducted during winter, we simply assumed this factor to be negligible as the morning rush hour period was before sunrise. Also during summer, morning rush hour period is not absent of sunlight and one cannot neglect the factor of photochemistry during that period. Calculations of emission ratios during hotter months need to consider the photochemical factor, which can be rather complicated.

There are several scopes to improve the analysis and calculation methods even further.

Here is a short list of recommendations for addressing certain points in future.

- i. As mentioned above, the emission ratios might have the same seasonal variability as of the air toxic itself. This could be further investigated by conducting a long term study over several months (or years) for a certain region.
- ii. In this study, calculating emission ratios with respect to CO and NO_x was an attempt to understand the influence of different fueled vehicles on air toxics. However, these two compounds are not exclusive to either gasoline or diesel fueled vehicle exhaust. So the calculated emission ratios were not fuel specific. Specific tracers are needed to pinpoint the exact amount of air toxic emitted by a specific fueled vehicle.
- iii. Recently EPA has developed a new emission predictor, the MOtor Vehicle Emission Simulator (MOVES) which will eventually replace MOBILE6.2 in the future. This study focused on the relationships between the measured emission ratios to the ones calculated from MOBILE6.2. When MOVES data are available to the public, it might be worth looking into how this new model predicts CO and toxics from mobile sources.
- iv. This study was conducted on formaldehyde, acetaldehyde and benzene- only couple of the numerous HAPs listed by EPA. A more extensive research including more MSATs can be highly useful to air toxic assessment programs to estimate ambient concentrations of air toxics from mobile sources.

BIBLIOGRAPHY

- (ACS) ACS Cancer Facts & Figures - 2010. Atlanta, GA.
- Air Improvement Resource I (2005) Examination of Temperature and RVP Effects on CO Emissions in EPA's Certification Database. Coordinating Research Council, Inc., 3650 Mansell Road, Suite 140 - Alpharetta, Georgia 30022.
- Altshuller AP (1993) Production of aldehydes as primary emissions and from secondary atmospheric reactions of alkenes and alkanes during the night and early morning hours. *Atmospheric Environment Part a-General Topics* 27:21-32.
- Anderson LG, Lanning JA, Barrell R, Miyagishima J, Jones RH, Wolfe P (1996) Sources and sinks of formaldehyde and acetaldehyde: An analysis of Denver's ambient concentration data. *Atmospheric Environment* 30:2113-2123.
- ATSDR (1999) Toxicological profile for formaldehyde. Agency for Toxic Substances and Disease Registry, Public Health Service, U.S. Department of Health and Human Services, Atlanta, GA.
- ATSDR (2007) Toxicological profile for benzene. Agency for Toxic Substances and Disease Registry, Public Health Service, U.S. Department of Health and Human Services, Atlanta, GA.
- Ban-Weiss GA, McLaughlin JP, Harley RA, Kean AJ, Grosjean E, Grosjean D (2008) Carbonyl and nitrogen dioxide emissions from gasoline- and diesel-powered motor vehicles. *Environmental Science & Technology* 42:3944-3950.
- Borbon A, Coddeville P, Locoge N, Galloo JC (2004) Characterising sources and sinks of rural VOC in eastern France. *Chemosphere* 57:931-942.
- Chen J, Vaughan J, Avise J, O'Neill S, Lamb B (2008) Enhancement and evaluation of the AIRPACT ozone and PM(2.5) forecast system for the Pacific Northwest. *Journal of Geophysical Research-Atmospheres* 113:20.
- Devlin RB, Raub JA, Folinsbee LJ (1997) Health Effects of Ozone. *Science and Medicine*.
- Duane M, Poma B, Rembges D, Astorga C, Larsen BR (2002) Isoprene and its degradation products as strong ozone precursors in Insubria, Northern Italy. *Atmospheric Environment* 36:3867-3879.

- EPA (1988) Health and Environmental Effects Profile for Formaldehyde. Environmental Criteria and Assessment Office, Office of Health and Environmental Assessment, Office of Research and Development, Cincinnati, OH.
- EPA (2000a) National Air Toxics Program : The Integrated Urban Strategy Office Of Air Quality Planning And Standards, Research Triangle Park, NC 27711
- EPA (2000b) Technical Support Document: Control of Emissions of Hazardous Air Pollutants from Motor Vehicles and Motor Vehicle Fuels. Assessment and Standards Division, Office of Transportation and Air Quality, U.S. Environmental Protection Agency.
- EPA (2010) 2002 National-Scale Air Toxics Assessment. U.S. Environmental Protection Agency.
- EPA (2011) 2005 National-Scale Air Toxics Assessment. U.S. Environmental Protection Agency.
- Friedfeld S, Fraser M, Ensor K, Tribble S, Rehle D, Leleux D, Tittel F (2002) Statistical analysis of primary and secondary atmospheric formaldehyde. *Atmospheric Environment* 36:4767-4775.
- Grosjean D (1982) Formaldehyde and other carbonyls in los-angeles ambient air. *Environmental Science & Technology* 16:254-262.
- Grosjean D, Grosjean E, Gertler AW (2001) On-road emissions of carbonyls from light-duty and heavy-duty vehicles. *Environmental Science & Technology* 35:45-53.
- Grosjean D, Grosjean E, Moreira LFR (2002) Speciated ambient carbonyls in Rio de Janeiro, Brazil. *Environmental Science & Technology* 36:1389-1395.
- Heirigs PL, Delaney SS, Dulla RG (2004) Evaluation of MOBILE Models: MOBILE6.1 (PM), MOBILE6.2 (Toxics), And MOBILE6/CNG. American Association of State Highway and Transportation Officials (AASHTO)
- Herron-Thorpe FL, Lamb BK, Mount GH, Vaughan JK (2010) Evaluation of a regional air quality forecast model for tropospheric NO₂ columns using the OMI/Aura satellite tropospheric NO₂ product. *Atmospheric Chemistry and Physics* 10:8839-8854.
- Ho KF, Lee SC, Louie PKK, Zou SC (2002) Seasonal variation of carbonyl compound concentrations in urban area of Hong Kong. *Atmospheric Environment* 36:1259-1265.
- IDEQ (2009) 2007 Treasure Valley Idaho Air Toxics Study

- Jobson BT, McCoskey JK (2010) Sample drying to improve HCHO measurements by PTR-MS instruments: laboratory and field measurements. *Atmospheric Chemistry and Physics* 10:1821-1835.
- Kavouras IG, DuBois DW, Etyemezian V, Nikolich G (2008) Ozone and its precursors in the Treasure Valley, Idaho. Department of Environmental Quality, State of Idaho
- McKeen SA, Mount G, Eisele F, Williams E, Harder J, Goldan P, Kuster W, Liu SC, Baumann K, Tanner D, Fried A, Sewell S, Cantrell C, Shetter R (1997) Photochemical modeling of hydroxyl and its relationship to other species during the Tropospheric OH Photochemistry Experiment. *Journal of Geophysical Research-Atmospheres* 102:6467-6493.
- NTP (2011) Report on Carcinogens. Twelfth edn. U.S. Department of Health and Human Services, Public Health Service, National Toxicology Program, Research Triangle Park, NC, p. 499.
- Possanzini M, Di Palo V, Cecinato A (2002) Sources and photodecomposition of formaldehyde and acetaldehyde in Rome ambient air. *Atmospheric Environment* 36:3195-3201.
- Possanzini M, Dipalo V, Petricca M, Fratacangeli R, Brocco D (1996) Measurements of lower carbonyls in Rome ambient air. *Atmospheric Environment* 30:3757-3764.
- Rappengluck B, Dasgupta PK, Leuchner M, Li Q, Luke W (2010) Formaldehyde and its relation to CO, PAN, and SO₂ in the Houston-Galveston airshed. *Atmospheric Chemistry and Physics* 10:2413-2424.
- Seinfeld JH, Pandis SN (2006) *Atmospheric chemistry and physics : from air pollution to climate change*. John Wiley & Sons, Inc.
- Starn TK, Shepson PB, Bertman SB, White JS, Splawn BG, Riemer DD, Zika RG, Olszyna K (1998) Observations of isoprene chemistry and its role in ozone production at a semirural site during the 1995 Southern Oxidants Study. *Journal of Geophysical Research-Atmospheres* 103:22425-22435.
- Stockwell WR, Kuhns H, Etyemezian V, Green MC, Chow JC, Watson JG (2003) The Treasure Valley secondary aerosol study II: modeling of the formation of inorganic secondary aerosols and precursors for southwestern Idaho. *Atmospheric Environment* 37:525-534.
- Tago H, Kimura H, Kozawa K, Fujie K (2005) Formaldehyde concentrations in ambient air in urban and rural areas in Gunma Prefecture, Japan. *Water Air and Soil Pollution* 163:269-280.

- Viskari EL, Vartiainen M, Pasanen P (2000) Seasonal and diurnal variation in formaldehyde and acetaldehyde concentrations along a highway in Eastern Finland. *Atmospheric Environment* 34:917-923.
- Warneke C, McKeen SA, de Gouw JA, Goldan PD, Kuster WC, Holloway JS, Williams EJ, Lerner BM, Parrish DD, Trainer M, Fehsenfeld FC, Kato S, Atlas EL, Baker A, Blake DR (2007) Determination of urban volatile organic compound emission ratios and comparison with an emissions database. *Journal of Geophysical Research-Atmospheres* 112.
- WHO (1989) Environmental Health Criteria for Formaldehyde. World Health Organization Geneva, Switzerland